

5-2011

Δnp63 Regulates A Complex Network Of Target Genes In Limb And Epidermal Development

Min Soon Cho

Follow this and additional works at: https://digitalcommons.library.tmc.edu/utgsbs_dissertations



Part of the [Genetic Phenomena Commons](#)

Recommended Citation

Cho, Min Soon, "Δnp63 Regulates A Complex Network Of Target Genes In Limb And Epidermal Development" (2011). *Dissertations and Theses (Open Access)*. 128.
https://digitalcommons.library.tmc.edu/utgsbs_dissertations/128

This Dissertation (PhD) is brought to you for free and open access by the MD Anderson UTHealth Houston Graduate School at DigitalCommons@TMC. It has been accepted for inclusion in Dissertations and Theses (Open Access) by an authorized administrator of DigitalCommons@TMC. For more information, please contact digcommons@library.tmc.edu.

$\Delta Np63$ REGULATES A COMPLEX NETWORK OF TARGET GENES

IN LIMB AND EPIDERMAL DEVELOPMENT

by

Min Soon Cho, M.S.

APPROVED:

Elsa R. Flores, Ph.D., Supervisory Professor

Richard R. Behringer, Ph.D.

Mong-Hong Lee, Ph.D.

Michael J. Galko, Ph.D.

Kenneth Y. Tsai, M.D., Ph.D.

APPROVED:

Dean, The University of Texas

Graduate School of Biomedical Sciences at Houston

**$\Delta Np63$ REGULATES A COMPLEX NETWORK OF TARGET GENES
IN LIMB AND EPIDERMAL DEVELOPMENT**

A
DISSERTATION

Presented to the Faculty of
The University of Texas
Health Science Center at Houston
and
The University of Texas
M.D. Anderson Cancer Center
Graduate School of Biomedical Sciences
in Partial Fulfillment

of the Requirements
for the Degree of

DOCTOR OF PHILASOPHY

By

Min Soon Cho, M.S.

Houston, Texas

May 2011

DEDICATION

I dedicate this work to my family whose love supports me in every way and to the Lord Jesus Christ, who is the creator and shepherd to all who trust in Him.

ACKNOWLEDGEMENTS

It would not be possible to complete this thesis without thoughtful advice and caring support from my mentor, colleagues and family members. I owe each of them my sincere appreciation.

First of all, I would like to thank my advisor and mentor, Dr. Elsa R. Flores for her support and advice throughout my academic development in the Ph.D. program. My academic achievements would not be possible without her help and support. She was my inspiration and the catalyst for my academic pursuit in mouse genetics and skin morphogenesis. Her advice and training have been indispensable for the progress of my project toward the right direction. I feel very fortunate to have her as my advisor and mentor.

It was my great honor and pleasure to have Drs. Richard Behringer, Mong-Hong Lee, Kenneth Tsai, Michael Galko, Randy Johnson, Pierre McCrea, Lei Li, Randy Legerski and Gulliermina Lozano as my committee members. Their suggestions and insight opened my eyes to things I could not have seen alone during my studies. I also thank Elisabeth Lindheim for her exceptional support and the Genes and Development program for providing me with such a high standard learning environment.

I would like to thank my colleagues in Dr. Flores' lab. I truly enjoyed working with a group of intelligent and hard working people. Their support and participation in the thesis discussions were invaluable and encouraged me to explore the subject matter

more thoroughly. I thank my friend Deepavali Chakravarti for her valuable friendship, challenging discussion and encouragement during my studies since she joined in Dr. Flores lab. I also thank Dr. Xiaohua Su, Young-jin Gi, Lingzhi Liu and Avinash Narayan for their input and assistance for this thesis. My summer interns, Arianexys Aquino, Nicole Müller, and Io Long Chan also contributed to RT-PCR, Western analysis and Luciferase construct cloning for this thesis.

Most of all, I could not have completed my academic journey without my supportive family, especially my husband, Dave Kim and my lovely son, Joseph Kim who filled my day with love and joy whether I was in the lab, in the library or at home. I also would like to remember my parents, Yoon Hak Cho and Boon Soon Jeong, my sisters in Korea for believing me and supporting me through their prayers with endless love. I would like to thank my parents in law, Rev. Suk In Kim and Chung Bok Kim for their support and prayers each and everyday.

Finally, I confess and praise my Lord savior for choosing me as His child and guiding me with His unfailing love, abundant patience and greatest wisdom.

$\Delta Np63$ regulates a complex network of target genes

in limb and epidermal development

Publication No. _____*

Min Soon Cho, M.S.

Supervisory Professor: Elsa R. Flores, Ph.D.

The skin is composed of two major compartments, the dermis and epidermis. The epidermis forms a barrier to protect the body. The stratified epithelium has self-renewing capacity throughout life, and continuous turnover is mediated by stem cells in the basal layer. *p63* is structurally and functionally related to *p53*. In spite of their structural similarities, *p63* is critical for the development and maintenance of stratified epithelial tissues, unlike *p53*. *p63* is highly expressed in the epidermis and previously has been shown to play a critical role in the development and maintenance of the epidermis. The study of *p63* has been complicated due to the existence of multiple isoforms: those with a transactivation domain (*TAp63*) and those lacking this domain ($\Delta Np63$). Mice lacking *p63* cannot form skin, have craniofacial and skeletal defects and die within hours after birth. These defects are due to the ability of *p63* to regulate multiple processes in skin development including epithelial stem cell proliferation, differentiation, and adherence programs. To determine the roles of these isoforms in skin development and maintenance, isoform specific *p63* conditional knock out mice were generated by our lab. *TAp63*^{-/-} mice age prematurely, develop blisters, and display wound-healing defects that result from hyperproliferation of dermal stem cells. That results in premature depletion of these cells, which are necessary for wound repair, that indicates *TAp63* plays a role in dermal/epidermal maintenance. To study the role of $\Delta Np63$, I generated a $\Delta Np63$ ^{-/-} mouse and analyzed the skin by performing immunofluorescence for markers

of epithelial differentiation. The $\Delta Np63^{-/-}$ mice developed a thin, disorganized epithelium but differentiation markers were expressed. Interestingly, the epidermis from $\Delta Np63^{-/-}$ mice co-expressed K14 and K10 in the same cell suggesting defects in epidermal differentiation and stratification. This phenotype is reminiscent of the $DGCR8^{fl/fl};K14Cre$ and $Dicer^{fl/fl};K14Cre$ mice skin. Importantly, $DGCR8^{-/-}$ embryonic stem cells (ESCs) display a hyperproliferation defect by failure to silence pluripotency genes. Furthermore, I have observed that epidermal cells lacking $\Delta Np63$ display a phenotype reminiscent of embryonic stem cells instead of keratinocytes. Thus, I hypothesize that genes involved in maintaining pluripotency, like *Oct4*, may be upregulated in the absence of $\Delta Np63$. To test this, q-RT PCR was performed for *Oct4* mRNA with wild type and $\Delta Np63^{-/-}$ 18.5dpc embryo skin. I found that the level of *Oct4* was dramatically increased in the absence of $\Delta Np63^{-/-}$. Based on these results, I hypothesized that $\Delta Np63$ induces differentiation by silencing pluripotency regulators, *Oct4*, *Sox2* and *Nanog* directly through the regulation of *DGCR8*. I found that *DGCR8* restoration resulted in repression of *Oct4*, *Sox2* and *Nanog* in $\Delta Np63^{-/-}$ epidermal cells and rescue differentiation defects. Loss of $\Delta Np63$ resulted in pluripotency that caused defect in proper differentiation and stem cell like phenotype. This led me to culture the $\Delta Np63^{-/-}$ epidermal cells in neuronal cell culture media in order to address whether restoration of *DGCR8* can transform epidermal cells to neuronal cells. I found that *DGCR8* restoration resulted in a change in cell fate. I also found that miR470 and miR145 play a role in the induction of pluripotency by repressing *Oct4*, *Sox2* and *Nanog*. This indicates that $\Delta Np63$ induces terminal differentiation through the regulation of *DGCR8*.

TABLE OF CONTENTS

Dedication.....	iii
Acknowledgements.....	iv
Abstract.....	vi
Table of Contents.....	viii
List of Illustrations.....	xv
List of Tables.....	xviii
List of Appendices.....	xix

CHAPTER 1: INTRODUCTION

1.1. Gene structure of p63.....	2
1.2. The general roles of TAp63 and Δ Np63 isoforms.....	4
1.2.1. The role of TAp63 isoforms	4
1.2.2. The role of Δ Np63 isoforms	7
1.3. The role of p63 in embryonic epidermal differentiation.....	9
1.3.1. Skin stratification.....	9
1.3.2 The roles of p63 in limb development.....	11
1.4. p63 point mutation in Human diseases	11
1.5. Stem cell maintenance.....	14
1.6. Asymmetric Cell division.....	15

1.7. MicroRNA biogenesis and regulation	20
1.8. Genes that play critical roles in epidermal stem cells	24
1.8.1. <i>Ink4a –Arf</i>	24
1.8.2. <i>Brachyury</i>	25
1.8.3. <i>DGCR8</i>	27

CHAPTER 2: MATERIALS AND METHODS

1. Generation of $\Delta Np63$ Conditional Knockout Mice.....	33
2. Genotyping.....	32
3. Mouse husbandry.....	33
4. Histology and immunostaining of E18.5 embryos.....	33
5. Mouse embryonic fibroblasts (MEFs) and keratinocytes isolation and culture	35
6. Tumor cell lines	36
7. Chromatin immunoprecipitation (ChIP)	36
8. Western blot analysis.....	38
9. RNA extraction and real–time PCR.....	39
10. Cloning of <i>brachyury-luciferase</i> reporter constructs.....	39
11. Dual-luciferase reporter assay	41
12. Keratinocyte proliferation assays.....	41
13. Proliferation assay (Tumor cell lines)	42
14. Keratinocytes differentiation and neuronal cell differentiation assay.....	42

15. miRNA TaqMan assay	43
16. Clonogenic assay, rhodamine B and BrdU staining	44
17. Murine <i>p63</i> siRNAs assay.....	44
18. Adenovirus-Cre infection.....	44
19. Retroviral infection (pSuper mouse DGCR8-1)	45
20. Boyden chamber assays for cell migration and invasion.....	45
21. Skeleton preparation and staining.....	45
22. Statistics.....	46
23. Graphs.....	46

CHAPTER 3: New targets of p63 in epithelial development, limb development and metastasis

3.1. The role of p63 as a transcriptional repressor of *Arf/Ink4a*

Rationale & Hypothesis.....	48
3.1.1. The phenotypic features of <i>p63</i> ^{-/-} mice are partially rescued by loss of <i>Arf</i> or <i>Ink4a</i>	48
3.1.2. Loss of <i>Arf</i> or <i>Ink4a</i> partially rescues the limb defect of the <i>p63</i> ^{-/-} mice.....	50
3.1.3. Loss of <i>Arf</i> or <i>Ink4a</i> restores the formation of stratified layers of skin in <i>p63</i> ^{-/-} mice.....	53
3.1.4. Proliferation of <i>p63</i> ^{-/-} keratinocytes is restored in the absence of <i>Arf</i> or <i>Ink4a</i>	58

3.1.5. p63 represses <i>p19^{Arf}</i> and <i>p16^{Ink4a}</i> leading to proper proliferation and differentiation, absent in <i>p63^{-/-}</i> cells.....	62
3.1.6. The <i>Arf</i> and <i>Ink4a</i> transcripts were repressed by restoration of p63 in double mutant MEFs.....	67

3.2. The role of p63 as a transcriptional activator of *Brachyury*

Rationale & Hypothesis.....	69
3.2.1. <i>Brachyury</i> gene expression is down regulated in the absence of <i>p63</i>	69
3.2.2. p63 is a unique p53 family member that binds to the promoter of <i>brachyury</i>	74
3.2.3. Δ Np63 α and β transcriptionally activate <i>brachyury</i>	77
3.2.4. The level of <i>brachyury</i> expression correlates with level of Δ Np63 expression in osteosarcoma cell lines.....	80
3.2.5. Loss of Δ Np63 results in concomitantly downregulation of <i>brachyury</i> expression	83
3.2.6. Downregulation of <i>p63</i> leads to loss of <i>brachyury</i> expression in a decrease in cell proliferation, migration and invasion.....	84

CHAPTER 4: Δ Np63 induces appropriate differentiation of the epidermis through regulation of *DGCR8*.

4. The roles of Δ Np63 in epithelial development

Rationale & Hypothesis	88
4.1. Generation of $\Delta Np63$ conditional knockout mice.....	88
4.2. $\Delta Np63$ knockout mice have a uniform layer of skin but still have a defect in cell adhesion.....	92
4.3. $\Delta Np63^{+/-}$ mice have wrinkled and expanded basal layer of skin.....	92
4.4. Inappropriate skin differentiation in the $\Delta Np63^{-/-}$ mice	95
4.5. Aberrant proliferation in spinous layer of epidermis in $\Delta Np63^{-/-}$ mice.....	97
4.6. Molecular mechanism contributing to the regulation of epithelial differentiation of $\Delta Np63$	100
4.6.1. $\Delta Np63$ cKO phenotypes were similar with DGCR8cKO skin.....	100
4.6.2. <i>DGCR8</i> is a unique target gene of $\Delta Np63$	100
4.6.3. $\Delta Np63$ transcriptionally regulates DGCR8 via direct binding to its promoter...	103
4.6.4. Loss of $\Delta Np63$ results in higher expression of pluripotency regulating genes, <i>Oct4</i> , <i>Sox2</i> and <i>Nanog</i>	106
4.6.5. Repression of mir470 and mir145 in $\Delta Np63^{-/-}$ and Δ/Δ epidermal cells correspond to elevated mRNA levels of <i>Oct4</i> , <i>Sox2</i> and <i>Nanog</i>	110
4.6.6. $\Delta Np63$ regulates cell fate and cell differentiation via the regulation of <i>DGCR8</i>	113
4.7. Loss of $\Delta Np63$ results in obtaining self-renewal capacity in keratinocytes.....	117

Chapter 5: Roles of $\Delta Np63$ in limb development, wound healing, and asymmetric cell division

5.1. Limb development and epidermal differentiation

Rationale and Hypothesis..... 121

5.1.1. Cre recombines 90% of $\Delta Np63$ alleles in $\Delta Np63^{fl/fl};K14Cre+$ (Δ/Δ) mice..... 122

5.1.2. $\Delta Np63$ plays early in limb development and epidermal skin differentiation
..... 124

5.2. The role of $\Delta Np63$ in Wound healing

Rationale and Hypothesis..... 128

5.2.1. Loss of $\Delta Np63$ accelerates healing process by faster proliferation after wound
.....128

5.2.2. Hyperproliferation results in rapid healing after wound in $\Delta Np63^{+/-}$ 131

5.2.3. Loss of $\Delta Np63$ cells have a defect in orientation of cell division during
development 133

5.2.4. $\Delta Np63$ regulates *LGN*, a marker of cell orientation, by indirectly binding to its
promoter.....135

5.2.5. Restoration of DGCR8 rescues expression of *LGN* in $\Delta Np63^{-/-}$
keratinocytes..... 138

5.2.6. Loss of $\Delta Np63$ shows a straight orientation of hair follicle growth..... 139

CHAPTER 6: CONCLUTIONS & DISCUSSIONS

6.1 Rescue of key features of the <i>p63</i>^{-/-} epithelial phenotype by inactivation of <i>Ink4a</i> and <i>Arf</i>	142
6.2 ΔNp63 transcriptionally regulates <i>brachyury</i>, a gene with diverse roles in limb development, tumorigenesis and metastasis	145
6.3. ΔNp63 induces terminal differentiation through transcriptional regulation of <i>DGCR8</i> and suppression of pluripotency factors	148
6.4. ΔNp63 indirectly controls asymmetric cell divisions through <i>LGN</i> via regulation of <i>DGCR8</i>.....	150
BIBLIOGRAHPY.....	153
APPENDIX.....	172
VITA.....	178

List of Illustrations

Figure 1. The schematic structure of p63 and its isoforms.....	3
Figure 2. Deletion of the <i>p63</i> gene in mice.....	5
Figure 3. K6 expression is high in $\Delta Np63^{-/-}$ skin at E 18.5.....	10
Figure 4. Phenotypic features of patients with AEC or EEC syndromes.....	13
Figure 5. A schematic model of asymmetric cell division of epidermis and terminal differentiation during embryo development.....	18
Figure 6. The Canonical pathway of microRNA (miRNA) biogenesis.....	22
Figure 7. The Hair follicle morphology of Dgcr8 cKO and Dicer cKO.....	28
Figure 8. Macroscopic analysis of embryos at day E18.5.....	51
Figure 9. Microscopic analysis of the epithelium of embryos at E18.5.....	55
Figure 10. Keratinocyte cultures derived from embryos at E18.5.....	60
Figure 11. Expression of p19 ^{Arf} , p16 ^{Ink4a} , and GFP in keratinocytes and stratified epithelium.....	65
Figure 12. p63 represses Arf and Ink4a.....	68
Figure 13. <i>Brachyury</i> is downregulated in the absence of <i>p63</i>	72
Figure 14. p63 binds to the <i>brachyury</i> promoter.....	76
Figure 15. <i>Brachyury</i> is transactivated by $\Delta Np63\alpha$ and $\Delta Np63\beta$	78
Figure 16. $\Delta Np63$ expression induces brachyury in tumor cell lines.....	81

Figure 17. Knockdown of $\Delta Np63$ results in decreased cell proliferation, migration and invasion.....	86
Figure 18. Generation of $\Delta Np63$ conditional knockout and knock out mice.....	90
Figure 19. Microscopic analysis of wild type, $\Delta Np63^{-/-}$ and $\Delta Np63^{+/-}$ embryos at day E18.5.....	94
Figure 20. Microscopic analysis of wild type, $\Delta Np63^{-/-}$ and $\Delta Np63^{+/-}$ embryos at day E18.5.....	96
Figure 21. Proliferation analysis of $\Delta Np63$ mutant embryos by incorporation of BrdU at day E18.5.....	99
Figure 22. $\Delta Np63$ deficient epidermal hair follicles are similar to <i>DGCR8cKO</i> epidermal phenotype.....	102
Figure 23. <i>DGCR8</i> is transactivated by $\Delta Np63\alpha$, $\Delta Np63\beta$ and $\Delta Np63\gamma$.....	104
Figure 24. <i>Oct4</i>, <i>Sox2</i> and <i>Nanog</i> are upregulated in $\Delta Np63$ deficient epidermal cells	108
Figure 25. Restoration of <i>DGCR8</i> rescues defect in differentiation in $\Delta Np63$ deficient cells	111
Figure 26. $\Delta Np63$ deficient epidermal cells are pluripotent and can self-renew	115
Figure 27. $\Delta Np63$ initiates epidermal differentiation through <i>DGCR8</i>.....	118
Figure 28. Stratification occurred in $\Delta Np63^{fl/fl};K14Cre+$ (Δ/Δ) mice epidermis... 	123

Figure 29. The view of $\Delta Np63^{fl/fl};K14Cre+$ (Δ/Δ) mice embryonic day at E18.5...	126
Figure 30. Wound healing is accelerated in $\Delta N63$ deficient mice skin.....	130
Figure 31. A graph of open wound (%) measured everyday after wound in 9-month-old mice.....	132
Figure 32. Asymmetric cell division is impaired by loss of $\Delta Np63$ embryo at day E18.5.....	134
Figure 33. LGN is downexpressed in $\Delta Np63^{-/-}$ epidermal cells through DGCR8 regulation.....	136
Figure 34. The orientation of hair follicle growth is straight not right angled in $\Delta Np63$ heterozygote embryos at E18.5.....	139

List of Tables

Table 1. Quantification of epithelial structures in day 18.5 embryos.....	57
Table 2. Quantification of length of limbs in day 18.5 embryos.....	64
Table 3. Cell division ratio	134

List of Appendices

Appendix 1. Mitotic Figures in Developing Epidermis from a wild type embryo at 18.5 Days of epidermal keratinocytes in the basal layer of developing epidermis undergo apical-basal cell divisions.....	172
Appendix 2. ΔNp63 ablation shows lower microRNA expression.....	173
Appendix 3. ΔNp63 ablation shows hyperproliferation in epidermal cells.....	174
Appendix 4. DGCR8 knock down reminiscent gene expression.....	175
Appendix 5. ΔNp63 initiates epidermal differentiation through <i>DGCR8</i>.....	177

CHAPTER 1.
INTRODUCTION

1. **Cho MS**, Chan IL and Flores ER. **Cell Cycle 9:12, 1-8; June 15, 2010** Δ Np63 transcriptionally regulates *brachyury*, a gene with diverse roles in limb development, tumorigenesis and metastasis. **Permission from Cho et al. and Copyright clearance center**

2. Su X, **Cho MS**, Gi Y, Ayanga BA, Sherr CJ, and Flores ER. **EMBO J. 2009 Jul 8;28(13):1904-15**. Rescue of key features of the p63-null epithelial phenotype by inactivation of Ink4a and Arf. **Permission from Su et al. and Copyright clearance center**

3. **Min Soon Cho**, Xiaohua Su, Deepavali Chakravarti, Arianexys Aquino, Nicole Müller, Avinashnarayan Venkatanarayan, Io Long Chan, Young Jin Gi, & Elsa R. Flores. Δ Np63 induces terminal differentiation through transcriptional regulation of DGCR8 and suppression of pluripotency factors.

Chapter 1. Introduction

1.1. Gene structure of p63, a p53 family member

p63, a *p53* family member, contains three domains: a transactivation domain (TA), a DNA binding domain and an oligomerization domain. All three domains bear homology to p53 and transactivate common target genes (Yang et al., 1998) (**Figure 1**). *p63* is located on chromosome 3q27-29 in human and chromosome 16 in mouse. The p63 gene uses two distinct promoters which results in multiple isoforms (TA contains a transactivation domain and ΔN lacks a conventional transactivation domain but has an alternative transactivation domain (proline repeat in 5' upstream)) and has alternative 3' end splicing variants that produce α , β and γ isoforms (**Figure 1**) (Yang et al., 1998). p63 is highly expressed in the basal layer of epidermis and is differentially expressed in various tissues in an isoform dependent manner, while p53 is ubiquitously expressed. The progenitor and stem cell populations reside in the basal layer of the epidermis. Normal epithelial tissues such as skin, mammary glands, prostate, tongue and esophagus show high expression of p63 (Yang et al., 1998) and in these tissues, expression of p63 is gradually lost by differentiation.

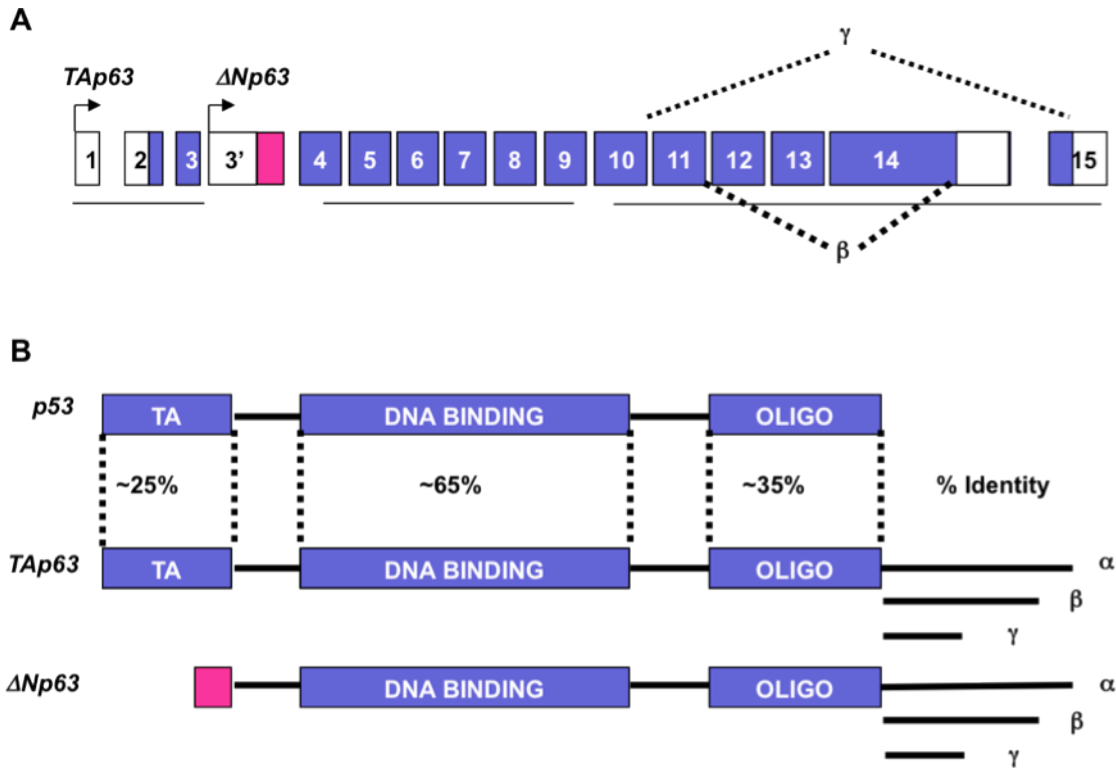


Figure 1. The schematic structure of p63 and its isoforms

A. *p63* has 15 exons and employs two independent promoters.

B. *p63* contains a transactivation (TA), a DNA binding and an oligomerization domain.

These have much similarity to p53.

1.2. The general roles of TAp63 and Δ Np63 isoforms

1.2.1. The roles of TAp63 isoforms

TAp63 isoforms transcribe *p63* gene that structurally resembles p53 and functions as a transcription activator (Yang et al., 1998). Since it has structural similarity to p53, it is largely believed that p63 functions as a tumor suppressor. However, *p63*^{-/-} mice show striking developmental defects that prompted study of the developmental roles of *p63*. Here I introduce the roles of TAp63 in advance of discussing the roles of Δ Np63 in embryonic development later in **Chapter 1**.

p63 knock out mice were generated by two groups (Mills et al., 1999; Yang et al., 1999) and striking knock out phenotypes were observed with apparent developmental defects such as truncated limbs, cleft plate and immature skin (**Figure 2**) (Mills et al., 1999; Yang et al., 1999). Identified functions for *p63* in the stratified epithelium include commitment to differentiation, the maintenance of cell junctions, and stem cell proliferation (Carroll et al., 2007; Carroll et al., 2006; Ihrie et al., 2005; Koster et al., 2007; Koster et al., 2004). Many of these functions are controlled by a numerous transcriptional networks of genes regulated by p63 (Vigano et al., 2006; Vigano and Mantovani, 2007; Yang et al., 2006). TAp63 isoforms act initially during early epidermal development, however TAp63 levels are almost undetectable in the mature epidermis and deregulated TAp63 results in hyperproliferation and failure of terminal differentiation (Koster et al., 2004; Koster et al., 2006; Liefer et al., 2000).

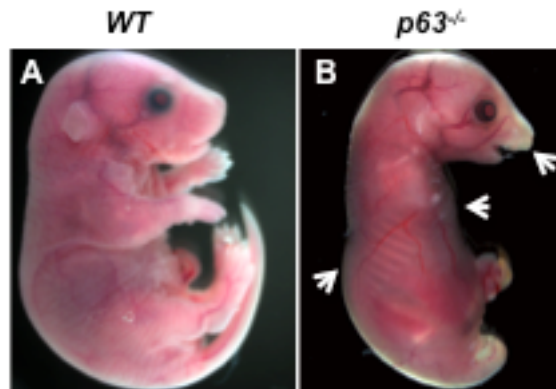


Figure 2. Deletion of the *p63* gene in mice

A. Sagittal view of E18.5 embryo wild type (*WT*) and **B.** *p63*^{-/-} embryo shows truncated limbs, cleft palate and transparent skin (Denoted by white arrows).

There are two distinct interpretations of roles of p63 in embryonic skin developmental defects: one is that p63 is essential for epidermal differentiation and another one is that p63 is critical for maintenance of epidermal stem cell renewal (Mills et al., 1999; Yang et al., 1999). Since those knock out mice do not possess any of p63 isoforms, it is difficult to accurately predict which isoforms play an important role in epidermal development.

However, the Flores laboratory (Su and Flores, 2009; Su et al., 2009b) demonstrated that TAp63 plays significant roles in skin development using a *TAp63*^{-/-} mice model. To generate TAp63 knockout mice, a conditional knockout strategy was used and uses it to ablate TAp63 in the germline (*TAp63*^{-/-}) or in keratin 14 expressing cells in the basal layer of the epidermis (*TAp63*^{fl/fl};*K14Cre*+) (Su et al., 2009b). *TAp63*^{-/-} mice have developed a fully differentiated epidermis during the embryonic stage, whereas they showed premature aging and developed skin ulcerations, spontaneous blister at adulthood, senescence of hair follicle-associated dermal and epidermal cells, delayed in wound healing and a decrease in hair morphogenesis (Su et al., 2009b). These phenotypes are due to loss of *TAp63* that result from premature depletion of epidermal and dermal precursor cells capacity (Su et al., 2009b). *TAp63*^{-/-} dermal precursor cells and epidermis prematurely senesced and showed genomic instability, indicating TAp63 plays essential roles in maintaining epidermal stem cells with an appropriate balance of senescence event and genomic stability.

In tumorigenesis, there is debate about the role of TAp63. The Roop laboratory reported that the expression of TAp63 in epithelial tumors is high, whereas expression of TAp63 is lower in the mature epidermis (Koster et al., 2006; Liefer et al., 2000). By the gene switch system, overexpression of TAp63 caused hyperproliferation with accelerating tumorigenesis but did not cause genomic instability arguing that TAp63 is as a proto-oncogene in epithelial tissue (Keyes et al., 2006; Koster et al., 2006). By contrast, the Jacks laboratory and others argued that TAp63 is a tumor suppressor when responding to apoptosis by irradiation (Flores et al., 2005; Flores et al., 2002; Park et al., 2000; Urist et al., 2002). This opposing interpretation results from the lack of isoform specific animal model since both groups used overexpression or knock down in wild type background.

Recently, the Flores laboratory generated *TAp63* specific knock out mice and showed that *TAp63* plays roles in senescence and tumor suppression and also controls metastasis which is controlled by dicer, a microRNA processing enzyme (Su et al.; Su and Flores, 2009; Su et al., 2009b). TAp63 coordinately regulates *Dicer* and miR-130b transcription in tumorigenesis and metastasis. Down modulation of Dicer and miR-130b remarkably affected the metastatic potential of *TAp63*^{-/-} cells, suggesting that TAp63 plays a key role as a regulator of microRNAs during tumorigenesis and metastasis. This data clearly demonstrated that *TAp63* is a tumor suppressor (Su & Chakravarti et al., 2010).

1.2.2. The role of Δ Np63 isoforms

p63, unlike p53, is known for its role in the development and differentiation of epithelial surfaces (Mills et al., 1999; Yang et al., 1999). So the main role of *p63* lies in the regulation of epithelial development, particularly in the formation of the epidermis (Candi et al., 2007a), whereas its function in cancer is less clear.

$\Delta Np63$ isoforms are transcribed using an alternative promoter of the gene (exon 3') and it lacks the transactivation domain (Yang et al., 1998). Different p63 isoforms have different functional properties. $\Delta Np63$ is the predominant isoform of p63 in epithelial tissue during embryonic development and even throughout life (Candi et al., 2007b). During mouse embryogenesis, the epidermis develops from a single-layered epithelium which expresses keratin 18 (K18) (Candi et al., 2007a). Stratification starts at embryonic day E9.5 when the first stratification markers, K5 and K14, are expressed. Epidermal stratification and maturation are complete by E19.5. p63 is necessary to achieve the terminal differentiation of epidermis. p63 proteins are mainly expressed in the basal layer, the expression of $\Delta Np63$ starts from E8.5 before stratification begins (Laurikkala et al., 2006). The current data do not clearly indicate whether $\Delta Np63$ modulates the stem cell or the differentiation compartment.

The $\Delta Np63$ gene has been implicated as an oncogene (Crook et al., 2000; Senoo et al., 2001) depending on the cellular context. Elevated levels of $\Delta Np63$ correlate with tumor aggressiveness (Candi et al., 2007a; Candi et al., 2007b; Flores, 2007; Flores et al., 2005). Previously, $\Delta Np63$ isoforms were found to induce cell proliferation and result in tumor and accelerated tumor growth (Massion et al., 2003; Yamaguchi et al., 2000).

$\Delta Np63$ possesses dominant negative activity against p53, and the maintenance of cell proliferation may rely on inhibition of endogenous *p53* function (Truong and Khavari, 2007). However mechanistic roles of $\Delta Np63$ in tumorigenesis and epidermal differentiation have not been fully elucidated.

1.3. The roles of p63 in embryonic epidermal differentiation

1.3.1. Skin stratification

The skin is composed of two major compartments, the dermis and the epidermis, that form the outer-most-barrier to protect the body from pathogens and environmental insults. The epidermis forms from a single layered structure, and stratifies to multiple epithelial layers. The stratified epithelium has self-renewing capacity throughout life, and continuous turnover is mediated by epithelial stem cells that reside in the basal layer, which give rise to all epidermal cells. The epidermis forms four different layers: basal, spinous, granular and cornified layers (Marks, 2006).

p63, especially $\Delta Np63$, is highly expressed in the basal layer of the epidermis and has previously been shown to play a critical role in the development and maintenance of the epidermis (Cho et al. 2010; Koster et al., 2004). However the roles of $\Delta Np63$ have not been well determined with regard to the regulation of stem cell renewal and appropriate differentiation because of their complexity. A recent study showed that TAp63 isoforms play an important role in dermal stem cell maintenance (Su et al., 2009b). My preliminary data show that $\Delta Np63^{-/-}$ skin expresses high levels of keratin 6

(K6), a marker for impaired stratified epithelial cells (**Figure 3**). K6 expression can also be implicated in hyperproliferative conditions, such as in wound healing or conditions that interfere with normal keratinocyte function (Rothnagel et al., 1999). This is suggesting that loss of $\Delta Np63$ leads to a defect in normal stratification or differentiation. However, the roles of $\Delta Np63$ have yet to be fully explained.

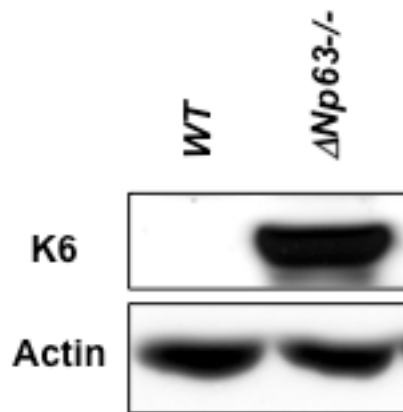


Figure 3. K6 expression is high in $\Delta Np63^{-/-}$ skin at E18.5. Western analysis was performed using protein from wild type and $\Delta Np63^{-/-}$ skin at E18.5 embryos using antibody for K6.

1.3.2. The roles of p63 in limb development

At the limb bud, limb formation begins by induction of fibroblast growth factor (FGF). FGF induces the formation of the apical ectodermal ridge (AER) and later it controls the apoptosis that is necessary to remove webbing between digits to form defined digits (Yonei-Tamura et al., 1999). During this interval of limb bud formation from embryonic day 9.5 to 12 (E9.5 to E12), expression of p63 is evident in the limb buds included in the apical ectodermal ridge (AER) at E8.5 (Koster et al., 2004; Laurikkala et al., 2006; Mills et al., 1999; Yang et al., 1999). The high levels of p63 expression in the AER suggest a potential role for *p63* in maintaining the structure or function of this specialized ectoderm (Koster et al., 2004; Mills et al., 1999; Yang et al., 1999). The AER is a region specified by expression of certain homeobox genes and T-box genes. Fore- and hind-limbs are specified by the anterior/posterior axis and secretion of the transcription factors, T-box 5 and T-box 4, respectively (Ohuchi et al., 1998; Rodriguez-Esteban et al., 1999). Limb formation results from a series of epithelial-mesenchymal transitions (EMT) between the limb bud mesenchymal cells (Hall, 2000a, b).

1.4. p63 point mutations in Human diseases

Interestingly, humans carrying dominantly inherited point mutations of *p63* in the DNA binding domain or SAM domain develop ectodermal dysplasias (**Figure 4**) (Barrow et al., 2002; McGrath et al., 2001). SAM domains are involved in protein-

protein interactions and play a role in developmental regulation. Ectodermal dysplasia in EEC syndrome (ectrodactyly-ectodermal dysplasia-cleft syndrome), which has mutations in the DNA binding domain of p63, affects the formations of skin, hair, teeth and other limb mammary development. AEC syndrome (ankyloblepharon-ectodermal dysplasia-clefting syndrome) is also one of p63 dominant mutant diseases in the SAM domain in humans that commonly has chronic inflammatory dermatitis of the scalp. The *p63* dominant mutation in humans gives rise to a phenotype that resembles that of *p63* knock out mice and these two diseases commonly have disfiguration of the limbs, cleft palate and skin dermatitis; however, the underlying mechanism remains elusive.

To determine whether this human disfiguring phenotype is p63 isoform specific will be very interesting and help understand the role of p63 in human disfiguring diseases. Recently, the Flores laboratory generated *TAp63* knock out mice that have fully developed limbs, mouth and skin (Su et al., 2009b). $\Delta Np63$ might be a very important regulator of human disfiguring diseases and generation of $\Delta Np63$ knock out mouse will provide a good animal model to study.

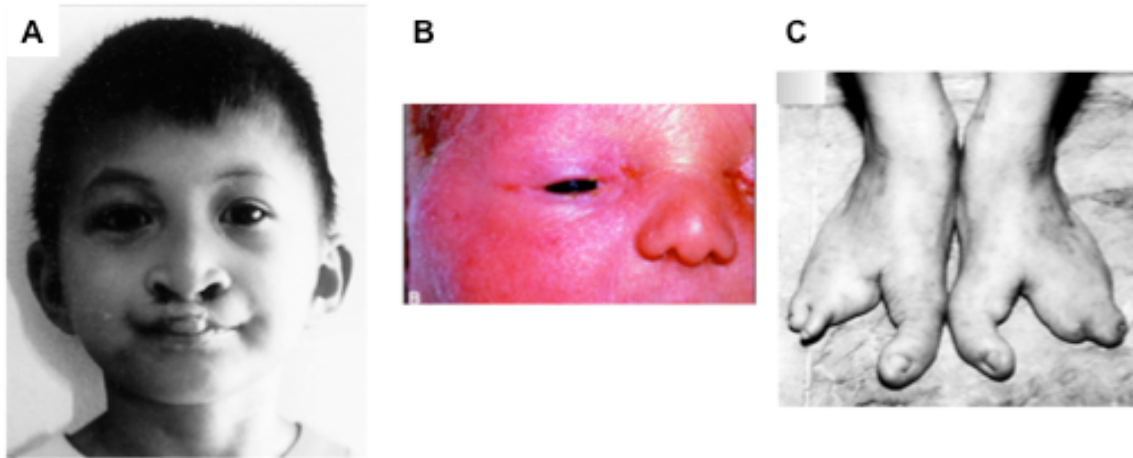


Figure 4. Phenotypic features of patients with AEC or EEC syndromes with *p63* dominant mutations

A. Bilateral cleft lip and sparse hair (shown); cleft palate and hypodontia (not shown) (McGrath et al., 2001), **B.** A newborn with partial fusion of the eyelids (ankyloblepharon) (Barrow et al., 2002) and **C.** Bilateral ectrodactyly of the feet (McGrath et al., 2001). **Reproduced and modified with permission from Barrow et al., 2002; McGrath et al., 2001 and Copyright clearance center**

1.5. Stem cell maintenance

All animals and land plants are multi-cellular organisms that have stem cells to maintain tissue homeostasis. Stem cells are defined with two characteristics; self-renewal to maintain the precise number of cells and the ability to differentiate into a diverse specialized cell types. Mammalian stem cells are classified into two broad types: embryonic stem cells and adult stem cells. Embryonic stem cells are pluripotent and differentiate to diverse cell types whereas adult stem cells (called a somatic stem cell) are thought to maintain and repair the tissue or organ.

This pluripotency is regulated by multiple transcription factors such as Oct4, Sox2, Nanog and others (Looijenga et al., 2003; Niwa, 2009; Rodda et al., 2005; Zaehres et al., 2005). In the oocyte, Oct4 is active as a maternal factor and it remains active through the embryonic stages before commitment to tissue organogenesis (Niwa, 2009). The expression of Oct4 is critical for governing pluripotency in order to keep the embryo away from differentiation in mice. Oct4 binds the octamer (ATTTGCAT) in the promoter regions of specific target genes. Oct4 and Sox2 form a heterodimer and Sox2 acts like a transcription co-factor to turn on *Nanog* expression (Grinnell and Bickenbach, 2007; Grinnell et al., 2007; Racila et al.).

The expression of Oct4 is associated with undifferentiated phenotypes, since it has been shown that it is capable of reprogramming somatic mouse keratinocytes to become more like embryonic stem (ES) cells (Grinnell and Bickenbach, 2007; Grinnell et al., 2007; Racila et al.). Nanog is associated with pluripotent phenotype. Therefore,

Nanog is also extinguished upon differentiation (Grinnell and Bickenbach, 2007; Grinnell et al., 2007).

p63 is highly expressed in the basal layer of the epidermis where epidermal stem cells reside and previously has been shown to play a critical role in epidermal development and maintenance (Mills et al., 1999; Yang et al., 1999). Specially, *TAp63* knock out mice show premature depletion of precursor cells in the dermis and epidermis (Su et al., 2009b). However the roles of Δ Np63 in epidermal stem cell compartment remain uncertain. According to previous studies, I hypothesize that Δ Np63 plays important roles in the epidermal stem cell compartment.

1.6. Asymmetric Cell division

During embryonic development, asymmetric cell divisions expand the diversity of cell types. Stem cells also divide asymmetrically to produce two distinct daughter cells. One daughter cell keeps its 'stemness' to give rise to equivalent cell fates and the other daughter cell differentiates to give rise to different cellular fates (Lambert and Nagy, 2002). Self-renewal of stem cells is an example of asymmetric division (Ulloa-Montoya et al., 2005). Asymmetric cell divisions take place not only in embryonic stem cells but also in somatic cells to contribute to aging of the organism through the human and mice life span. Stem cells are precisely controlled depending on the rate of depletion of differentiated cells. In this way the production of differentiated cell types is precisely balanced by renewal of the stem cell population (Hall, 1989; Hall and Watt, 1989).

Asymmetric cell division is an example of biological cell polarization events and plays fundamental roles in precisely regulating various progenitor cells and maintenance of fully differentiated functional cells such as epithelial cells (**Figure 5**). Basal layer cells of epidermis function as skin stem cells and asymmetric vs. symmetric divisions result from regulation of spindle orientation. Asymmetric cell divisions result in asymmetric localization of proteins, RNA transcript and other macromolecules between daughter cells. For instance, β 1-integrin or α -catenin null mice, basal epidermal cells lose their polarity resulting in misorientation of their spindles, demonstrating the importance in stem cell polarity and oriented divisions.

In *Drosophila*, asymmetric cell division was studied in neuroblast development where asymmetric divisions generate neuroblasts or glia. This event is precisely regulated by two apically localized multi-protein complexes, which are evolutionarily well conserved. In *Drosophila*, the Insc-Pins-aPKC complex is required for correct execution of the asymmetric division (Chia et al., 2001; Yu et al., 2002).

In mammalian epithelial cells, there is a homologue of Pins, LGN (named after the repetitive Leu-Gly-Asn tripeptide in the protein), which is composed of seven tetratricopeptide repeats in the N-terminal region, and in the C-terminus four GoLoco motifs (G-protein regulatory motif) for binding to $G\alpha$ that appears to control asymmetric cell-fate decision.

In contrast to mammalian Par 3 (partition defective protein 3) and Pins, little is known about mammalian homologues of Insc. The *C. elegans* Par protein complex is

highly conserved across species including mammals (Izumi et al., 1998; Joberty et al., 2000; Johansson et al., 2000; Kempfues, 2000; Kempfues et al., 1988a; Kempfues et al., 1988b); however, it is unclear whether this polarity protein complex regulates asymmetric cell division of progenitors. Although the human *Insc* gene has been described based on analyses in silico, the structure and function of the gene products remain to be elucidated.

Lechler and Fuchs describe the characterization of the mouse homolog of *Inscuteable*, *mInsc*, and find that protein complexes containing LGN, *mInsc*, and Par3 localize to the apical cortex of perpendicularly dividing basal cells of epidermis (Lechler and Fuchs, 2005). Asymmetric cell divisions play important roles in differentiation and proliferation in skin. They also show that *p63* null epidermal cells have a defect in asymmetric cell division indicating that *p63* implicates asymmetric cell divisions (Lechler and Fuchs, 2005). However specific roles of *p63* to regulate of these genes complex largely remain to be elucidated during embryonic epidermal development.

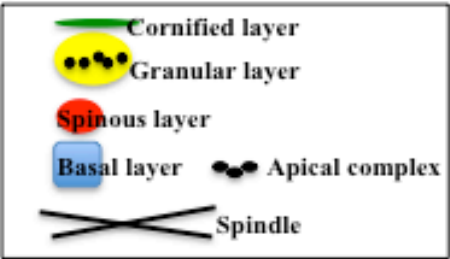
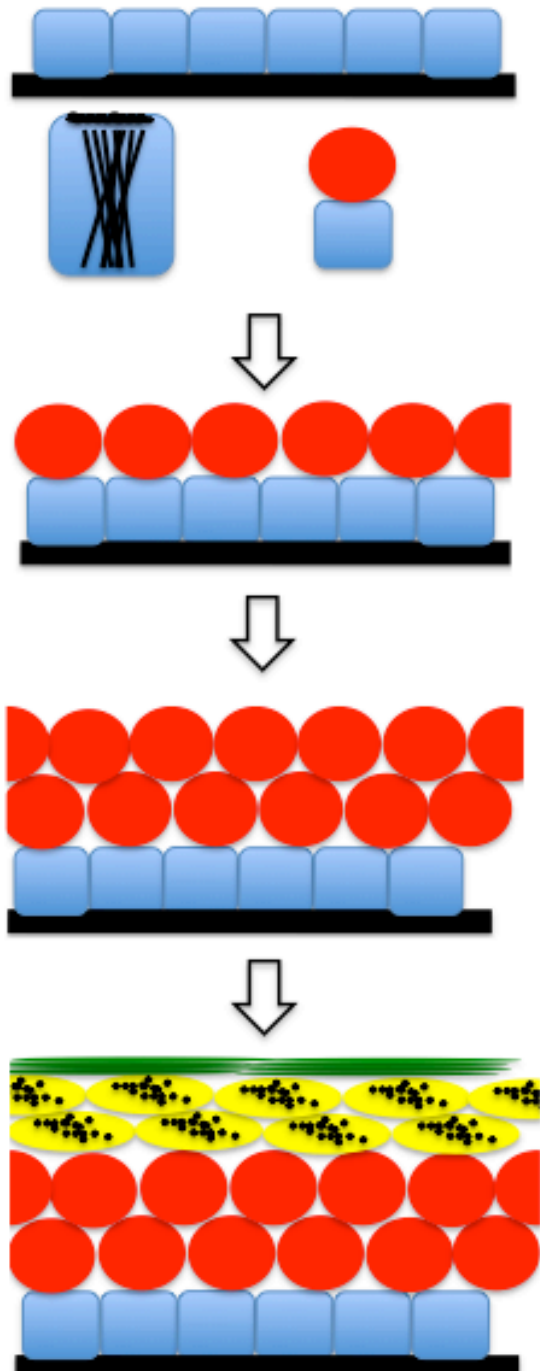


Figure 5. A schematic model of asymmetric cell division of epidermis and terminal differentiation during embryo development.

The major role of cell division in normal adult skin is to maintain the rate between production and loss of cells through injury or death, thereby maintaining cell number at an approximately constant level, which is called homeostasis (Hall, 1989; Hall and Watt, 1989). The entire epidermis is continuously replaced by new cell growth from the basal cell layer to the top of the granular cell layer by terminal differentiation: this process is called cornification (Miller et al., 2006; Candi et al., 2005). The cells of the basal layer divide in an asymmetric way: one daughter cell keeps stemness that resides on basal layer and the other daughter cell undergoes differentiations that migrate to spinous layer and keeps going to differentiation event (**Cho & Flores, unpublished**).

1.7. MicroRNA biogenesis and regulation

MicroRNA (miRNA) functions are implicated in numerous biological stages and human diseases: developmental timing, embryogenesis, programmed cell death, proliferation, stem cell differentiation, organogenesis, and angiogenesis, hematopoiesis, tumorigenesis and viral defense (Alvarez-Garcia and Miska, 2005; Lim et al., 2003). *miRNA* genes are transcribed by RNA polymerase II as long primary transcripts (pri-miRNAs) (Kim, 2005). Then pri-miRNAs are processed in the nucleus by the RNase III enzyme Drosha, acting with its double-stranded RNA binding partner protein DGCR8 (in vertebrates) or Pasha (in invertebrates), called a microprocessor. The microprocessor complex cleaves pri-miRNAs to generate small stem-loop structures called precursor miRNAs (pre-miRNAs), which are then processed further by a second RNase III enzyme (Dicer) (Sontheimer and Carthew, 2005) into mature miRNAs (**Figure 6**).

MicroRNAs (miRNAs) are on average only 22 nucleotides long and are found in all eukaryotic cells. miRNAs post-transcriptionally regulate target mRNAs by binding to complementary sequences, resulting in repression of protein expression and gene silencing. Thousands of miRNAs are encoded in the human genome and regulate more than 30% of human genes. This occurs when mature miRNAs become coupled with a multiple-protein nuclease complex called the RNA-induced silencing complex (RISC). Once incorporated into the RISC, the miRNA is situated to regulate target genes by degradation of the mRNA through direct cleavage or by inhibiting protein synthesis.

Eukaryotic organisms have well conserved miRNAs, approximately half of known microRNAs, that reside in non-protein coding RNAs (intron and exon) or within the

intron of protein coding genes. RNA polymerase II transcribes miRNA genes, generating long primary transcripts (pri-miRNAs). Subsequently, the process yields mature miRNAs through two steps involving RNase-III enzymes, Drosha and Dicer, and companion double-stranded RNA-binding domain (dsRBD) proteins (**Figure 6**).

In the nucleus, Drosha forms a complex with DGCR8, which recognizes double stranded RNA and processes the long primary miRNA, yielding premature miRNA (pre-miRNA) with a hairpin structure composed of approximately 70 nucleotides in length. The premature miRNA with hairpin structure is exported to the cytoplasm by exportin 5, where they are processed 19-25 nucleotides long miRNA duplex structures by Dicer (Yi et al., 2003); (Sontheimer and Carthew, 2005). The double stranded RNAs are incorporated into the RISC complex, which regulates protein expression. In most cases studied so far, animal miRNAs are not completely complementary to their mRNA targets. They seem to inhibit protein synthesis while retaining the stability of the mRNA target (Ambrosio et al., 2004; Lee et al., 2004). Target gene transcripts are regulated by multiple miRNAs and an individual miRNA targets numerous transcripts. DGCR8 only processes miRNAs while Dicer processes both miRNAs and endogenous siRNA.

The Flores laboratory (Su & Chakravarti et al., 2010) showed that TAp63 regulates *Dicer* during development and tumor metastasis and others showed that miRNA203 down regulates Δ Np63 in differentiated epidermal cell layers, including the spinous layer. However Δ Np63's role in microRNA biogenesis and regulation remains to be elucidated.

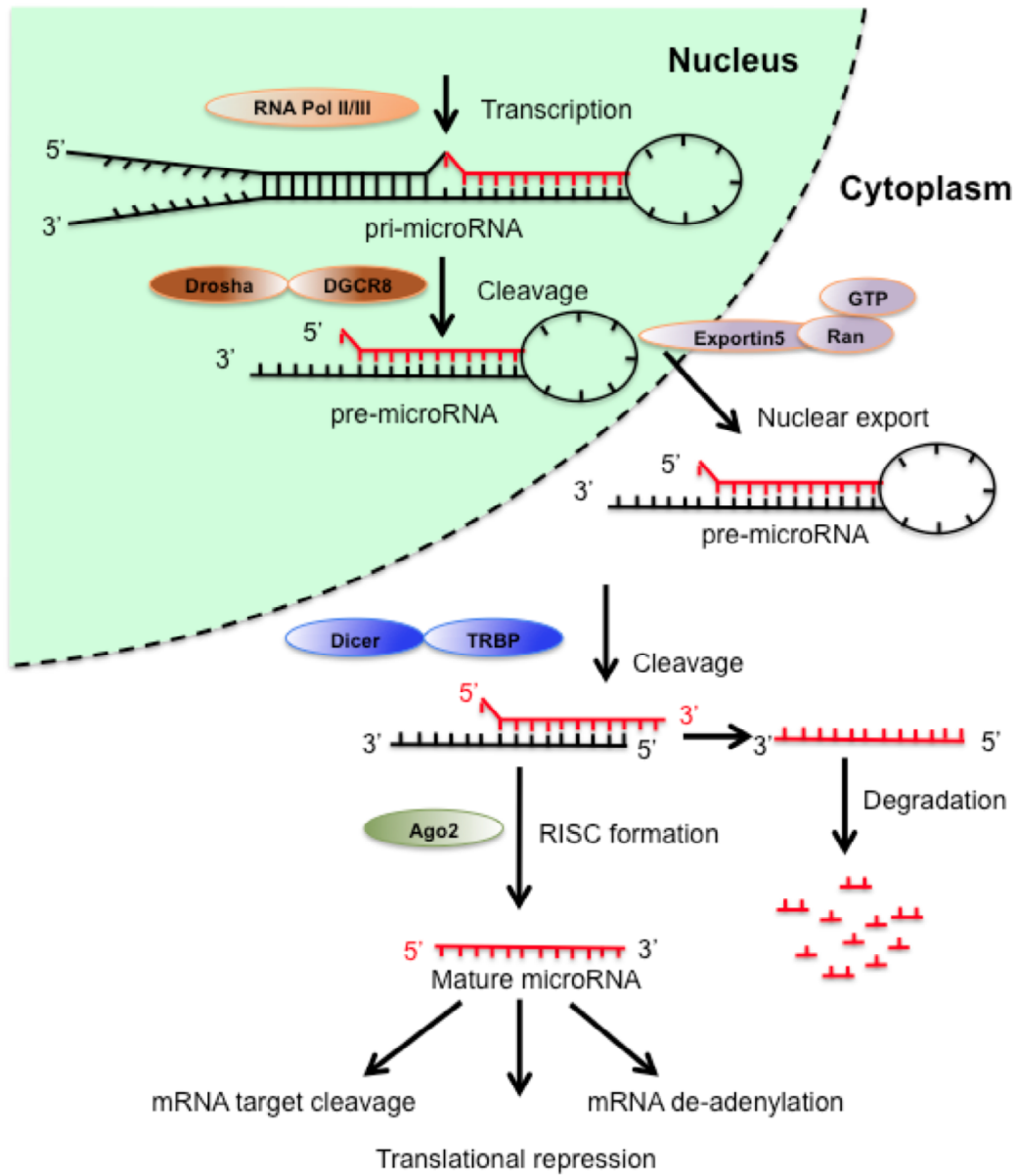


Figure 6. The Canonical pathway of microRNA (miRNA) biogenesis

The canonical microRNA maturation processing pathway has been viewed as linear and universal to vertebrate microRNAs. This maturation pathway implicates the production of the precursor microRNA from cleavage of primary microRNA by the

microprocessor complex Drosha–DGCR8 (also called Pasha) in the nucleus. The resulting precursor microRNA hairpin structure is exported from the nucleus to the cytoplasm by the Exportin-5-Ran-GTP. In the cytoplasm, the RNaseIII Dicer in complex with TRBP (the double-stranded RNA-binding protein) cleaves the precursor microRNA to a mature microRNA. The RNA-induced silencing complex (RISC), with the mature miRNA, silence target mRNAs through mRNA cleavage, translational repression or deadenylation, whereas the passenger strand (black) is degraded **(Winter et al., 2009)**
(Reproduced with a permission from copyright clearance center).

1.8. Genes that play critical roles in epidermal stem cells

1.8.1. *Ink4a-Arf*

Arf is a tumor suppressor located at the *INK4a/Arf* locus. $p16^{Ink4a}$ and $p19^{Arf}$ are encoded from the same locus and are transcribed from alternative reading frames. *Ink4a* and *Arf* mRNA are composed of three exons. Arf is regulated in response to aberrant growth signaling, apoptosis, and cell cycle arrest (Sherr and McCormick, 2002). It accumulates in the nucleolus and forms a complex with MDM2. This complex initiates p53 dependent cell cycle arrest and apoptosis. Important roles of the *Ink4a/Arf* locus, which are epigenetically silenced by polycomb complexes, have been implicated in the maintenance of hematopoietic stem cells (HSCs) and neural stem cells (NSCs) (Bracken et al., 2007; Bruggeman et al., 2005; Molofsky et al., 2005; Molofsky et al., 2003). By contrast, the overexpression of polycomb complex results in aggressive metastatic cancer. Loss of bone marrow-derived HSCs result from the *Ink4a-Arf* locus being epigenetically sequestered by polycomb complexes, such as CBX7, CBX8 and Bmi (Bracken et al., 2007; Bruggeman et al., 2005). *Bmi* knock out mice rescue the bone marrow loss of *Ink4a-Arf*-null mice (Bruggeman et al., 2005; van der Lugt et al., 1994) and likewise, this occurred in neural stem cells (NSCs), indicating *Bmi1* is essential for the self-renewal of hematopoietic and neural stem cells. These data also implicate inhibition of the *Ink4a-Arf* locus as an essential event in the process of stem cell renewal. Therefore, inhibition of *Ink4a-Arf* may also take place not only in HSCs and NSCs, but also other stem cells like those that reside in the epidermis. However putative repressors

other than *Bmi1* in other stem cell lineages have yet to be identified. p63, which is highly expressed in the basal layer of the epidermis (Fuchs, 2008; Senoo et al., 2007). We hypothesized that p63 represses *Ink4a-Arf* in epidermal stem cells.

1.8.2. *Brachyury*

Brachyury is a transcription factor within the T-box complex of genes, which in mammals is comprised of 18 T-box genes. A specific DNA element (a near palindromic sequence TCACACCT) is recognized and bound to T (*brachyury*) through a region in its N-terminus (called the T-box). *Brachyury* heterozygous mutants have shortened tails and *brachyury* homozygous mutants are lethal around embryonic day E10 due to defects in mesoderm formation, notochord differentiation and the absence of the forelimb bud. By genome nomenclature of human and mouse, *brachyury* is used as a gene symbol and the gene is called as *T* although *brachyury* is maintained as the gene description. *Brachyury* has a conserved role in the establishment of the anterior-posterior axis. It also defines the mesoderm during gastrulation. Brachyury is required for mesoderm formation and cellular differentiation and *brachyury* mutant mice exhibit a disruption in the apical ectodermal ridge (AER) morphogenesis. The AER is a thickened ridge of ectoderm that is essential for limb morphogenesis (Johnson and Tabin, 1997; Kengaku et al., 1998). In mice, brachyury is expressed in the inner cell mass of the blastocyst stage embryo (but not in the majority of mouse embryonic stem cells) in early development and its

expression is localized to the node and notochord in later development. This indicates that *brachyury* plays diverse roles with critical functions during embryonic development.

Recently, brachyury has been shown to be upregulated in a variety of tumors and tumor cell lines, including those of the small intestine, stomach, kidney, bladder, uterus, ovary, testis, lung, colon, and prostate (Palena et al., 2007), and chordoma, a rare malignant bone tumor (Vujovic et al., 2006; Yang et al., 2009). Expression of the *brachyury* gene is used as a diagnostic marker of a malignant tumor, chordoma, which arises from remaining notochordal cells accumulated in the **vertebrate**. Furthermore, duplication of brachyury in the germ line confers major susceptibility to chordoma. *Brachyury* also regulates epithelial to mesenchymal transition (EMT) and mesenchymal to epithelial transition (MET), which, in addition to being critical processes in development, are also involved in tumor metastasis (Liu et al., 2003a; Palena et al., 2007; Yang et al., 2009) that results from overexpression of brachyury (Liu et al., 2003a; Palena et al., 2007; Yang et al., 2009).

Our previous genome-wide analysis using a 15,000 cDNA microarray in the absence of *p63* mouse embryonic fibroblasts (MEFs) identified *brachyury* as a putative transcriptional target of p63 (Lin et al., 2009). *Brachyury* is an attractive target of p63 based on the *p63* mutant mouse phenotypes. During the interval of limb bud formation from embryonic day 9.5 to 12 (E9.5 to E12), p63 expression is evident in the limb buds including in the apical ectodermal ridge (AER).

1.8.3. DGCR8

Drosha and Dicer are required for microRNA processing. DGCR8 contains a double-stranded RNA (dsRNA) binding domain and is thought to recognize and bind pri-miRNA to stabilize it for processing by Drosha. DGCR8 only processes miRNAs while Dicer processes both miRNAs and endogenous siRNA (Suh et al.). *Dicer*^{-/-} and *Dgcr8*^{-/-} have shown that miRNAs have essential roles in the proliferation and differentiation of embryonic stem cells (ESC). When embryonic stem cells differentiate, they must both silence the ESC self-renewal program and activate new tissue-specific programs (Melton et al.; Suh et al.; Yi et al., 2009). In the absence of DGCR8, mouse ESCs fail to silence self-renewal. *Dgcr8*^{-/-} ESCs were unable to silence *Oct4*, *Sox2* and *Nanog* gene expression resulting in a defect in differentiation. Conditional knock out of *Dcgr8* (*K14cre-Dgcr8*^{fl/fl}: designated to *Dgcr8cko*) in animal skin showed a defect in epidermal stratification and differentiation resulting in dry skin. Hair follicle growth occurred in the opposite orientation in *Dgcr8cko* compare to wild type (**Figure 7**).

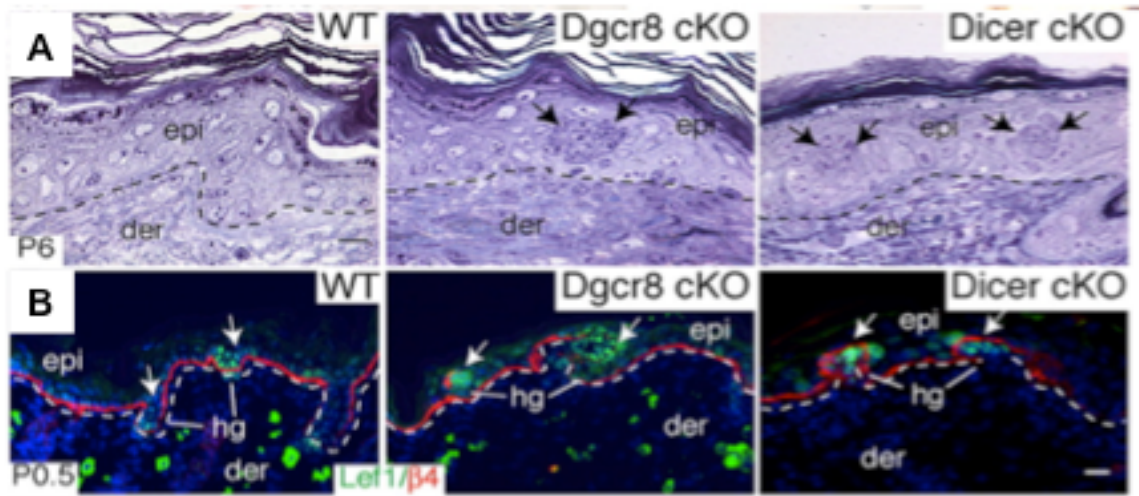


Figure 7. The Hair follicle morphology of *Dgcr8* cKO and *Dicer* cKO

A. P6 *Dgcr8* and *Dicer* cKO skins display evaginating hair germs (hg) that appear as balls of undifferentiated cells (arrows) that distort the epidermis (epi). (Scale bar, 10 μ m.) and **B.** Immunofluorescence identifies germs molecularly by transcription factor Lef1 and by hemidesmosomal β 4 integrin (nonspecific dermal staining is caused by the secondary antibody). (Scale bar, 20 μ m.). **Reproduced with permission from Yi R et al. PNAS 2009;106:498-502**

The epidermal cells from *Dgcr8*cko were hyperproliferative and showed delayed-differentiation. It was resulting from incomplete stratification and differentiation, that later, caused death by desiccation (Yi et al., 2009). This is similar to the phenotype of *ΔNp63* null mice.

According to others studies, application of stem cell activity has been used for some considerable time. However, ex-vivo grafted keratinocytes have limitations, and do not satisfy the homeostatic view of stem cell activity. Because of this limitation, understanding the developmental steps leading to the generation of epidermal stem cells that raise more hope in human embryonic stem cell research and the characterization of the key signaling pathways involved in skin morphogenesis will be beneficial for therapeutic aspects. For instance, in zebrafish studies, p63 plays roles as an inducer of epidermal development and an inhibitor of neuroectodermal formation, and later it is required for epidermal cell proliferation. To understand the roles of p63 in mammalian epidermal cell proliferation, *p63* knock out mice were generated by two groups. One group hypothesized that p63 is necessary for maintenance of stem cells (Yang et al., 1999; Senoo et al. 2007), whereas the second suggests epidermal commitment and stratification impairments (Mills et al., 1999; Koster et al. 2004, 2007a). The two hypotheses and the nature of the p63 isoform involved in these critical embryonic steps remain highly controversial (Koster et al. 2007b).

TAp63^{-/-} mice have already been generated and characterized with respect to epidermal development (Su et al., 2009). *TAp63*^{-/-} mice exhibit genomic instability,

dermal stem cell hyperproliferation, and depletion of the epidermal stem cell compartment, whereas *TAp63*^{-/-} embryonic skin has a fully developed epidermis. TAp63 transcriptionally regulates *Dicer*, which is a critical RNaseIII enzyme that processes microRNAs and endogenous siRNAs. *TAp63* is a stress response gene and its expression in the epidermis is undetectable in the absence of stress. However $\Delta Np63$ ^{-/-} mice have different phenotypes than *TAp63*^{-/-} mice in embryonic development, especially in the epidermis. $\Delta Np63$ ^{+/-} epidermis has expansion in basal layer and epidermis of $\Delta Np63$ ^{+/-} and $\Delta Np63$ ^{-/-} has an aberrant hyperproliferation. Expression of the pluripotency regulating genes, *Oct4*, *Sox2* and *Nanog* were high in $\Delta Np63$ deficient epidermal cells, even though these are supposedly somatic differentiated cells. The phenotypes of *TAp63* null mice and the difference between *TAp63*^{-/-} and $\Delta Np63$ ^{-/-} mice led me to hypothesize that TAp63 and $\Delta Np63$ function differentially in the epidermal development. My hypothesis is that $\Delta Np63$ is required for embryonic epidermal differentiation through silencing pluripotency genes.

Chapter 2.

Materials and Methods

Some parts of this chapter were modified from the following journals.

1. **Cho MS**, Chan IL and Flores ER. **Cell Cycle 9:12, 1-8; June 15, 2010** Δ Np63 transcriptionally regulates *brachyury*, a gene with diverse roles in limb development, tumorigenesis and metastasis. **Permission from Cho et al. and Copyright clearance center**

2. Su X, **Cho MS**, Gi Y, Ayanga BA, Sherr CJ, and Flores ER. **EMBO J. 2009 Jul 8;28(13):1904-15**. Rescue of key features of the p63-null epithelial phenotype by inactivation of Ink4a and Arf. **Permission from Su et al. and Copyright clearance center**

3. **Min Soon Cho**, Xiaohua Su, Deepavali Chakravarti, Arianexys Aquino, Nicole Müller, Avinashnarayan Venkatanarayan, Io Long Chan, Young Jin Gi, & Elsa R. Flores. Δ Np63 induces terminal differentiation through transcriptional regulation of DGCR8 and suppression of pluripotency factors.

Chapter 2. Materials and Methods

Generation of $\Delta Np63$ Conditional Knockout Mice

The cre-loxP strategy was used to generate the $\Delta Np63$ conditional knockout allele ($\Delta Np63fl$). Genomic *p63* DNA from intron 3 to intron 3' was amplified from a BAC clone DNA (BAC RP23-186N8, Children's Hospital Oakland Research Institute). LoxP sites flanking exon 3' of *p63* and neomycin (*neo*) gene flanked by *frt* sites inserted in intron 3' were cloned into pL253 (Liu et al., 2003). Mouse embryonic stem cells (ESCs) were analyzed by Southern blot analysis for proper targeting of the $\Delta Np63$ allele.

Chimeras resulting from ESC clones injected into C57BL/6 blastocysts were mated with C57BL/6 albino females and genotyped as described below. Mice with germ line transmission of the targeted allele (conditional, flox neo allele, *fn*) were crossed to the FLPeR mice to delete the neo cassette (Farley et al., 2000). Resulting progeny were intercrossed with *Zp3-Cre* (C57BL/6) (Lewandoski et al., 1997) transgenic mice. $\Delta Np63fl/+;Zp3-Cre$ females were mated with C57BL/6 males to generate $\Delta Np63^{+/-}$ mice. The $\Delta Np63^{+/-}$ mice were intercrossed to generate $\Delta Np63^{-/-}$ mice. All procedures were approved by the IACUC at U.T. M.D. Anderson Cancer Center.

Genotyping

Genomic DNA from tail biopsies was genotyped by Southern blot analysis by digesting genomic DNA with *Bgl*I or by PCR using the following primers and annealing

temperature: 1.) for wild-type (388bp): wt-F, 5'- ACAGTCCTCTGCTTTCAGC-3' and wt-R (fl-R), 5'- CACACAGCA CTGGCCTTGC -3', annealing temp: 62°C, 2.) for Δ Np63flox (256bp): fl-F, 5' – TTAGGTGGA TCCCTAGGAAGAG - 3' and fl-R (wt-R), 5' – CACACAGCACTGGCCTTGC - 3', annealing temp: 62°C, and 3.) for Δ Np63KO (468bp): ko-F, 5'- TACAGCTCCTGGAGGATC CCATGC-3' and wt-R, annealing temp: 62°C. Primers used to genotype the CRE gene are as follows: Cre-F, 5' –TGGGCGGCATGGTGCAAGTT - 3' and Cre-R, 5' – CGGTGCTAACCAGCGTTTTTC - 3', annealing temp: 60° C. The PCR products were electrophoresed on a 1% agarose gel.

Mouse husbandry

$p63^{+/-}$ mice on (C57BL/6_129SvJae) a background enriched for C57BL/6 (95%) (Yang et al, 1999; Flores et al, 2005) were intercrossed with $Ink4a^{-/-}$ (Sharpless et al., 2001), $Arf^{GFP/GFP}$ (Zindy et al., 2003a) or $p53^{-/-}$ (Jacks et al., 1994) mice to obtain compound mutant mice and embryos of the following genotypes: $Ink4a^{-/-};p63^{-/-}$, $Arf^{GFP/GFP};p63^{-/-}$, and $p53^{-/-};p63^{-/-}$. Wild type and $p63^{-/-}$ mice were also generated from each cross and analyzed. All procedures were approved by the IACUC at U.T. M.D. Anderson Cancer Center.

Histology and immunostaining of E18.5 embryos

Pregnant females at day E18.5 of gestation were injected with BrdU (100 mg /

gram of total body weight) 3 times of 1 hour interval (Su et al., 2009b). Embryos were extracted 1 hour later after the last injection and fixed in 10% formalin at room temperature for 18 hours. The next day fixed embryos were changed into 70% ethanol for overnight. Fixed embryos were embedded in paraffin, sectioned, and stained with hematoxylin and eosin (H&E) for microscopic analysis. For immunofluorescence (IF), paraffin-embedded sections were rehydrated in xylene and gradually decreasing concentrations of ethanol (100%~70%). Sections were subjected to antigen unmasking in citrate buffer unmasking solution (Vector Laboratory) followed by incubation with blocking solution for 1hour at room temperature, and 18 hour incubation at 4°C with the following primary antibodies: K5 (1:1000) (Abcam), K14 (1:500) (LifeSpan BioSciences), K10 (1:1000) (Covance), K15 (1:1000) (Abcam), filaggrin (1:1000) (Abcam), collagen IV (1:80) (Abcam), Lef1 (1:200) (Cell Signaling), Δ Np63 antibody (1:1000) (BioLegend) and Lhx2 (1:200) (SantaCruz). For staining with collagen IV antibody, unmasking was performed with Protease XXV (Fisher, AP-9006-002) at 37 °C for 10 min.

For immunofluorescence, visualization was performed using an anti-rabbit secondary antibody conjugated to Texas-red (1:5000) (Jackson ImmunoResearch Laboratories), an anti-guinea pig secondary antibody conjugated to FITC (1:1000, Jackson Immuno- Research), or an anti-chicken secondary antibody conjugated to Alexa 488 (1:1000) (Molecular Probes) followed by counterstaining with DAPI (Vector Laboratory) or ToPro3 (Invitrogen). Incorporation of BrdU was analyzed using the BrdU

detection kit II (Roche). For BrdU analysis by immunocytochemistry, a FITC conjugated BrdU antibody (1:200) (TEX-Gene) was used. GFP immunofluorescence was performed on frozen sections prepared from E18.5 embryos. Briefly, the epidermis was peeled from day 18.5 embryos and frozen in OCT compound (Tissue Tek). Frozen sections were fixed in 2% formaldehyde/0.2% glutaraldehyde solution for 2 min before incubation with anti-GFP (1:1000) (Invitrogen) at 4 °C overnight followed by incubation with anti-rabbit secondary antibody conjugated to Texas-red (1:2000) (Jackson ImmunoResearch Laboratories) and counterstaining with DAPI (Vector Laboratory).

For immunohistochemistry, visualization was performed using Vector VIP kit (Vector Laboratory).

Mouse embryonic fibroblasts (MEFs) and keratinocytes isolation and culture

Wild type, $p53^{-/-}$, $p63^{-/-}$, $Arf^{GFP/GFP}$, and $Arf^{GFP/GFP};p63^{-/-}$ MEFs were isolated from embryos at day 13.5 and cultured in DMEM with 10%FBS as described earlier (Flores et al, 2002). Wild type, $p63^{-/-}$, $p53^{-/-};p63^{-/-}$, $Arf^{GFP/GFP}$, $Arf^{GFP/GFP};p63^{-/-}$, $Ink4a^{-/-}$, and $Ink4a^{-/-};p63^{-/-}$, $\Delta Np63^{-/-}$ and $\Delta Np63^{fl/fl}$ keratinocytes were isolated from E18.5 embryos. Briefly, the skin was peeled off and incubated in dispase II (Roche) for 18 h at 4 °C to separate the epidermis from the dermis. Epidermal sheets were minced into small pieces and incubated in 0.25% trypsin–EDTA (Gibco-BRL) for 20min at 37 °C. Cells were plated on mitomycin treated J2-3T3 feeder cells and cultured in F media (Sigma) supplemented as described earlier (Barrandon and Green, 1987; Flores et al., 2000).

Tumor cell lines

Tumor cell lines were derived from $p53^{+/-}$ or $p53^{+/-};p63^{+/-}$ mice with tumors of the indicated types. Each cell line was re-genotyped as described previously to assay for loss of heterozygosity (LOH) of $p53$ or $p63$ (Yang et al., 1998). The six tumor cell lines used are as follows: (1) Os-1 is derived from a metastatic osteosarcoma ($p53^{-/-};p63^{+/-}$). (2) Os-2 is derived from a non-metastatic osteosarcoma (genotype $p53^{-/-}$) (3) Os-3 is derived from a metastatic osteosarcoma (genotype $p53^{+/-};p63^{-/-}$), (4) RS is derived from a rhabdomyosarcoma (genotype $p53^{+/-}$), (5) MAd is derived from a mammary adenocarcinoma (genotype $p53^{+/-};p63^{-/-}$), and (6) LAd is derived from a lung adenocarcinoma (genotype $p53^{+/-};p63^{-/-}$).

Chromatin immunoprecipitation (ChIP)

Wild type and $\Delta Np63^{-/-}$ keratinocytes were grown to near confluence on J2-3T3 feeder cells in F media as described previously (Su et al., 2009b). Feeder cells were removed with 0.02% EDTA 24 hours prior to collecting keratinocytes for chromatin extraction. Cellular proteins were crosslinked to DNA using 1% formaldehyde and chromatin was prepared as described earlier (Flores et al., 2002). ChIP analysis was performed using a pan-p63 antibody (4A4, Abcam) and p53 antibody (FL-393) (Santa Cruz) as described previously (Flores et al., 2002; Su et al., 2009a). Each ChIP was performed in triplicate using keratinocytes from three embryos of each genotype. q-RT PCR was performed by using primers specific for the indicated regions of the DGCR8

promoter: Site1 -3393 - forward 5'-AGTCACCTTGGTGCC TCTCATAG-3' and -3348
 -reverse 5'-AAACAGGTGGCAAGGCTTCTT-3', Site2 -1459 - forward 5'-
 CTTTTTTTTCTGTGGATCTTTTGGT-3' and -1397 - reverse 5'-CACAGGGCAGGC
 AGATCAG-3', and nonspecific site -3893 - forward 5'-
 CAAATCAAATCTGCATCCATAGG -3' and -3833 - reverse 5'-
 GCCCTCCTGCCTGTAAACCT-3' and LGN promoter: site1F 5'-
 TGAAGGCATGAATAGAATGGGAAT-3', site1R 5'-
 GGAAAAGCAGAGATGGCGAAT-3', site2F 5'-TCCCACCTTTTCGCCATCTG-3',
 site2R 5'-TCCTCCGCCAACTAGAAGCTT-3', site3F 5'-
 GCCCTGGTTGTCCTGGATCT-3' and site3R 5'-
 CAAGTGGGTCTCTGTGTGTTTGA-3'.

Mouse embryo fibroblasts (MEFs) were grown to near confluence in 15 cm
 dishes. Cells were cross-linked with 1% formaldehyde for 10 min at 37°C in DMEM.
 The chromatin was prepared as described previously and diluted 10-fold in ChIP dilution
 buffer and incubated overnight at 4°C with 2 µg of p53 (FL-393) (Santa Cruz), p63
 (4A4) (Santa Cruz), or p73 antibody (IMG-246) (Imgenex) or 2 µg immunoglobulin G
 (IgG). Immunoprecipitated DNA was purified and PCR was performed using the
 primers flanking the identified p53/p63 consensus binding site, forward primer (5'-
 AGTCTGATATGGCCGCGCAC-3') and reverse primer (5'-AAAGATTACACCTGG
 GTCCCTG-3'), and 58°C as the annealing temperature to generate a 279 bp amplicon.

Western blot analysis

Total cell lysates were generated from keratinocytes or skin from 18.5day embryos. 50 µg total protein was electrophoresed on a 10% SDS PAGE and transferred to PVDF membrane as described previously. Blots were probed with anti ΔNp63 (1:2000) (BioLegend), K5 (1:1000) (Abcam), K10 (1:1000) (Covance), filaggrin (1:1000) (Abcam), DGCR8 (1:200) (Abcam), p19Arf (5C3-1) (Bertwistle et al., 2004), GFP (1:1000) (Invitrogen) or p16Ink4a (1:200) (Santa Cruz) at 4°C for 18 hours followed by incubation for 1 hour at room temperature with goat anti-mouse or goat anti-rabbit secondary antibodies conjugated to horseradish peroxidase (1:5000) (Jackson Lab). Actin (Sigma 1:5000) was used as a loading control. Detection was performed using the ECL Plus Kit (Amersham) following the manufacturer's protocol and x-ray autoradiography.

Total cell lysates were generated from tumor cell lines (Os-1 and Os-2) 24 hours after transfection, or MEFs. 20 µg were electrophoresed on a 10% SDS PAGE and transferred to PVDF membrane as described previously. Blots were probed with anti-p63 (4A4) (1:500) (Santa Cruz) at 4°C overnight followed by incubation for one hour at room temperature with goat anti-mouse secondary antibodies conjugated to horseradish peroxidase (1:5,000) (Jackson Lab). Anti-actin (Sigma 1:5,000) was used as a loading control. Detection was performed using the ECL Plus Kit (Amersham) following the manufacturer's protocol and x-ray autoradiography.

RNA extraction and quantitative real-time PCR (q-RT PCR)

RNA was prepared from the dermis/epidermis peeled from wild type, *p63*^{-/-}, *Arf*^{GFP/GFP}, *Arf*^{GFP/GFP};*p63*^{-/-}, Δ *Np63*^{-/-} or *TAp63*^{-/-} 18.5 day embryos and wild type, *p63*^{-/-} or *TAp63*^{-/-} 9.5 day embryos using an RNeasy plus kit (Qiagen Ltd.). cDNA was synthesized from 2 ug of total RNA using TriZol (Invitrogen) according to the manufacturer's protocol. The RNA levels of *Ink4a*, *Arf*, and *GFP* encoded by the cellular *Arf* promoter were determined by q-RT PCR and performed in triplicate using an ABI 7900 machine. The following primers were used for performing real-time PCR: *Ink4a*, *p19Arf* (Bruggeman et al., 2005), and *GFP* sense 5'-GTCCGCCCTGAGCAAAGA-3', *GFP* antisense 5'-TCCAGCAGGACCATGTGATC-3'. Primers for *GAPDH* were used as an internal control. The primers for *mOct4*, *mSox2*, *mNanog* (Taube et al.), *mDGCR8* (Han et al., 2009), *mNestin* (Pattyn et al., 2003), and *mNeuN* (Hu et al.) were used as described previously. *Brachyury* mRNA, sense 5'-CGGTGCTGAAGGTAAATGTG-3', and antisense 5'-GTTGTCAGCCGTCACGAG T-3' were designed by Cho (Cho et al., 2010). Primers for Δ *Np63*, *TAp63* and *GAPDH* were used as described previously (Su et al., 2009b).

Cloning of *brachyury-luciferase* reporter constructs.

The *brachyury* promoter was amplified from BAC clones, RP24-530D23 and RP23-376B1 (Children's Hospital Oakland Research Institute), and cloned into the pGL3 basic luciferase reporter vector (Promega). To generate the Brach1 luciferase

construct, primers were designed containing the p63 binding site shown by ChIP and 5' XhoI and 3' BglIII cloning restriction enzyme sites: forward primer (5'-CCGCTCGAGTGCGAGGCCACCTCGGCT-3') and reverse primer (5'-GGAAGATCTCAAAGGAGCACCGAGATCGGG-3'). The primers to generate the Brach2 luciferase construct were designed to encompass the identified p63 binding site, exon 1 and intron 1 of *brachyury* and 5' XhoI and 3' BglIII cloning restriction enzyme sites: forward primer (5'-CCGCTCGAGTGCGAGGCCACCTCGGCT-3') and reverse primer (5'-GGAAGA TCTAAGACAGCGCACGGCAGGA-3'). PCR amplicons were digested with XhoI and BglIII and ligated into pGL3 basic (Promega). The QuickChange® Multi Site-Directed Mutagenesis kit was used to generate Brach1m using the Brach1 luciferase construct as a template and the following primers: forward 5'-

CATTTTCTCTTCCCCAGAGACTTACTTTTTTCGCGCTTTTCGGGAGTTCAAGT
 G-3' and reverse 5'-
 CACTTGAACTCCCGAAAAGCGCGAAAAAAGTAAGTCTCTGGGGAAGAGAAA
 AATG-3'.

To generate the *Dgcr8* S luciferase construct, DNA was amplified from wild type mouse genomic DNA (C57BL/6) using primers containing the p63 binding site shown by ChIP and 5' XhoI and 3' BglIII cloning restriction enzyme sites: (*DGCR8- Luc* F: XhoI 5'-CCGCTCGAGGCTTCTAGTTGTCTATTCC-3', *DGCR8- Luc* R: BglIII 5'-GGA AGATCTGCTCACCAGATAGCTTGGA -3') PCR amplicons were digested with

XhoI and BglII and ligated into pGL3 basic luciferase reporter vector (Promega). The QuickChange® Multi Site-Directed Mutagenesis kit was used to generate *dgcr8 Sm-luc* using the *dgcr8 S luciferase* construct as a template and the following primers: 1 forward 5'-ATGCCTGTCTAAAGTCACTTTTGTGCCTCTCATAGGCCTG-3', 2 forward 5'-GCATGTATCTCCTAAGAAGCTTTTCCACCTGTTTACAACACCAG-3', 3 forward 5'-TGGTGCCTCTCATAGGCCTGTTTTTATCTCCTAAGAAGCCTTGC-3'.

Dual-luciferase reporter assay

Luciferase reporter assays were performed as described previously. *p53^{-/-};p63^{-/-}* MEFs were plated on 6-well plates (3.5×10^5 cells per well). Twelve hours after plating, the MEFs were transiently transfected using Fugene HD (Roche) with 1 µg of Brach1, Brach2, Brach1m, dgcr8S or dgcr8 Sm, 0.5 µg of Renilla luciferase plasmid (transfection control), and 0.5 µg plasmids encoding the p63 isoforms [TAp63α, TAp63β, TAp63γ, ΔNp63α, ΔNp63β or ΔNp63γ or 0.5 µg of empty vector (pcDNA3)]. After 24 hr, cells were harvested, lysed with manufacturer's protocol and luciferase activity was measured using the Dual-Luciferase Reporter Assay system (Promega) and a Veritas microplate luminometer (Turner BioSystems). Each experiment was performed in triplicate.

Keratinocytes proliferation assays

Keratinocytes, wild type, *p63^{-/-}*, *Ink4a^{-/-}*, *Arf^{GFP/GFP}*, *Ink4a^{-/-};p63^{-/-}*, *Arf^{GFP/GFP};p63^{-/-}* and *p63^{-/-};p53^{-/-}* of 1×10^4 were plated in triplicate on mitomycin

treated J2-3T3 feeder cells. Keratinocytes were counted every day for 8 days. Keratinocytes were also subjected to serial passages at 5-day intervals. After isolation, 1×10^4 keratinocytes were plated in triplicate, passaged, and the cumulative number of population doublings was calculated.

After adeno-Cre virus infection for 24 hours, passage-0 keratinocytes, wild type and $\Delta Np63\Delta/\Delta$, were plated at a density of 4×10^5 in 10cm dish on J2-3T3 feeder cells. Keratinocytes were trypsinized and counted at 5 and 10 days.

Proliferation assay (Tumor cell lines)

Os-1 and Os-2 tumor cell lines were plated at a density of 1×10^5 cells in a 6-well dish and transfected with *p63*-siRNA. Forty-eight hours after transfection, tumor cells in 6-well dishes were treated with 10 mM BrdU for 15 hours as described previously.¹⁶ Cells were fixed with 70% ethanol and immunostained using anti-BrdU-FITC (1:200) (GeneTex). DAPI was used as a counterstaining. The percentage of BrdU positive cells were calculated by counting the number of BrdU positive cells and dividing by the total number of cells with and without BrdU positivity in each well. Each experiment was performed in triplicate.

Keratinocyte differentiation and neuronal cell differentiation assay

Passage-0 $\Delta Np63^{fl/fl}$ keratinocytes were plated at a density of 1×10^6 in 10cm dish on J2-3T3 feeder cells. When confluency of the cells reached 80%, keratinocytes

were infected with adenovirus-Cre-GFP (5000 particles per cell) to recombine $\Delta Np63$ allele ($\Delta Np63\Delta/\Delta$) and adenovirus-GFP (Vector Development Lab, Baylor College of Medicine) was used as a control. After 24 hours, keratinocytes were trypsinized. Passage-1 keratinocytes were plated at a density of 1×10^6 in 10cm dish on J2-3T3 feeder cells in F media supplemented with high calcium at a final concentration of (1.6mM) and refed every day for 3days. Differentiation was assessed using western blot analysis using antibodies against K5, K10 and filaggrin as described above. To test rescue differentiation defects in keratinocytes, 2 μ g of flag-DGCR8 was transfected into 4×10^5 in 6 well dish $\Delta Np63\Delta/\Delta$ for 24hours and cultured in F media supplemented with high calcium condition (1.6mM) and refed with high calcium F-media every day for 3days. For neuronal cell differentiation test, $\Delta Np63\Delta/\Delta$ epidermal cells with or without flag- DGCR8 transfection were cultured in neuroectodermal media as described in 2007 paper. Neuronal cell differentiation was assessed using q-RT PCR for *mNestin* and *mNeuN* as described above.

miRNA TaqMan assay

Applied Biosystems TaqMan miRNA assays were employed to detect and quantify mature miRNAs using looped-primer real time PCR for *miR145*, *miR 470.*, *miR295*, *miR 302a* and *miR130b*. Total RNAs were prepared from keratinocytes by TRIzol LS Reagent (Invitrogen). Two-step TaqMan MicroRNA Assay kit was used as described previously (Su and Chakravarti et al., 2010)

Clonogenic assay, rhodamine B and BrdU staining

4×10^5 $\Delta Np63\Delta/\Delta$ epidermal cells were plated on mitomycin c (Roche)-treated J2-3T3 feeder cells in F media as described (Barrandon and Green, 1987; Flores et al., 2000; Su et al., 2009b). Keratinocytes cultured for 7 days were trypsinized and some dishes were fixed in 10% formalin for 30min, and stained with 2% rhodamine B (Sigma). Some dishes were treated with 10 mM BrdU for 15 hr prior to harvesting. The BrdU treated cells were fixed in 70% ethanol for 30min and then denatured by 0.01N NaOH. Cells were double stained with anti-cytokeratin 5 (Abcam) (1:1000) and anti-BrdU-FITC conjugated antibody (GeneTex, Inc.) (1:200). Secondary antibody used is anti-rabbit-Texas Red-conjugated (Jackson ImmunoResearch) (1:500).

Murine p63 siRNAs assay.

A murine p63 siRNA was designed spanning amino acids 134–141 of p63 (5'-AAGAGACCGGAAGGCAGATGA-3') as described previously (Cho et al.; Iwakuma et al., 2005). Non-targeting scrambled siRNA #1 (Dharmacon) was used as a negative control. 100 nM of p63-siRNA (Dharmacon) was transfected into tumor cell lines using Fugene HD (Roche) following the manufacturer's protocol.

Adenovirus-Cre infection

1×10^6 $\Delta Np63^{fl/fl}$ keratinocytes were plated on J2-3T3 feeder in 10cm dish and infected with 5×10^3 Ad-Cre-GFP (Vector Development Lab, Baylor College of

Medicine) particles per cell. The efficiency of infection was calculated by GFP expression and rate was about 99%. Western analysis was performed for Δ Np63 to verify recombination.

Retroviral infection (pSuper mouse DGCR8-1)

1 X 10⁶ wild-type keratinocytes were plated on J2-3T3 feeder in 10cm dish and infected with pSuper mouse DGCR8-1 (Addgene) as described previously (Su and Chakravarti et al., 2010).

Boyden chamber assays for cell migration and invasion.

Twenty-four hours after transfection, Os-1 and Os-2 cell lines transiently expressing p63-siRNA were plated at a density of 2.5 x 10⁴ on a membrane or matrigel (BD Biosciences). Migrated or invaded cells were visualized using Diff-Quik stain (Sigma).

Skeleton preparation and staining

Embryos were collected at E18.5. Skin and internal organs were discarded, and the remaining embryo was fixed overnight in 95% ethanol at room temperature. The following day, the cartilage was stained in 0.05% alcian blue (Sigma) in 95% ethanol in acetic acid for 6 hours and then destained in 1% KOH overnight. Bone staining was performed in 0.015% alizarin red (Sigma) in 1% KOH. The embryonic skeleton was

washed in 20% glycerol in 1% KOH and changed twice per day until the solution was clear.

Statistics.

Data are represented as mean \pm SEM. Data were analyzed using a Student's t test. A p value of 0.05 was considered significant. All experiments were done at least in triplicate.

Graph.

All graphs were plotted with PRISM5 software (GraphPad).

Chapter 3.

New targets of p63 in epithelial development, limb development and metastasis

Some parts of this chapter were modified from the following journals.

1. **Cho MS**, Chan IL and Flores ER. **Cell Cycle 9:12, 1-8; June 15, 2010** Δ Np63 transcriptionally regulates *brachyury*, a gene with diverse roles in limb development, tumorigenesis and metastasis. **Reproduced with permission from Cho et al., and Copyright clearance center.**
2. Su X, **Cho MS**, Gi Y, Ayanga BA, Sherr CJ, and Flores ER. **EMBO J. 2009 Jul 8;28(13):1904-15.** Rescue of key features of the p63-null epithelial phenotype by inactivation of Ink4a and Arf. **Reproduced with permission from Su et al., and Copyright clearance center.**

3.1. The role of p63 as a transcriptional repressor of *Arf/Ink4a*

Rationale: Deletion of *p63* in the mouse results in a generalized loss of stratified epithelium due to defects in the maintenance of stem cell proliferative capacity, differentiation, and cell-cell adherence (Mills et al., 1999; Senoo et al., 2007; Yang et al., 1999). We therefore interbred *p63*^{+/-} mice with animals lacking either *Ink4a* or *Arf* (since inhibition of *Ink4a-Arf* locus is essential for the process of stem cell renewal in hematopoietic stem cell) to generate mice lacking both *Ink4a* and *p63* or *Arf* and *p63*.

Hypothesis: The formation of stratified epithelium is restored in the compound mutant, *Arf*^{GFP/GFP};*p63*^{-/-} and *Ink4a*^{-/-};*p63*^{-/-} mice by rescuing of the proliferative capacity of epidermal stem cells and differentiation.

3.1.1. The phenotypic features of *p63*^{-/-} mice are partially rescued by loss of *Arf* or *Ink4a*.

The *p63*^{-/-} mice have striking defects in the epidermis, cleft lip and palate, and craniofacial abnormalities during embryonic development (Mills et al., 1999; Yang et al., 1999). Due to defects in the incomplete stratified epidermis and ectodermal malformation that result in desiccation of the newborn and maternal neglect, *p63*^{-/-} mice die after birth. Others studies suggested that these phenotypes of *p63*^{-/-} mice were because of defects in stem cell proliferative maintenance or incomplete differentiation

and cell-cell adhesion (Mills et al., 1999; Yang et al., 1999; Zindy et al., 2003a). However there is not yet a clear mechanism, which would explain the defects observed in $p63^{-/-}$ developing mice. Recently, repression of both *Arf* and *Ink4a* has been implicated in stem cell renewal and proliferation (Bracken et al., 2007; Bruggeman et al., 2005; Molofsky et al., 2005; Molofsky et al., 2003). *Arf* and *Ink4a* are known to be tumor suppressors. To tease out whether incomplete stratified epidermis results from the role of p63 in stem cell renewal, *Arf* and/or *Ink4a* mutant mice were generated in $p63^{-/-}$ background. The hypothesis is that loss of *Arf* and/or *Ink4a* lead to rescue of the $p63^{-/-}$ phenotype observed in the incomplete stratified epidermis of the mouse. To test this hypothesis, $p63^{+/-}$ mice (Yang et al., 1999) were intercrossed with the $Arf^{GFP/GFP}$ (Zindy et al., 2003a) and $Ink4a^{-/-}$ (Sharpless et al., 2001) mice to first obtain double heterozygous mice ($Arf^{GFP/+};p63^{+/-}$ and $Ink4a^{+/-};p63^{+/-}$). In order to restore stem cell renewal potential in the $p63^{-/-}$ mice, sequential matings by intercrossing $Arf^{GFP/+};p63^{+/-}$ and $Ink4a^{+/-};p63^{+/-}$ mice gave rise to $Arf^{GFP/GFP};p63^{-/-}$ and $p16^{Ink4a^{-/-}};p63^{-/-}$ mice respectively. Pups were born at a Mendelian ratio and $Arf^{GFP/GFP};p63^{-/-}$ and $Ink4a^{-/-};p63^{-/-}$ mice were viable as neonates, however they also died hours after birth as seen in $p63^{-/-}$ mice. By macroscopic examination of 10 neonates of each genotype, it was found that they were born with skin covering more than 80% of the body, but 10-20% of embryos retained craniofacial and limb defects. They died due to maternal neglect within hours after birth. Intriguingly, both double mutant, $Arf^{GFP/GFP};p63^{-/-}$ and $Ink4a^{-/-};p63^{-/-}$, embryos at embryonic day E18.5 and newborn mice had a thin single layer of skin

covering 85-95% of the body by microscopic examination (**Table 1**). 20 embryos of each $Arf^{GFP/GFP};p63^{-/-}$ and $Ink4a^{-/-};p63^{-/-}$ were analyzed at E18.5. These embryos had dull and opaque skin with partially patched stratified epithelium (**Figure 8C & D**), compared to the shiny and translucent appearance of the $p63^{-/-}$ embryos devoid of such epithelium (**Figure 8B**). Interestingly, both double mutant embryos exhibited elementary limbs and a long tail (**Figure 8C & D**). Strikingly, 18 of 20 $Arf^{GFP/GFP};p63^{-/-}$ and 16 of 20 $Ink4a^{-/-};p63^{-/-}$ had retained the appearance of normal facial features and fully developed ears (**Figure 8C & D**) (**Table 1**).

3.1.2. Loss of *Arf* or *Ink4a* partially rescues the limb defect of the $p63^{-/-}$ mice.

There is incomplete limb development in $p63^{-/-}$ mice and because 18 out of 20 $Arf^{GFP/GFP};p63^{-/-}$ and 16 out of 20 $Ink4a^{-/-};p63^{-/-}$ embryos had the appearance of primitive limbs, a careful analysis of the skeletal structure was performed (**Figure 8E-P**) using cartilage/bone staining method. The forelimbs of $Arf^{GFP/GFP};p63^{-/-}$ and $Ink4a^{-/-};p63^{-/-}$ embryos were well developed with scapula, humerus and ulna that were most cases similar in size to wild-type embryos (**Figure 8I-L**) (**Table 2**). In addition, in both $Arf^{GFP/GFP};p63^{-/-}$ and $Ink4a^{-/-};p63^{-/-}$ embryos (**Figure 8K & L**) immature digits were observed whereas the forelimbs were significantly smaller in the $p63^{-/-}$ embryos (**Figure 8J**) (**Table 2**). As in the $Arf^{GFP/GFP};p63^{-/-}$ and $Ink4a^{-/-};p63^{-/-}$ embryos, the pubic bone is similar in size to wild-type and fused but still does not completely develop hind limbs. The $p63^{-/-}$ embryos do not have well developed hind limbs: (compare **Figure 8O & P** to

Figure 8M) (Table 2). Additionally this fusion does not occur in the $p63^{-/-}$ mice (Figure 8N). Limb development will be discussed in chapter 3.2 and chapter 5.1 sections in more detail.

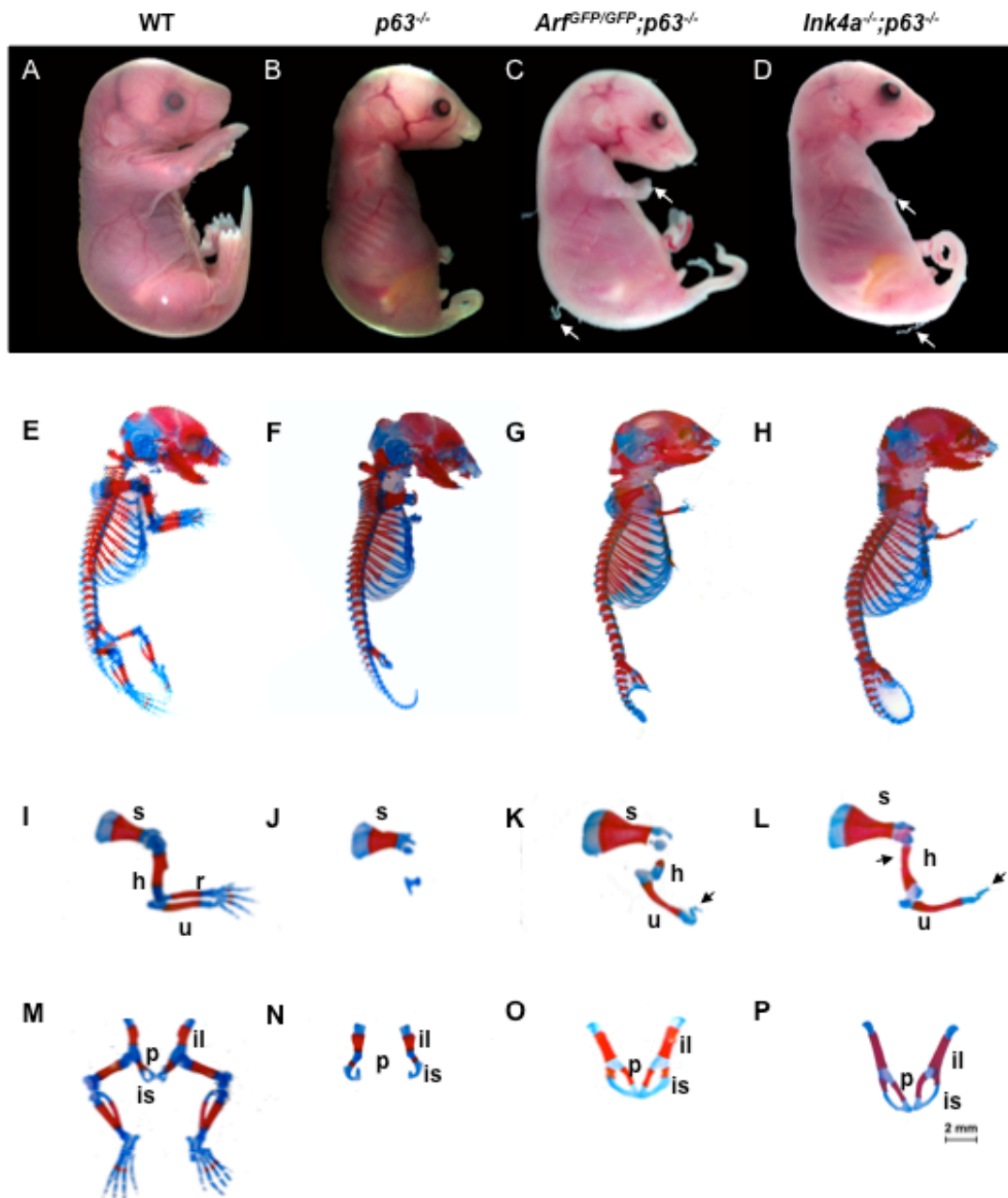


Figure 8. Macroscopic analysis of embryos at day E18.5. (A–D) Representative images of embryos with their respective genotypes indicated above each panel; WT indicates wild type. The white arrow in (B) points to cleft lip and palate in $p63^{-/-}$ embryo. White arrows in (C, D) designate strings of desquamated epithelium and forelimbs. (E–P) Show skeletal preparations from E18.5 embryos stained with Alcian Blue for cartilage and alizarin red for bone. Whole embryos (E–H) were of the following genotypes: (E), wild type; (F), $p63^{-/-}$; (G), $Arf^{GFP/GFP};p63^{-/-}$; and (H), $Ink4a^{-/-};p63^{-/-}$. Analysis of forelimbs (I–L) from (I), wild type; (J), $p63^{-/-}$; (K), $Arf^{GFP/GFP};p63^{-/-}$; and (L), $Ink4a^{-/-};p63^{-/-}$ embryos. The arrowheads in (K) and (L) point to rudimentary digits. Designated bones include the scapula (s), humerus (h), radius (r), and ulna (u). (M–P) Analysis of pubic bones and hind limbs from (M), wild type; (N), $p63^{-/-}$; (O), $Arf^{GFP/GFP};p63^{-/-}$; and (P), $Ink4a^{-/-};p63^{-/-}$ embryos. Designated bones include the ilium (il), ischium (is), and pubic bone (p). A 2 mm scale bar is included in the corner of (P).

Reproduced with permission from Su et al., EMBO J. 2009 July 8; 28(13): 1904-1915 and Copyright clearance center.

3.1.3. Loss of *Arf* or *Ink4a* restores the formation of stratified layers of skin in *p63*^{-/-} mice.

Macroscopic examination of double mutant embryos showed that they retained the appearance of epidermis unlike *p63*^{-/-} mice skin. We, thus, hypothesized that loss of *Arf* or *Ink4a* rescues the epidermal defect observed in the *p63*^{-/-} embryos. To test the extent of epithelial rescue that occurs in double mutant embryos, microscopic analyses for epidermal structure and epidermal markers were performed by hematoxylin and eosin (H&E) staining and immunofluorescence (IF) for keratin 5 (K5) for basal layer markers, keratin 15 (K15) for a hair follicle marker, keratin 10 (K10) for a spinous layer marker and filaggrin (Fila) for a granular layer marker (**Figure 9; Table 1**). The H&E-stained sections of embryonic day E18.5 *Arf*^{GFP/GFP};*p63*^{-/-} embryos revealed a well-layered basal layer of epithelium surrounding the embryo (**Figure 9C**). Twenty *Arf*^{GFP/GFP};*p63*^{-/-} embryos had an average coverage of 85% by H&E staining. The extent of rescue in the 20 *Ink4a*^{-/-};*p63*^{-/-} embryos examined was even more striking with the appearance of structures that resembled hair follicles (**Figure 9D; Table 1**). 10±2 hair follicles per centimeter were apparent in all 20 of the *Ink4a*^{-/-};*p63*^{-/-} embryos compared to 64±4/cm in the wild-type and 0/cm in the *Arf*^{GFP/GFP};*p63*^{-/-} and *p63*^{-/-} mice (**Table 1**). To further analyze the structure of the epithelium in order to determine whether there is a rescue in *Ink4a*^{-/-};*p63*^{-/-} and *Arf*^{GFP/GFP};*p63*^{-/-} embryos, IF was performed using K5 and K14, markers of the basal layer, K10, a marker of the spinous layer, and Fila, a marker of the granular layer of the epithelium. To determine whether the cell adhesion defect is

rescued in *Ink4a*^{-/-}; *p63*^{-/-} and *Arf*^{GFP/GFP}; *p63*^{-/-} embryos, IF was also performed using antibodies: collagen IV for the basement membrane and E-cadherin for cell adhesion. These epidermal layer markers were completely absent or stained feebly in the *p63*^{-/-} embryos (Mills et al., 1999; Yang et al., 1999). Consistent with previously published data (Mills et al., 1999; Yang et al., 1999), 3 of the 20 *p63*^{-/-} embryos had an average of 2% K5 positive cells in patches on the area above the dermis (**Figure 9F; Table 1**). K5 staining in the *Arf*^{GFP/GFP}; *p63*^{-/-} and *Ink4a*^{-/-}; *p63*^{-/-} mice stained encircle the embryos (**Figure 9G & H; Table 1**) indicating the presence of a stratified multilayer basale. More remarkably, K10 staining was apparent and stained around the embryos (**Figure 9K & L; Table 1**). Strikingly, in the *Ink4a*^{-/-}; *p63*^{-/-}, the appearance of a multilayer stratified epithelium, which stained positive for K5, K10 and Fila (**Figure 9G, H, K, L, O & P**), was more apparent and evidence of hair follicle-like structures staining positively for K15 was also visible (**Figure 9**) (Liu et al., 2003b) . K15 staining indicated the presence of epidermal precursor cells in double mutant embryos (**Figure 9S & T**).

We also determined whether loss of *p53* rescued the *p63*^{-/-} phenotype. We analyzed twenty *p53*^{-/-}; *p63*^{-/-} embryos at embryonic day E18.5. Seventy percent (14 of 20) of *p53*^{-/-}; *p63*^{-/-} embryos died *in utero* at embryonic day E15.5 (Sah et al, 1995). However viable embryos at embryonic day E18.5 had a similar phenotype as *p63*^{-/-} embryos (**Table 1**) indicating that the rescue of the *p63*-null phenotype by loss of the *Ink4a-Arf* locus is independent of the p53 pathway.

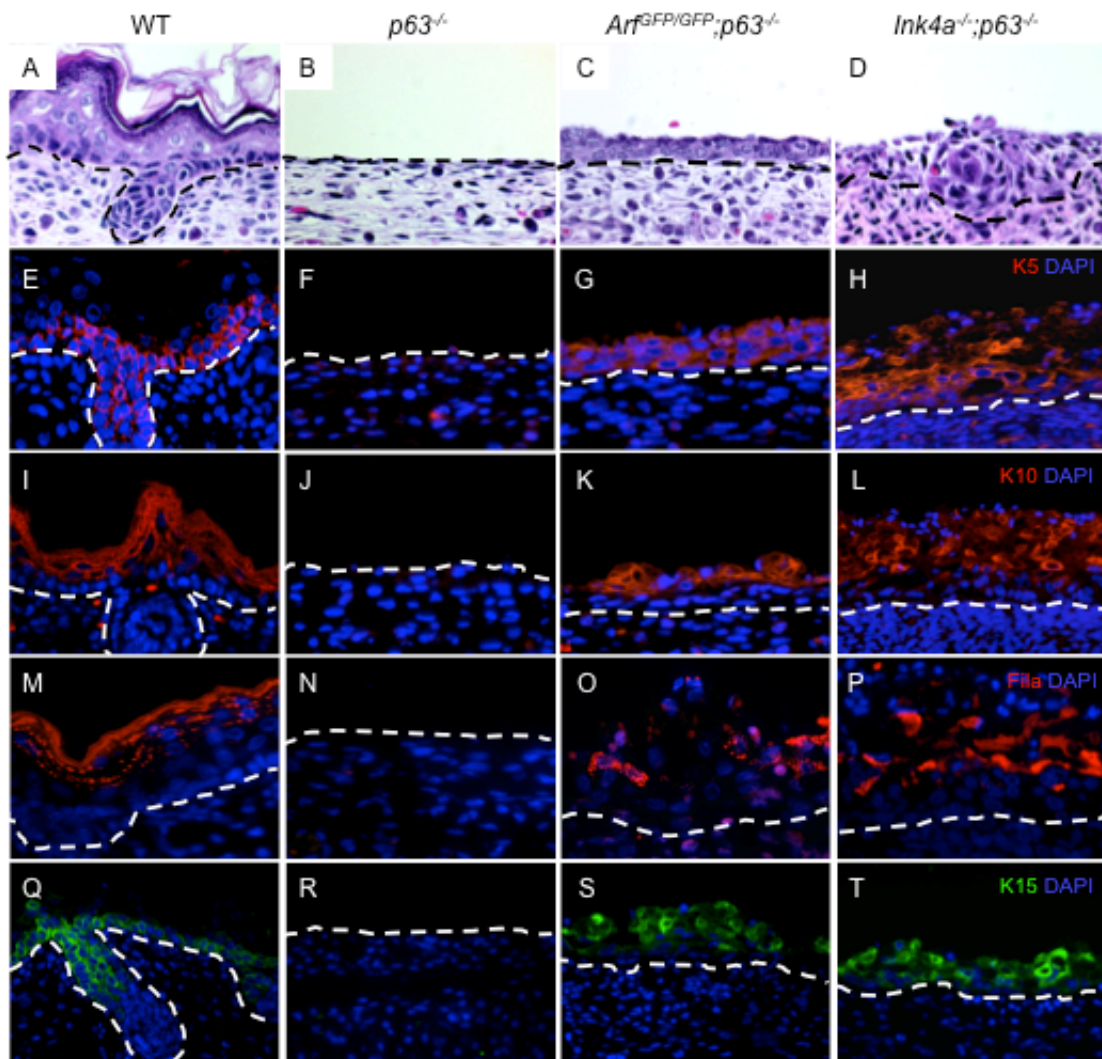


Figure 9. Microscopic analysis of the epithelium of embryos at E18.5. Cross sections of skin stained with hematoxylin and eosin (A–D) and immunofluorescence using antibodies to keratin 5 (red) (E–H), keratin 10 (red) (I–L), filaggrin (red) (M–P), and keratin 15 (green) (Q–T) and counterstained with DAPI (blue) are illustrated. The

genotypes for each vertical set of panels are indicated at the top of the figure. Broken lines define the border between the dermis and epidermis. **Reproduced with permission from Su et al., EMBO J. 2009 July 8; 28(13): 1904-1915.**

Table 1. Quantification of epithelial structures in day 18.5 embryos

Genotype	# of embryo	K5	K10	Fila	Embryo w/ hair follicle	Embryo w/ cleft palate	Embryo w/fore-limbs
WT	20	100%	100%	100%	20	0	20
<i>p63</i> ^{-/-}	20	2%	5%	0%	0	20	3
<i>Arf</i> ^{G/G} ; <i>p63</i> ^{-/-}	20	85%	75%	50%	0	4	18
<i>Ink4a</i> ^{-/-} ; <i>p63</i> ^{-/-}	20	85%	85%	75%	20	2	20
<i>p53</i> ^{-/-} ; <i>p63</i> ^{-/-}	6*	0%	0%	0%	0	6	0

Shown are the numbers of embryos analyzed per genotype. Numbers in columns with % represent the mean from 20 embryos analyzed per group. The asterisk (*) indicates that only 6 of 20 *p53*^{-/-};*p63*^{-/-} embryos could be analyzed at E18.5; the remaining 14 embryos died *in utero* at day 15.5.

3.1.4. Proliferation of $p63^{-/-}$ keratinocytes is restored in the absence of *Arf* or *Ink4a*.

Extraction of keratinocytes from $p63^{-/-}$ mice is difficult because of the defect in complete formation of stratum epithelia of the $p63^{-/-}$ mice. Consistent with previously published data, cells could be extracted from the surface of $p63^{-/-}$ and also $p63^{-/-};p53^{-/-}$ embryos; however, they do not proliferate on J2-3T3 feeder cells (**Figure 10**) (Barrandon and Green, 1987). *Arf* and *Ink4a* are known to be repressors of stem cell self-renewal (Molofsky et al., 2005; Molofsky et al., 2003). To determine whether loss of *Arf* or *Ink4a* could restore the proliferation defect of the $p63^{-/-}$ keratinocytes, the epidermal cells were isolated from $Arf^{GFP/GFP};p63^{-/-}$ and $Ink4a^{-/-};p63^{-/-}$ embryos at embryonic day E18.5 (**Figure 10**). These keratinocytes were cultured on J2-3T3 feeder cells to maintain stem cell properties (Barrandon&Green 1987; Flores et al., 2000). Excitingly, double mutant keratinocytes formed colonies similar to those formed by wild-type keratinocytes (**Figure 10A-E**). However, $Arf^{GFP/GFP};p63^{-/-}$ and $Ink4a^{-/-};p63^{-/-}$ keratinocytes did not form condensed colonies due to the lack of adhesion to each other (**Figure 10C, E, H, and J**). These cells were stained with K5, a marker of the stratum basale (**Figure 10F-J**). Both the $Arf^{GFP/GFP};p63^{-/-}$ and $Ink4a^{-/-};p63^{-/-}$ keratinocytes express K5 indicating that the isolated cells originated from keratinocytes. The fact that the $Arf^{GFP/GFP};p63^{-/-}$ and $Ink4a^{-/-};p63^{-/-}$ keratinocytes were less adherent to each other is not surprising given that *p63* has also been shown to regulate genes involved in cell adhesion (Carroll et al., 2006; Ihrle et al., 2005). This data is consistent with the macroscopic appearance of $Arf^{GFP/GFP};p63^{-/-}$ and $Ink4a^{-/-};p63^{-/-}$ mice, which have fragile skin.

To further understand the extent of rescue of the proliferation defect of $p63^{-/-}$ keratinocytes by loss of *Arf* or *Ink4a*, keratinocytes were cultured on J2-3T3 feeder cells (Barrandon and Green, 1987; Flores et al, 2000). Beginning at passage 2, wild-type, $p63^{-/-}$, $Arf^{GFP/GFP}$, $Ink4a^{-/-}$, $Arf^{GFP/GFP};p63^{-/-}$, and $Ink4a^{-/-};p63^{-/-}$ keratinocytes were monitored and counted every day for 8 days. While the $p63^{-/-}$ keratinocytes did not proliferate, cells of all other genotypes (wild-type, $Arf^{GFP/GFP}$, $Ink4a^{-/-}$, $Arf^{GFP/GFP};p63^{-/-}$, and $Ink4a^{-/-};p63^{-/-}$) continued to proliferate over the 8-day time course (**Figure 10K**). The most proliferative keratinocyte lines were the $Ink4a^{-/-}$ and $Arf^{GFP/GFP}$ while the $Arf^{GFP/GFP};p63^{-/-}$, and $Ink4a^{-/-};p63^{-/-}$ keratinocytes were as proliferative as wild-type keratinocytes. Additionally, these cells were passaged 7 times every 5 days and the accumulated population doublings were assessed (**Figure 10L**). The $p63^{-/-}$ keratinocytes senesced at passage 1, however all other genotypes continued to proliferate in later passages. The wild-type keratinocytes senesced at passage 3, while the $Ink4a^{-/-}$, $Arf^{GFP/GFP}$, $Ink4a^{-/-};p63^{-/-}$, and $Arf^{GFP/GFP};p63^{-/-}$ keratinocytes reached 12 to 14 accumulated population doublings by passage 7 (**Figure 10L**). $p53^{-/-};p63^{-/-}$ keratinocytes also senesced at passage 1 comparable to $p63^{-/-}$ keratinocytes (**Figure 10K-L**). This data suggested that the proliferation defect in the $p63^{-/-}$ keratinocytes cannot be rescued by the loss of p53, however it was dependent on loss of the *Ink4a-Arf* locus.

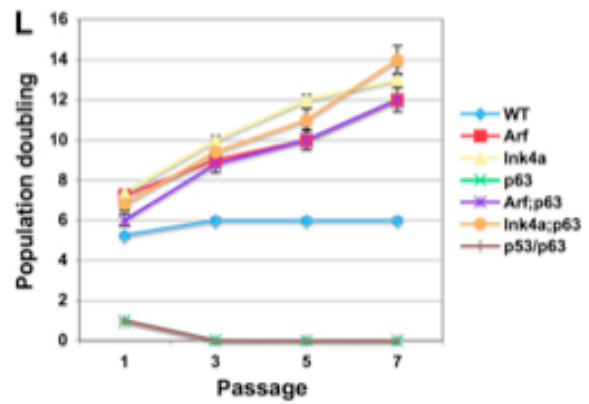
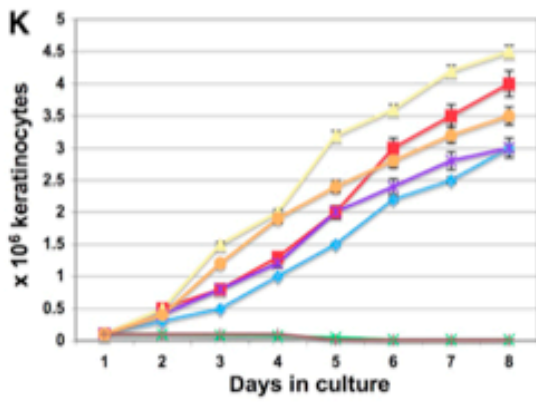
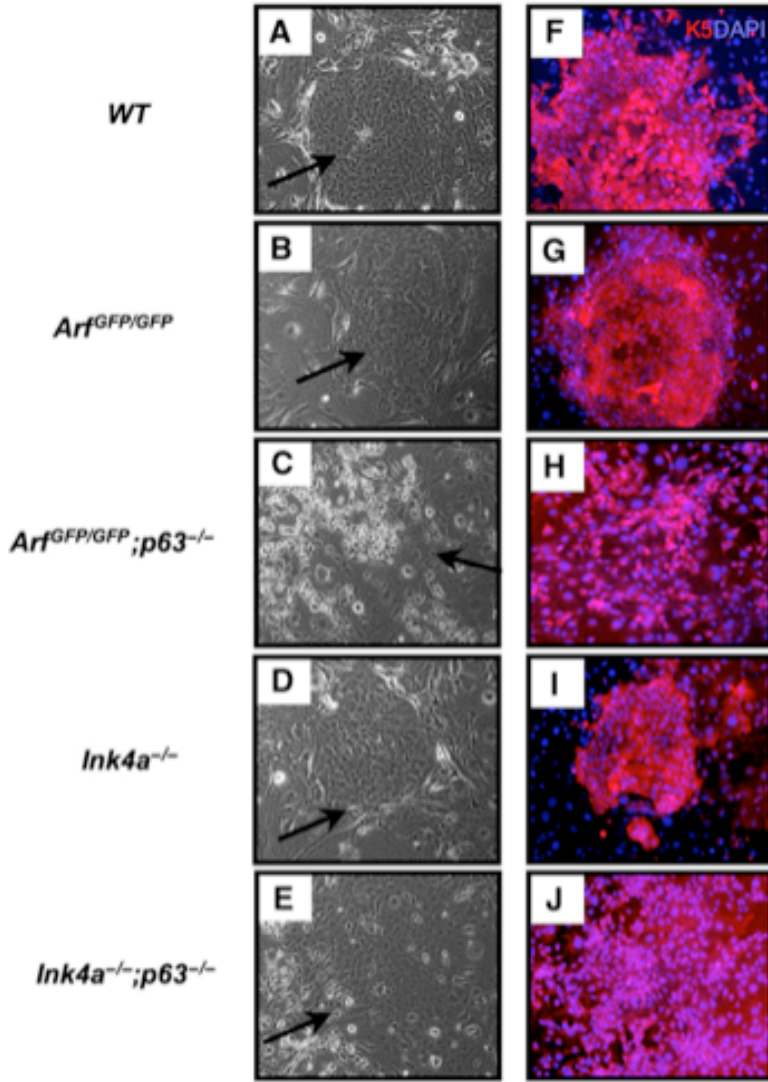


Figure 10. Keratinocyte cultures derived from embryos at E18.5. (A–E) Light micrographs of keratinocytes cultured on J2-3T3 feeder cells with their respective genotypes indicated to the left of the panels. Black arrows indicate the positions of keratinocytes colonies. (F–J) Immunofluorescence obtained with an antibody to keratin 5 (red), a marker of basal epithelial cells; cells were counterstained with DAPI (blue). (K) Indicates the proliferation rates of cultured keratinocytes of the following genotypes: wild type (WT, blue), *Arf*^{GFP/GFP} (Arf, red), *Ink4a*^{-/-} (Ink4a, yellow), *p63*^{-/-} (p63, green), *p53*^{-/-};*p63*^{-/-} (brown), *Arf*^{GFP/GFP};*p63*^{-/-} (Arf;p63, purple), and *Ink4a*^{-/-};*p63*^{-/-} (Ink4a;p63, orange). (L) Computes the cumulative population doublings of keratinocytes cultures passaged every 5 days for seven passages. The average of results obtained with three independent keratinocytes lines each assayed in triplicate is shown. The genotypes are indicated as in (K). **Reproduced with permission from Su et al., EMBO J. 2009 July 8; 28(13): 1904-1915.**

3.1.5. p63 represses $p19^{Arf}$ and $p16^{Ink4a}$ leading to proper proliferation and differentiation.

The failure to generate proliferative keratinocytes from $p63^{-/-}$ mice, together with the rescue of this process in *Arf* null and *Ink4a*-null backgrounds strongly suggested that p63 negatively regulates *Arf* and *Ink4a* expression. $p19^{Arf}$ knock out mice used a GFP reporter knock in strategy (Zindy et al., 2003a). To understand further whether the untimely expression of Arf and Ink4a proteins in the absence of *p63* can inhibit the outgrowth of keratinocytes leading to the profound defects in epidermal development.

To test this hypothesis, the GFP reporter gene was used to detect whether there is any differential expression in $Arf^{GFP/GFP}$ and $Arf^{GFP/GFP};p63^{-/-}$ cells, since Arf is not detectable during normal mouse epithelial development (Zindy et al., 2003b). Interestingly, GFP levels were 2.5 fold higher in MEFs and 3 fold higher in keratinocytes in the absence of *p63* providing further evidence that p63 represses *Arf* expression (**Figure 11C & D**). The difference in GFP levels between $Arf^{GFP/GFP}$ and $Arf^{GFP/GFP};p63^{-/-}$ keratinocytes was also detected by immunofluorescence (**Figure 11E & F**). Remarkably, GFP levels were also found to be higher *in vivo* in the epithelium of $Arf^{GFP/GFP};p63^{-/-}$ compared to $Arf^{GFP/GFP}$ embryos at embryonic day E18.5 suggesting that this repression of $p19^{Arf}$ is necessary for the complete formation of epidermis of $p63^{-/-}$ mice (**Figure 11A-F**). Interestingly, western blot analysis also revealed that $p19^{Arf}$ expression is higher in $p63^{-/-}$ MEFs and keratinocytes than in their wild-type counterparts indicating that p63 represses expression of $p19^{Arf}$ (**Figure 11G & H**). To

further verify whether the repression of p63 affects levels of *Arf* and *Ink4a* transcripts, q-RT PCR was performed (**Figure 11J & K**). *Arf* RNA levels were increased 15 fold in the absence of *p63* and likewise, the levels of *p16^{Ink4a}* were slightly increased in the absence of *p63* suggesting that p63 transcriptionally represses *p16^{Ink4a}* and *p19^{Arf}* (**Figure 11J & K**).

Table 2. Quantification of length of limbs in day 18.5 embryos

Genotype	Scapula	Humerus	Ulna	Pubic bone
WT	4.8±0.2	4.4±0.1	4.8±0.2	3.9±0.3
<i>p63</i> ^{-/-}	3.8±0.1	0.5±0.1	1.5±0.2	2.6±0.1
<i>Arf</i> ^{G/G} ; <i>p63</i> ^{-/-}	5.0±0.1	1.5±0.2	2.8±0.3	3.9±0.1
<i>Ink4a</i> ^{-/-} ; <i>p63</i> ^{-/-}	5.0±0.1	2.8±0.3	4.5±0.3	3.9±0.2

Shown is the mean (±s.d.) measured in mm of the indicated skeletal structures. Measurements were taken from 10 embryos per genotype.

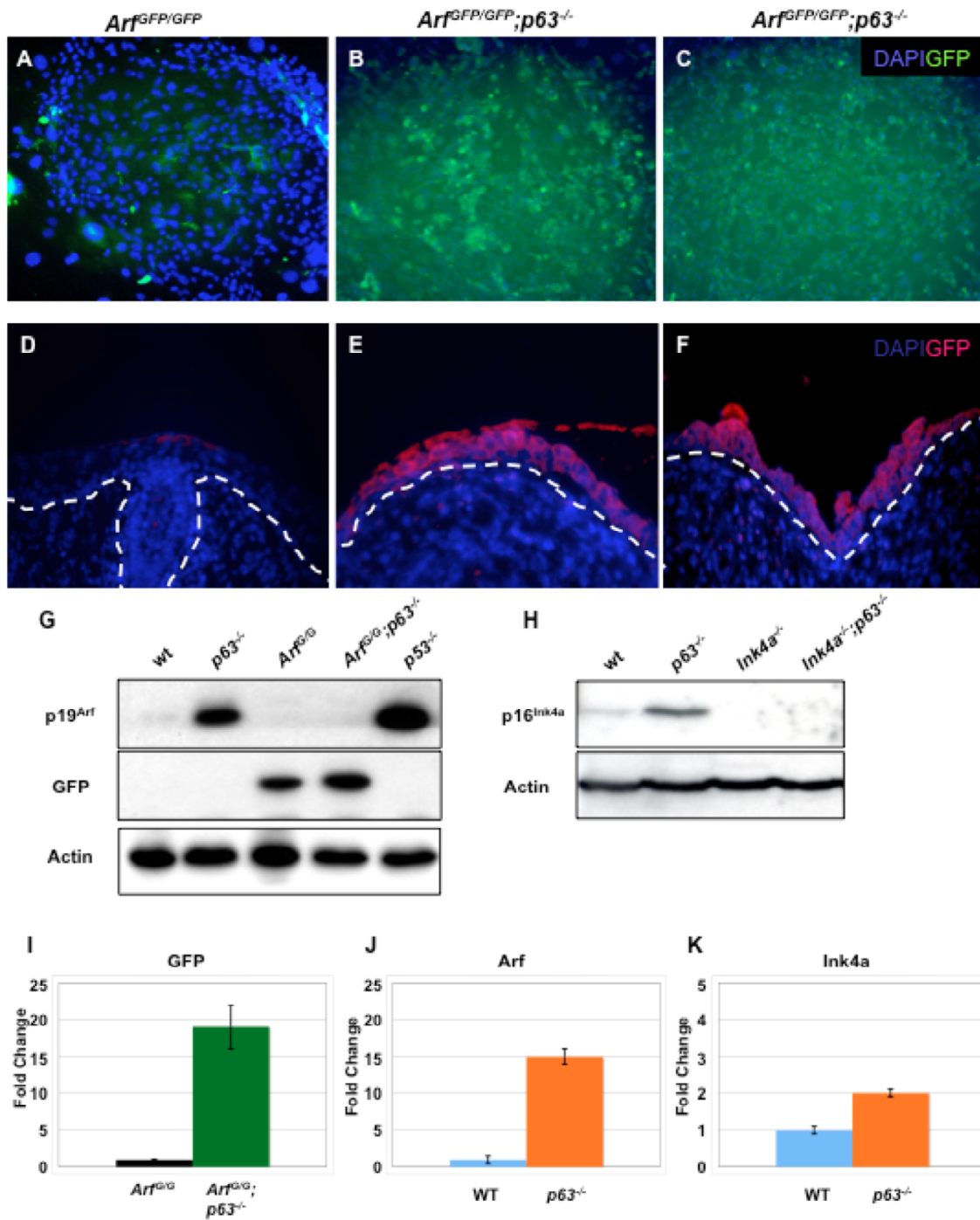


Figure 11. Expression of p19^{Arf}, p16^{Ink4a}, and GFP in keratinocytes and stratified epithelium. (A–C) GFP expression in keratinocytes of the indicated genotypes (top).

Cells were counterstained with DAPI (blue). Representative colonies of cultured *Arf*^{GFP/GFP};*p63*^{-/-} keratinocytes (B, C) were vividly fluorescent when compared (matched exposures) with cultures at the same passage derived from *Arf*^{GFP/GFP};*p63*^{+/+} mice (A). (D–F) Cross sections of stratified epithelium from E18.5 embryos stained with antibodies to GFP (red). DAPI (blue) was used as a counterstain. The respective genotypes correspond to those indicated above (A–C). Matched exposures are shown. (G, H) Immunoblotting analysis of selected proteins (indicated at the left) identified in detergent lysates of age-matched passage-2 keratinocytes (B) of the indicated genotypes (top). Passage-2 *p53*^{-/-} MEFs were used as a positive control (G). Actin was used as a loading control. (I–K) q-RT PCR of the indicated mRNAs (top) extracted from E18.5 dermis/epidermis of the indicated genotypes (bottom). GAPDH was used as an internal control. **Reproduced with permission from Su et al., EMBO J. 2009 July 8; 28(13): 1904-1915.**

3.1.6. The *Arf* and *Ink4a* transcripts were repressed by restoration of p63 in double mutant MEFs.

Because expression of Arf RNA and protein was high in *p63*^{-/-} MEFs, to further understand whether there is repression of *Arf* and *Ink4a* by p63, p63 isoform specific plasmids were transfected into *p63*^{-/-} or *Arf*^{GFP/GFP};*p63*^{-/-} MEFs. Q-RT PCR was performed to determine whether p63 restoration affects levels of *Arf* and *Ink4a* mRNA transcription (**Figure 12A & B**). *Arf* and *Ink4a* RNA levels were diminished in the presence of *p63* and GFP levels were slightly decreased in the presence of *p63* suggesting that *Arf* and *Ink4a* are transcriptionally repressed by p63 restoration (**Figure 12A & B**). The Flores laboratory showed that p63 directly binds to the promoters of *Arf* and *Ink4a* to repress transcription of the genes (Su et al., 2009). Taken together, these data suggest that p63 plays a role as a transcriptional repressor of *Ink4a* and *Arf* and the repression of *Ink4a* and *Arf* is necessary for epithelialization.

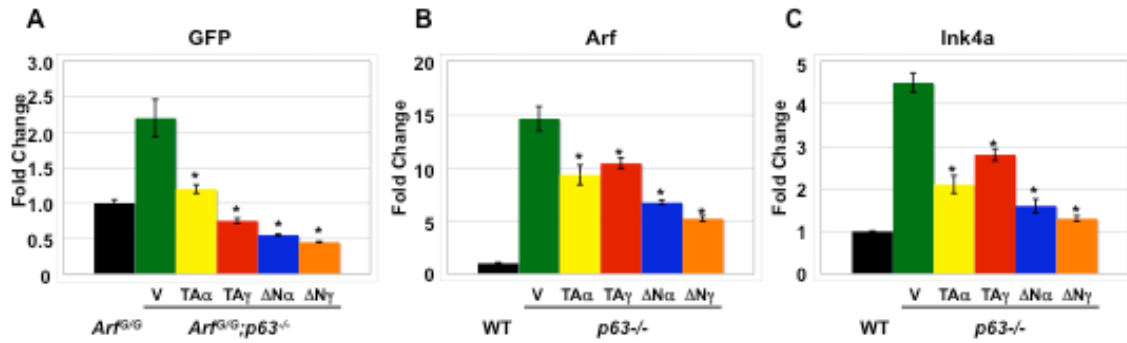


Figure 12. p63 represses *Arf* and *Ink4a*.

(A, B & C) q-RT PCR of the indicated mRNAs (top) extracted from the specified MEFs transfected with the indicated expression vectors (bottom). GAPDH was used as an internal control. The asterisk denotes statistical significance ($P < 0.01$). **Reproduced and modified with permission from Su et al., EMBO J. 2009 July 8; 28(13): 1904-1915.**

3.2. The role of p63 as a transcriptional activator of *Brachyury*

Rationale: Human patients with dominantly inherited point mutations of *p63* in the DNA binding domain or SAM domain develop ectodermal dysplasias, including ectrodactyly (Celli et al., 1999; McGrath et al., 2001); however, the underlying mechanism is not yet well understood. Mice deficient for *p63* display similar defects to those seen in humans and mice in the malformation of ectodermal appendages and epithelial tissues (Mills et al., 1999; Yang et al., 1999). The Flores laboratory's previous genome-wide analysis identified *brachyury* as a putative transcriptional target of p63 (Lin et al., 2009). The *p63* mutant mice display multiple defects including failure of proper limb formation and as well as tumor formation in heterozygous mice (Flores, 2007; Flores et al., 2005; Mills et al., 1999; Yang et al., 1999). Mice mutant for both *p63* and *p53* (*p53*^{+/-}; *p63*^{+/-}) develop metastatic tumors at high frequency (Flores et al., 2005).

Hypothesis: p63 regulates *brachyury*, which is critical for appropriate limb formation, tumorigenesis, and metastasis.

3.2.1. *Brachyury* gene expression is down regulated in the absence of *p63*

Mice in the absence of p63 have truncated or absent limbs (Mills et al., 1999; Yang et al., 1999). However the roles of p63 in limb development have not been well elucidated. Our laboratory has reported recently that many genes were down regulated in the absence of *p63* by genome wide screening using a 15,000cDNA microarray, and the

brachyury was one of the downregulated genes in *p63*^{-/-} MEFs (Lin et al., 2009). *Brachyury* is an important gene playing diverse roles in the apical ectodermal ridge (AER) formation during limb development (Liu et al., 2003a) and contributing to tumor metastasis (Palena et al., 2007; Yang et al., 2009). During development, in early embryonic stages, *brachyury* mRNA is expressed from E5.5 to E12.5 and interestingly, *p63* mRNA is also highly expressed at the AER at embryonic day E10.5 within the window of AER formation (Lo Iacono and Gross, 2008) in the developing mouse embryo (Inman and Downs, 2006; Wilkinson et al., 1990), leading to the hypothesis that p63 plays a role in regulating *brachyury* gene expression during limb development. Interestingly, we found that *brachyury* gene expression pattern is similar to the expression pattern of $\Delta Np63$ mRNA during wild-type mouse embryo development (**Figure 13A & B**). To determine whether *brachyury* expression is down regulated in the developing *p63*^{-/-} embryo, RNA was isolated from wild type and *p63*^{-/-} whole embryos at embryonic day E9.5, when AER formation takes place and *brachyury* mRNA highly expressed in the AER (Liu et al., 2003). q-RT PCR was performed using *brachyury* primers, brachyury expression was found to be 7.5 fold lower in *p63*^{-/-} compared to wild-type embryos ($p < 0.01$, Figure 13A), indicating that p63 probably transcriptionally regulates *brachyury* expression since p63 is a transcription factor (Yang et al., 1998).

The Flores laboratory has shown recently that mice develop normal limbs in the absence of *TAp63* (Su et al., 2009), leading us to hypothesize that the $\Delta Np63$ isoforms

are essential for proper limb development. First, to ask whether *brachyury* expression is downregulated in *TAp63^{-/-}* whole embryos, wild type and *TAp63^{-/-}* embryos were generated at embryonic day E9.5 and q-RT PCR for *brachyury* was performed using RNA from wild type and *TAp63^{-/-}* embryos. As expected, expression of *brachyury* was comparable to the wild-type levels in *TAp63^{-/-}* embryos (**Figure 13B**), indicating that Δ Np63, and not TAp63, regulates *brachyury* gene expression within a window of embryonic limb development.

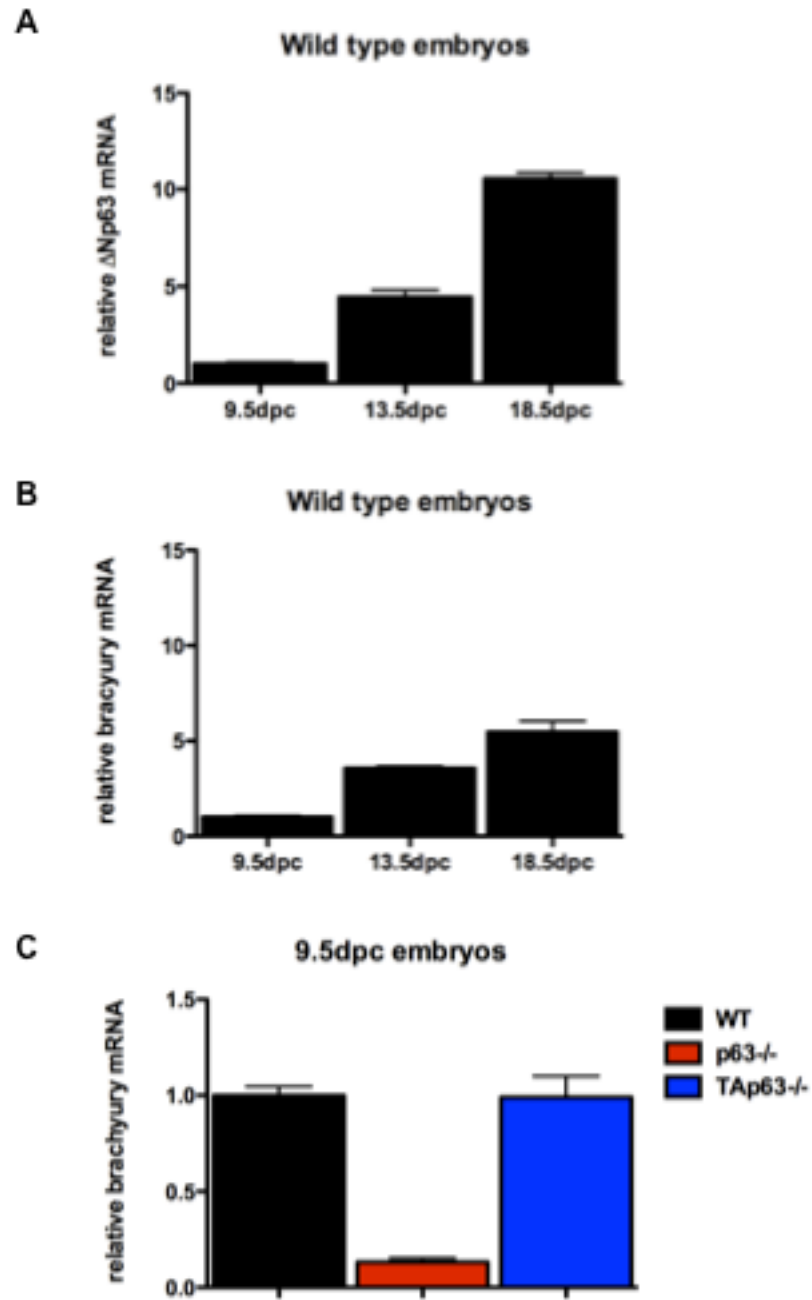


Figure 13. *Brachyury* is downregulated in the absence of *p63*. Quantitative RT-PCR (q-RT PCR) for (A) $\Delta Np63$ or (B) *brachyury* in wild-type embryos at 9.5, 13.5 and 18.5

days post coitum (dpc). (C) q-RT PCR for *brachyury* in wild-type (Wt), *p63* deficient (*p63*^{-/-}) and *TAp63* deficient (*TAp63*^{-/-}) embryos at day 9.5 dpc. Fold change relative to wild-type levels of $\Delta Np63$ or *brachyury* mRNA is shown on the y-axis for each genotype on the x-axis each bar represents the average of three independent experiments. The asterisk indicates statistical significance (p-value <0.01). **Reproduced with permission from Cho et al., Cell Cycle 9:12, 1-8; June 15, 2010**

3.2.2. p63 binds to the promoter of *brachyury*.

As a transcription factor, p63, like p53, has been known to bind to a consensus sequence of the promoter and transcriptionally regulates its target genes. The consensus binding site is PuPuPuC(A/T)(T/A)GPyPyPy - 0-13bp spacer - PuPuPuC(A/T)(T/A)GPyPyPy (Lin et al., 2009; Flores et al., 2002). By following this rule, Dr. Flores identified a putative p53/p63 consensus site 138 nucleotides upstream of exon 1 (-138 site) (**Figure 14A**). This site, actCTTGtcgcgCCTTGcgg, that follows the rule of p53/p63 consensus site with some base pair mismatches (Lin et al., 2009; Flores et al., 2002). To determine whether p63 can bind to this putative consensus site on the promoter of *brachyury*, chromatin immunoprecipitation (ChIP) assay was performed using nuclear extracts from wild type and *p63*^{-/-} mouse embryonic fibroblasts (MEFs) derived from embryonic day E13.5 embryos. Using two different antibodies for p63, ChIP analysis from wild type MEFs demonstrated that p63 binds to the -138 site of the *brachyury* promoter (**Figure 14B**).

All p53 family members, p53, p63 and p73, share some target genes consensus sites and all p53 family members are predicted to bind to this identified consensus site (Flores et al., 2002). To determine if p53 and p73 can also bind to the *brachyury* promoter, ChIP analysis was performed using antibodies for p53 and p73 in wild type, *p63*^{-/-} and *p53*^{-/-} MEFs. Although these family members bound to the p21 promoter (**Figure 14C**), which is a representative target gene of p53, but the binding of p53 and

p73 was not detected to this -138 site of *brachyury* promoter indicating that p63 is the only family member of p53 that binds to the *brachyury* promoter (**Figure 14B**).

Previously, the Flores laboratory has reported that p53, p63 and p73, have interdependent binding at some promoter sites (Lin et al., 2009). To figure out whether p63 binding to *brachyury* promoter is impaired in the absence of p53, ChIP analysis was performed using antibodies for p63 from wild type, *p53*^{-/-}, and *p63*^{-/-} MEFs. Indeed, p63 binding to the -138 sites was not dampened in the absence of *p53*, suggesting that p63 does not require the presence of p53 to bind to the *brachyury* promoter and clearly showing that the only p53 family member who regulates transcription of *brachyury* is p63.

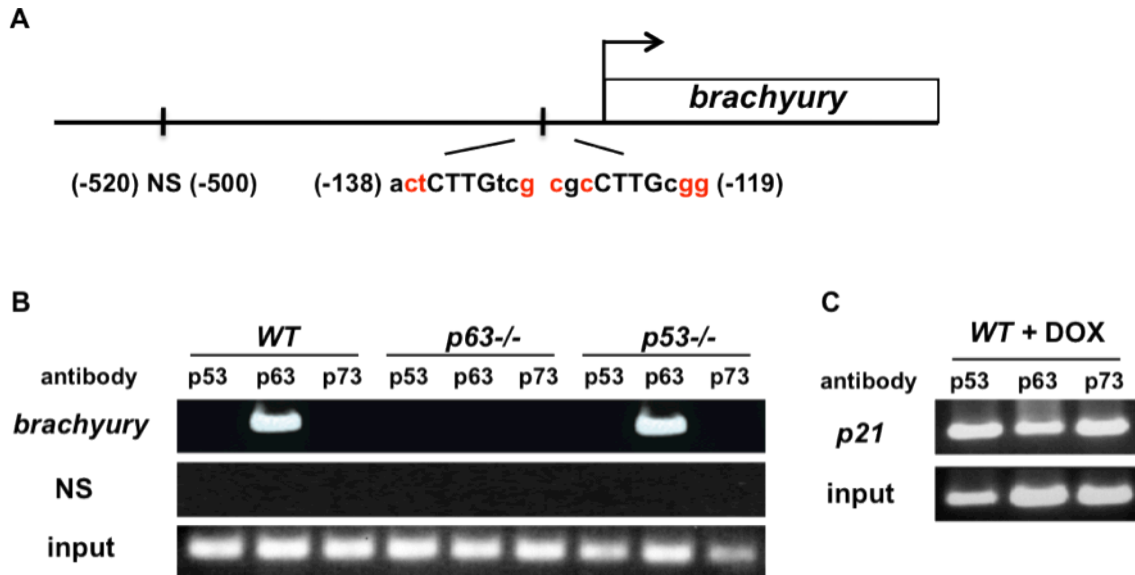


Figure 14. p63 binds to the *brachyury* promoter. (A) Schematic of the promoter of *brachyury* including the sequence of the p53/p63-binding site located 138 nucleotides upstream of the start site. Mismatches are shown in red. (B) ChIP analysis of wild-type (WT), *p63*^{-/-}, and *p53*^{-/-} mouse embryonic fibroblasts (MEFs) using antibodies against p53, p63 or p73. PCR was performed using primers flanking the p63 binding site and an upstream non-specific site (NS) shown in (A). (C) ChIP analysis of the p21 promoter using antibodies for p53, p63 and p73. Total input chromatin for each PCR ChIP reaction is shown. ChIP experiments were performed on 3 MEF lines of each genotype in triplicate. **Reproduced with permission from Cho et al., Cell Cycle 9:12, 1-8; June 15, 2010**

3.2.3. $\Delta Np63\alpha$ and β transcriptionally activate *brachyury*.

To further understand whether p63 physically binds to the promoter of *brachyury* that turns on gene transcription, a *luciferase* reporter gene assay was performed using a p63 consensus site from the *brachyury* promoter (-138 site). Two *brachyury* promoter luciferase reporter constructs were generated: brach1 and brach2. Brach1 contained the 5' upstream region of the transcriptional start site, including the p63 consensus element, and Brach 2 contained the sequence of Brach1, exon1 and intron 1 of *brachyury* (**Figure 15A**). To know which isoforms of p63 bind and turn on gene transcription, TAp63 (α , β , γ) or $\Delta Np63$ (α , β , γ) isoforms expressing plasmids were transfected with brach1 or brach2 into *p53*^{-/-}; *p63*^{-/-} (MEFs). Consistent with q-RT PCR result (**Figure 13**), we found that $\Delta Np63\alpha$ and β were the only isoforms that transactivated both the brach1 and brach2 luciferase reporter gene activity (**Figure 15B**) indicating only $\Delta Np63\alpha$ and β isoforms transactivate *brachyury* gene promoter. The TAp63 isoforms do not have this activity, consistent with the phenotype of the *TAp63*^{-/-} mice, which show no limb development defect (Su et al., 2009). To further confirm whether the p63 consensus site was specific for the transactivation activity on the *brachyury* promoter in the luciferase assay, the construct was mutated with the minimal site necessary for *brachyury* transactivation by p63 (Brach1). The mutant construct, named as Brach 1m, includes two point mutations in the half sites required for p63 binding (**Figure 15A**). Using Brach 1m in the luciferase assays, transactivation by the p63 isoforms was not detected indicating

that the identified p63 consensus site is specific for *brachyury* transactivation (Figure 15B).

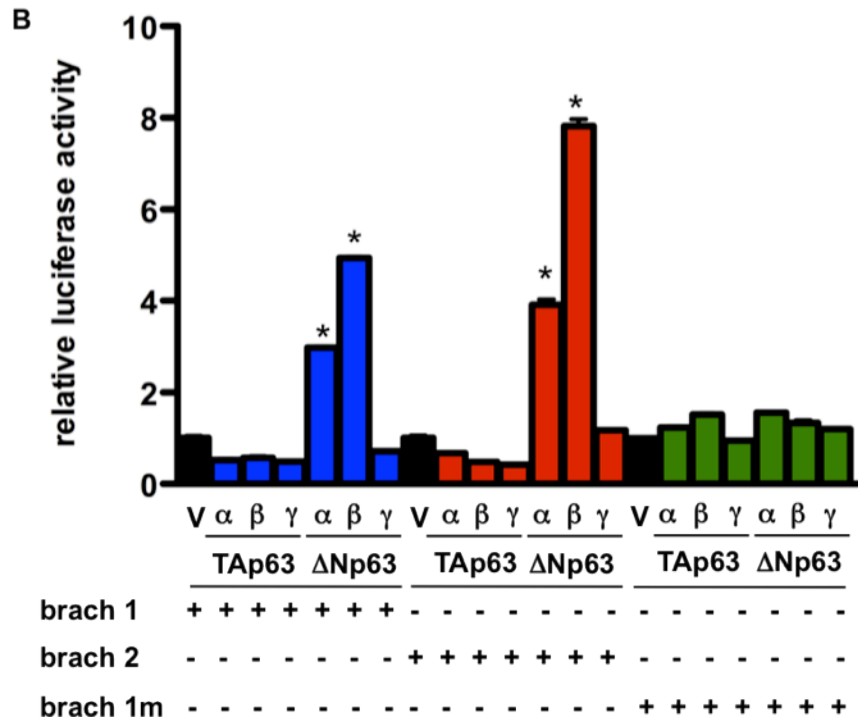
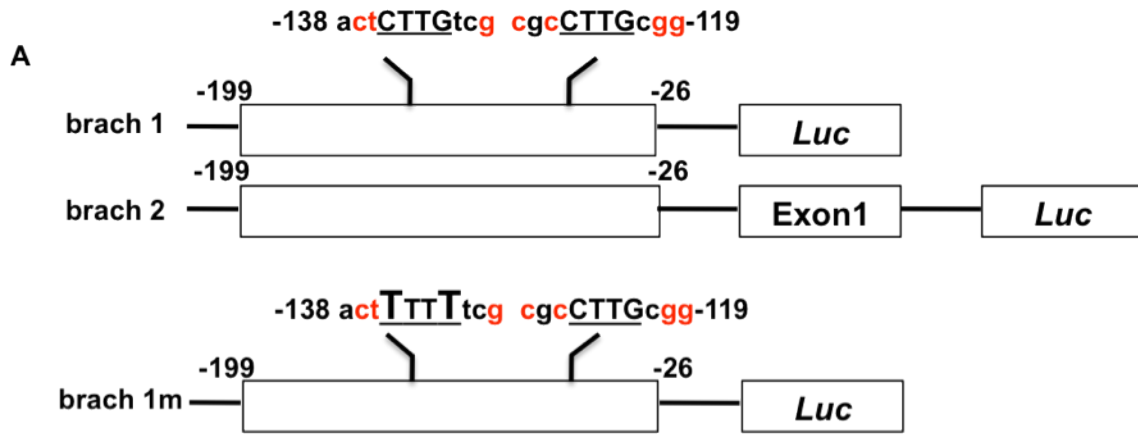


Figure 15. *Brachyury* is transactivated by Δ Np63 α and Δ Np63 β . (A) Schematic structure of *brachyury luciferase* gene reporter constructs, Brach1, Brach2 and Brach1m. (B) Bar graph showing luciferase assay in *p53*^{-/-};*p63*^{-/-} MEFs transfected with the indicated *p63* isoform expressing plasmids and the indicated luciferase reporter gene. Each bar represents the average of the fold activation of three independent experiments. The asterisks indicate statistical significance (p-value <0.01). **Reproduced with permission from Cho et al., Cell Cycle 9:12, 1-8; June 15, 2010**

3.2.4. The level of *brachyury* expression correlates with the level of $\Delta Np63$ expression in osteosarcoma cell lines

Brachyury plays diverse roles during development and is also highly expressed in several human cancers (Palena et al., 2007; Vujovic et al., 2006; Yang et al., 2009). Indeed, $\Delta Np63$ has also been suggested to play oncogenic roles since it is highly expressed in many human cancers (Cox et al., 2009; Flores, 2007). To determine whether $\Delta Np63$ expression correlates with *brachyury* expression in tumors, q-RT PCR was performed using tumor cell lines from $p53^{+/-}$ and $p53^{+/-};p63^{+/-}$ mice. They expressed various level of $\Delta Np63$ (**Figure 16A**). To tease out whether $TAp63$ and $\Delta Np63$ differentially correlate with *brachyury* expression in these tumor cell lines, q-RT PCR was performed using primers for *TAp63*, *$\Delta Np63$* , and *brachyury* from total RNA derived from cell lines of 1 rhabdomyosarcoma (RS), 3 osteosarcomas (Os-1, Os-2 and Os-3), 1 mammary adenocarcinoma (MAd), and 1 lung adenocarcinoma (LAd). By q-RT PCR, all tumor cell lines showed low levels of *TAp63* expression (**Figure 16A**). Interestingly, two of 3 osteosarcoma cell lines (Os-1 and Os-2) expressed high levels of $\Delta Np63$ and those concomitantly expressed high levels of *brachyury* (**Figure 13A**). As expected, other cell lines with low levels of $\Delta Np63$ also expressed low levels of *brachyury*, indicating that the expression of these two mRNA transcripts does indeed have some correlation.

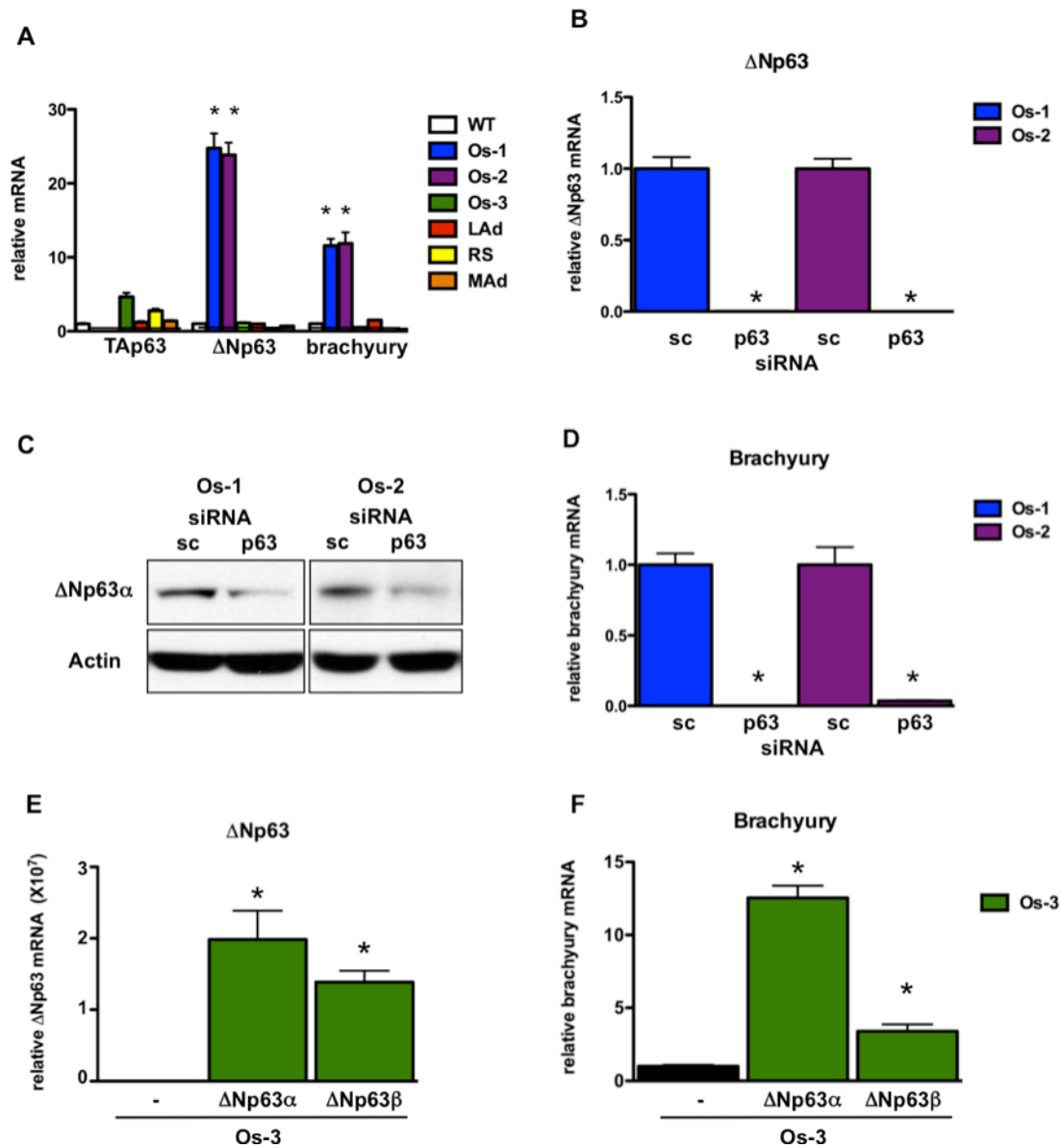


Figure 16. ΔNp63 expression induces brachyury in tumor cell lines. (A) q-RT PCR using total RNA from the indicated tumor cell lines for *TAp63*, *ΔNp63* and *brachyury*. (B) q-RT PCR and (C) Western blot analysis for expression of *ΔNp63* in Os-1 and Os-2

osteosarcoma cells transfected with scrambled (sc) or p63 siRNA (p63). (D) q-RT PCR of *brachyury* mRNA in Os-1 and Os-2 cells after transfection with scrambled (sc) or p63 siRNA (p63). (E and F) q-RT PCR for (E) $\Delta Np63$ and (F) *brachyury* in Os-3 osteosarcoma cell lines transfected with $\Delta Np63\alpha$ and $\Delta Np63\beta$. each experiment was performed in triplicate. the asterisks indicate statistical significance (pvalue <0.01).

Reproduced with permission from Cho et al., Cell Cycle 9:12, 1-8; June 15, 2010

3.2.5. Loss of $\Delta Np63$ results in concomitant downregulation of *brachyury* expression

To further explain the correlations between $\Delta Np63$ and *brachyury* expression, levels of $\Delta Np63$ were knocked down using a siRNA approach. Specifically, siRNA was used for p63, targeted to the DNA binding domain of p63, (Iwakuma et al., 2005) and it was transfected into two osteosarcoma cell lines (Os-1 and Os-2). Scrambled siRNA (sc-siRNA) was used as a control (**Figure 16 B- D**). As expected, knock down *p63* (**Figure 16B & C**) led to the knock down of $\Delta Np63$. Transfection efficiency from both cell lines with the si-*p63* exhibited at least an 80~ 90% knockdown of $\Delta Np63$ (**Figure 16B & C**). To detect whether $\Delta Np63$ knock down resulted in a concomitant decrease in *brachyury* expression, q-RT PCR was performed in these cells and *brachyury* expression was seen to be dramatically decreased (greater than 98%) in both Os-1 and Os-2 cell lines compared to the scrambled siRNA (sc-siRNA) transfected cell lines (**Figure 16D**). Additionally, $\Delta Np63\alpha$ or $\Delta Np63\beta$ were overexpressed in Os-3 cells which expressed low levels of $\Delta Np63$ and *brachyury*. Endogenous *brachyury* expression was restored with high levels of $\Delta Np63\alpha$ and $\Delta Np63\beta$ (**Figure 16E & F**). Taken together, these results further support that $\Delta Np63$ regulates *brachyury* expression.

3.2.6. Downregulation of *p63* leads to loss of *brachyury* expression and a decrease in cell proliferation, migration and invasion

Previously, it has been shown that *brachyury* expression is high in tumors and tumor cell lines, which also exhibit increased proliferation. To determine whether knockdown of $\Delta Np63$ with a concomitant downregulation of *brachyury* has a consequence on cellular proliferation, bromo-deoxyuridine (BrdU) incorporation assay was performed to measure the percentage of S-phase cells. This assay was performed in the osteosarcoma cell lines, Os-1 and Os-2, which have high $\Delta Np63$ and *brachyury* expression. These cells were transfected with siRNA-p63 or scrambled (sc) as a control. This transfection with siRNA specific for p63, resulted in greater than 90% knockdown of $\Delta Np63$ and a diminution in *brachyury* expression (**Figure 16B & D**), the number of cells incorporating BrdU was lower compared to cells transfected with a scrambled siRNA (**Figure 17A**). The percentage of BrdU positive Os-1 cells was initially 79% and diminished to 60% after transfection with the siRNA-p63. Likewise, the level of BrdU positivity in Os-2 cells decreased from 64% to 52% after transfection with the si-p63 (**Figure 17B**). The level of BrdU positivity did not change in the cells treated with scrambled siRNA (sc-siRNA). These data imply that loss of $\Delta Np63$ results in lower expression of *brachyury* and fewer proliferative cells. Metastatic tumor cells are highly migrative and invasive (Friedl and Wolf, 2003). To determine whether the migration and invasion characteristics are altered in these cells, Boyden chamber assay was used to measure migration and invasion. Indeed, Os-1 and Os-2 cells with down regulated

ΔNp63 and *brachyury* had a diminished capacity to migrate and invade (**Figure 17C & D**). Taken together, these data suggest that the high expression of *ΔNp63* detected in many human cancers is critical for upregulation of *brachyury* and increased cell proliferation, migration and invasion in cancer cell lines. Overall, my data suggests that *ΔNp63* controls limb development via transcriptionally activating *brachyury*, and in tumor, *ΔNp63* also regulates cell proliferation, migration and invasion through *brachyury* gene activation.

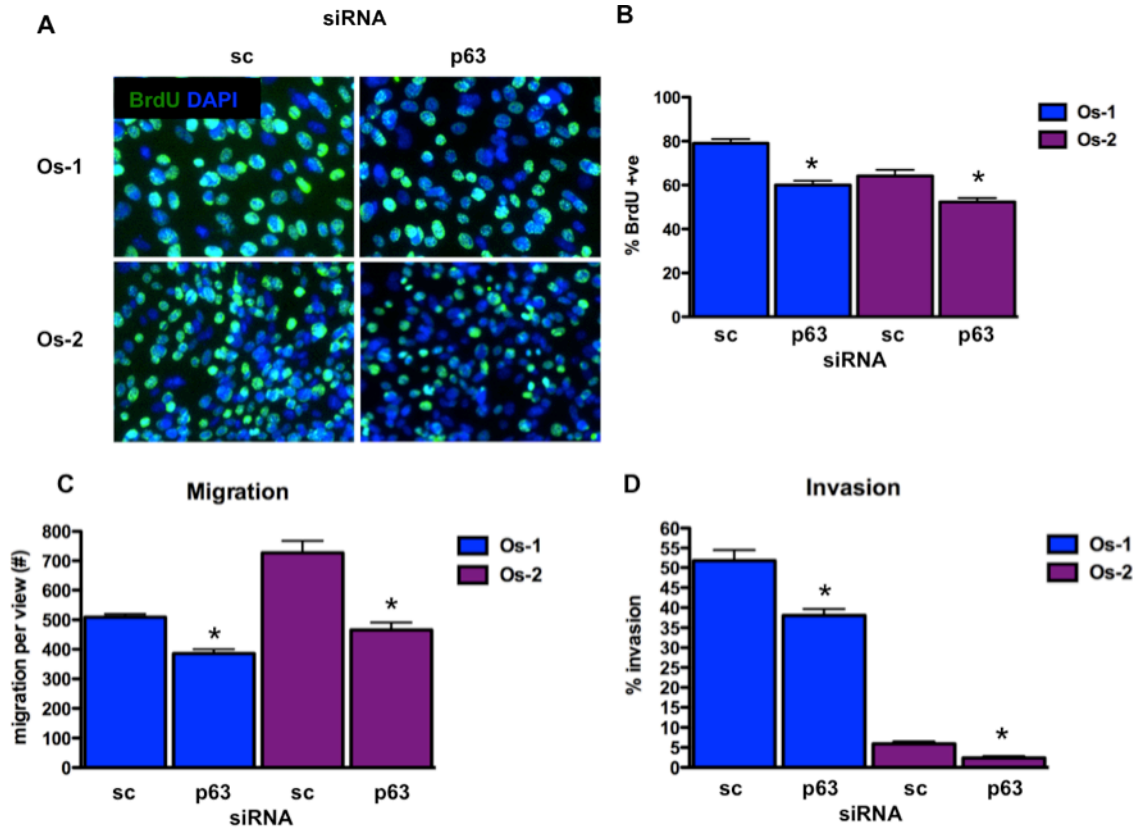


Figure 17. Knockdown of Δ Np63 results in decreased cell proliferation, migration and invasion. (A) BrdU positive (green) os-1 and os-2 cells transfected with scrambled siRNA (sc) or *p63*-siRNA (p63). DAPI (blue) was used as a nuclear counterstain. (B) Bar graph showing the percentage of BrdU positive cells after transfection with scrambled (sc) or *p63*-siRNA. Bar graphs showing (C) the number of cells migrated in a Boyden chamber assay and (D) the percentage of cells that have invaded through Matrigel in this assay. The asterisks indicate statistical significance (pvalue <0.01).

Reproduced with permission from Cho et al., *Cell Cycle* 9:12, 1-8; June 15, 2010

Chapter 4.

Δ Np63 induces terminal differentiation of the epidermis through transcriptional regulation of *DGCR8*.

Some parts of this chapter were modified from the following manuscript.

1. **Min Soon Cho**, Xiaohua Su, Deepavali Chakravarti, Arianexys Aquino, Nicole Müller, Avinashnarayan Venkatanarayan, Io Long Chan, Young Jin Gi, & Elsa R. Flores. Δ Np63 induces terminal differentiation through transcriptional regulation of *DGCR8* and suppression of pluripotency factors.

Chapter 4. The roles of $\Delta Np63$ in epithelial development

Rationale: The phenotypes of the $\Delta Np63cKO$ (K14Cre) and the $\Delta Np63$ null are reminiscent of the $DGCR8$ (a microprocessor for microRNAs) conditional knockout (cKO) mice and knock out embryonic stem cells (ESCs). Specifically, these mice display a hair follicle outgrowth skin phenotype (Yi et al., 2006; Yi et al., 2009) as detected in the $\Delta Np63^{+/-}$ mice. Importantly, $DGCR8^{-/-}$ ESCs display a hyperproliferation phenotype and failure of silencing pluripotency genes (Suh et al.; Wang et al., 2007) which results in differentiation defects. Interestingly, I have observed that $\Delta Np63$ deficient epidermal cells display phenotypic characteristics that resemble embryonic stem cells instead of keratinocytes.

Hypothesis: $\Delta Np63$ induces terminal differentiation of the epidermis through the regulation of $DGCR8$.

4.1. Generation of $\Delta Np63$ conditional knockout mice

To understand the role of $\Delta Np63$ in skin development, a $\Delta Np63^{-/-}$ mouse was generated by intercrossing the $\Delta Np63$ conditional knock out mice ($\Delta Np63fn/fn$) to FLPeR transgenic mice (Farley et al., 2000) to eliminate the intervening *neo* cassette ($\Delta Np63fl/fl$) (**Figure 18C**) and tissue-specific deletion of the $\Delta Np63$ isoforms using the cre-loxP system with the retention of the $TAp63$ isoforms. LoxP sites were inserted into

the *p63* gene flanking exon 3', which contains the unique translational start site of the $\Delta Np63$ isoforms, to generate a floxed allele ($\Delta Np63fl$) (**Figure 18A**). Properly targeted embryonic stem cells (ESCs) were injected into 129/B6 hybrid donor blastocysts and subsequently into pseudo pregnant females. The resulting male chimeras (founder) were intercrossed with albino C57/B6 females for germ line transmission detected by Southern blot analysis and genotyping PCR (**Figure 18B & C**).

To further understand the role of $\Delta Np63$ in skin epithelial development, $\Delta Np63^{-/-}$ mice were generated by intercrossing the $\Delta Np63fl$ mouse ($\Delta Np63^{fl/fl}$) with germ line-specific Cre-transgenic mice (Zp3-cre specific for the egg) (Lewandoski et al., 1997) and resulting $\Delta Np63^{+/+}$ male and female were intercrossed to generate $\Delta Np63^{-/-}$. Pups died within a few hours after birth due to postnatal desiccation. Q-RT PCR performed on timed embryos (9.5 and 18.5dpc) isolated from $\Delta Np63^{-/-}$ embryos confirmed absence of $\Delta Np63$ mRNA ($p < 0.0001$) (**Figure 18D**) or protein expression (**Figure 18E**) with retention of *TAp63* mRNA as wild-type levels (**Figure 18F**) throughout embryonic development.

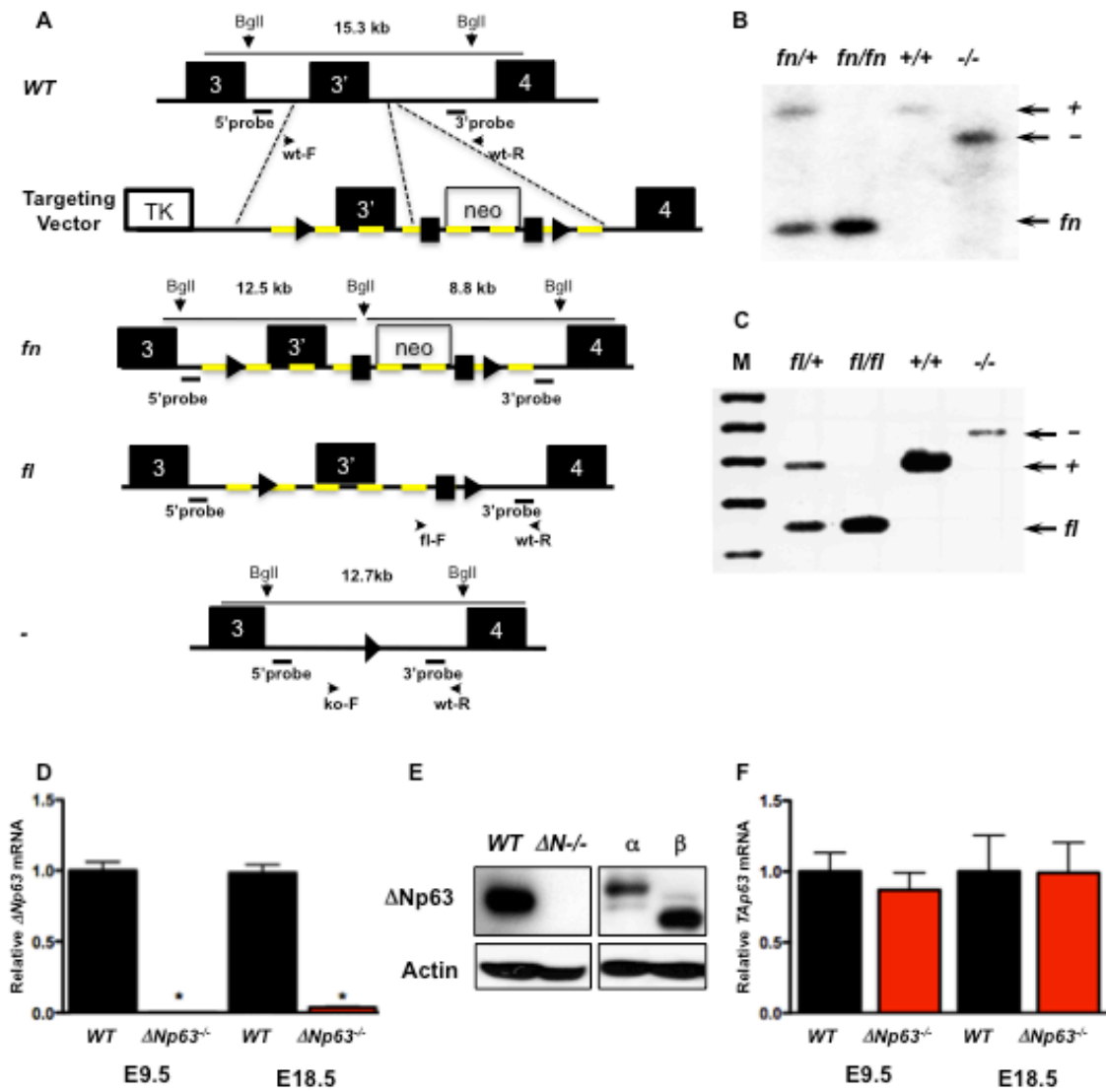


Figure 18. Generation of $\Delta Np63fl/fl$ conditional knockout and $\Delta Np63^{-/-}$ knock out mice.

A) The $\Delta Np63$ targeting vector was generated by inserting loxP sites (triangles) flanking

exon 3' and a neomycin cassette (neo) flanked by frt sites (squares). Location of primers used for genotyping is indicated by arrows. The targeted region of the allele is depicted by a dashed yellow line. Flox neo (fn) mice were crossed to the FLPeR mice expressing the flp recombinase to delete the neo cassette in vivo and to generate the flox (fl) allele. The knock out (KO) allele is shown after cre recombination. B) Southern analysis of genomic DNA from: $\Delta Np63fn/+$, $\Delta Np63fn/fn$, $\Delta Np63+/+$ and $\Delta Np63-/-$ mice. C) PCR analysis of genomic DNA from: $\Delta Np63fl/+$, $\Delta Np63fl/fl$, $\Delta Np63+/+$ and $\Delta Np63-/-$ mice. D) Q RT PCR analysis of $\Delta Np63$ mRNA from E9.5 and E18.5 wild-type and $\Delta Np63-/-$ embryos. E) Western blot analysis for $\Delta Np63$ using epidermal cells derived from wild-type and $\Delta Np63-/-$ embryos (E18.5) (left panel) and $p53-/-;p63-/-$ MEFs expressing $\Delta Np63\alpha$ and $\Delta Np63\beta$ cDNAs. Actin was used as a loading control. F) Q RT PCR analysis of $TAp63$ mRNA from E9.5 and E18.5 wild-type and $\Delta Np63-/-$ embryos. Q RT PCR values are normalized to GAPDH. Asterisks indicate statistical significance, ($p<0.001$).

4.2. $\Delta Np63$ knock out mice have a uniform layer of skin but still have a defect in cell adhesion

$\Delta Np63^{-/-}$ pups were born but died within hours as a result of a fragile skin that could not retain body fluid. Pups still had defects in craniofacial and limb development that resulted in lacking nutrition that resulted in maternal neglect (**Figure 19A-D**). To further analyze of $\Delta Np63^{-/-}$ phenotypic characteristics, E18.5 embryos were used. Interestingly, microscopic analyses highlighted the phenotypic differences between the $\Delta Np63^{-/-}$ and $p63^{-/-}$ animal skin (**Figure 19A-D**). The $\Delta Np63^{-/-}$ animals have greater epidermal development and even hair follicle like structures are observed (**Figure 19G**).

To confirm the deletion of $\Delta Np63$ in the epidermal skin, immunohistochemistry (IHC) was performed using an antibody against $\Delta Np63$ on sections of embryos. Animals from different genotypes, which include the *wild type*, $p63^{-/-}$, $\Delta Np63^{+/-}$ and $\Delta Np63^{-/-}$. $\Delta Np63$ signals are not observed from $\Delta Np63^{-/-}$ and $p63^{-/-}$ skin (**Figure 19I-L**).

4.3. $\Delta Np63^{+/-}$ mice have wrinkled and expanded basal layer of skin

Skin from heterozygote embryos, $\Delta Np63^{+/-}$, macroscopically looked thicker compared to the wild type, which led me to question whether there are any phenotypic differences in heterozygote skin (**Figure 19B**). To further analyze the thicker skin phenotype from heterozygote embryos, skin from $\Delta Np63^{+/-}$ embryos was fixed, paraffin embedded, sectioned and stained with hematoxylin and eosin (H&E) (**Figure 19F**) to

observe epidermal architectural differences. Interestingly, the skin from $\Delta Np63^{+/+}$ mice had expanded and more enucleated cells in the basal layer of epidermis compared to wild-type animals.

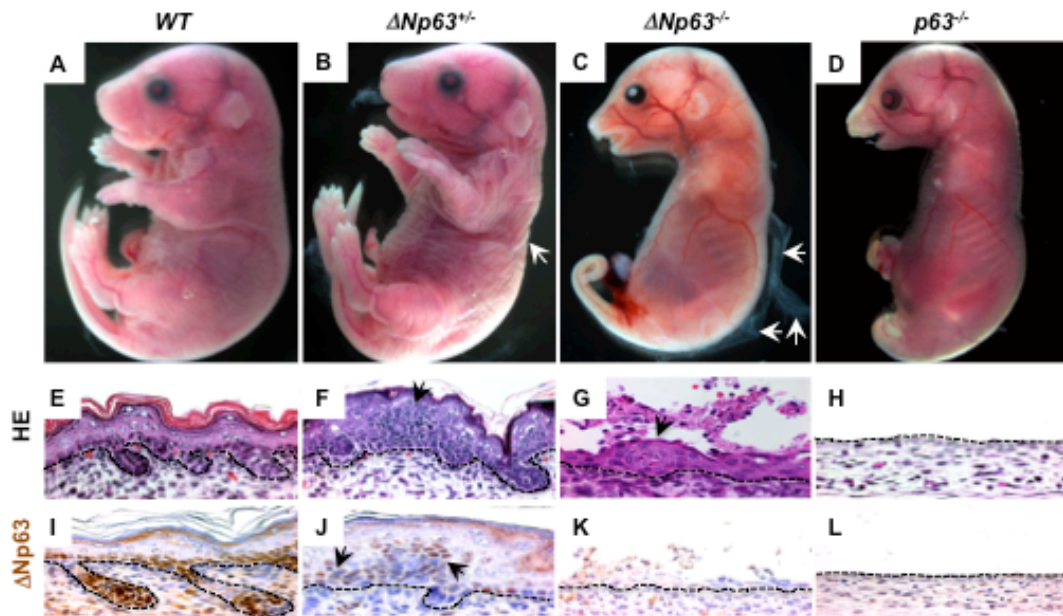


Figure 19. $\Delta Np63$ mutant mice exhibit epidermal abnormalities.

A-D) Embryos at day E18.5 of the following genotypes: wild-type (**A**), $\Delta Np63^{+/-}$ (**B**), $\Delta Np63^{-/-}$ (**C**), and $p63^{-/-}$ (**D**). Arrows in panel (**B**) indicate extra folds of skin and in panel (**C**) indicate non-adherent skin. **E-H)** Hematoxylin and eosin stained cross sections of the skin of E18.5 embryos of the following genotypes: wild-type (**E**), $\Delta Np63^{+/-}$ (**F**), $\Delta Np63^{-/-}$ (**G**), and $p63^{-/-}$ (**H**). Arrows indicate basaloid cells above the basal layer of the epidermis. **I-L)** Immunohistochemistry for $\Delta Np63$ in cross sections of E18.5 skin from embryos of the following genotypes: wild-type (**I**), $\Delta Np63^{+/-}$ (**J**), $\Delta Np63^{-/-}$ (**K**), and $p63^{-/-}$ (**L**).

4.4. A defect in skin differentiation in the $\Delta Np63^{-/-}$ mice

Studies from others and the Flores laboratory have shown that TAp63 and $\Delta Np63$ have different roles in skin differentiation (Koster et al., 2005; Keyes et al., 2004; Truong et al., 2006; Su et al., 2009). In particular, Su et al. (2009) generated $TAp63^{-/-}$ mice that showed no defects in skin differentiation during embryonic development. Hence, I hypothesize that $\Delta Np63$ is essential for proper epidermal differentiation. To test this hypothesis, differentiation marker analyses were performed with keratin 5 (K5) and keratin 14 (K14) as a basal layer marker, keratin 10 (K10) as a spinous layer marker and filaggrin (Fila) as a granular layer marker on E18.5 embryo skin. Surprisingly, all differentiation markers were expressed in $\Delta Np63^{-/-}$ but the expression was not as robust as in wild-type embryos (compare **Figures 20G & K** to **Figures 20F & J**) suggesting an inhibition of differentiation in the absence of $\Delta Np63$ (**Figure 20C, G, and K**). All differentiation marker expression was also expanded in $\Delta Np63^{+/-}$ embryos (**Figure 20B**). Given the apparent disorganization of epidermis in $\Delta Np63$ deficient embryos, I investigated whether expanded expression of differentiation markers in the $\Delta Np63$ embryos is due to improper epidermal differentiation. Double staining was performed using antibodies, K14 and K10. These overlap expression (**Figure 20N & O**) of two different layer markers, K14 and K10 in $\Delta Np63^{+/-}$ and $\Delta Np63^{-/-}$ embryos (**Figure 20N & O**).

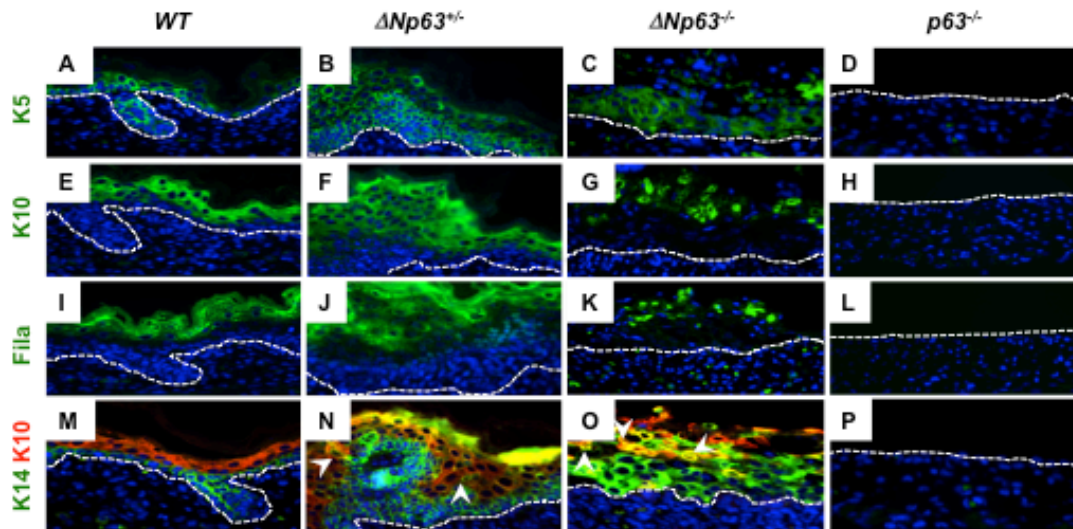


Figure 20. $\Delta Np63$ mutant mice display defects in epidermal differentiation.

Immunofluorescence using skin from E18.5 day embryos of the indicated genotypes.

Antibodies used are as follows: (A-D) keratin 5, (E-H) keratin 10, (I-L) filaggrin, and

(M-P) keratin 14 (green) and keratin 10 (red). DAPI was used as a counterstain.

Magnification 400X.

4.5. Aberrant proliferation in spinous layer of epidermis in $\Delta Np63^{-/-}$ mice

Improper differentiation and expansion of basal layer cells led me to ask whether this differentiation defect resulted from altered proliferation in the $\Delta Np63$ ablated epidermis. To address this question, first, a BrdU incorporation assay was performed on embryonic day E18.5 embryos. The pregnant females were timed at 18.5 days through $\Delta Np63^{+/-}$ females intercrossing with $\Delta Np63^{+/-}$ males and embryos were collected from the pregnant females at 18.5 dpc. BrdU was injected 3 times in 1 hour interval into pregnant females and 1 hour after the last injection embryos were harvested (Su. et al., 2009). To count the number of proliferative cells in basal layer of epidermis, double staining was performed using antibodies against to K5 and BrdU (**Figure 21A- C**). Since there were BrdU positive cells above the basal layer, to determine the origin of the signal, double staining with K10 and BrdU was also performed (**Figure 21D- F**). Double positivity for K10 and BrdU was not clearly visualized in wild type skin, while there were double K10 and BrdU positive signals sectioned skins from $\Delta Np63^{+/-}$ and $\Delta Np63^{-/-}$ embryos. These results indicate that loss of $\Delta Np63$ results in aberrant proliferation compared to wild type skin (**Figure 21G & H**). Since loss of $\Delta Np63$ led to aberrant proliferation in epidermal layers, it prompted me to hypothesize that $\Delta Np63^{-/-}$ keratinocytes proliferate in vitro.

Epidermal keratinocytes were harvested from $\Delta Np63^{-/-}$ epidermis and cultured. To measure the proliferation rate of epidermal cells from wild type and $\Delta Np63^{-/-}$, epidermal cells were cultured for 5 days and 10 days on J2-3T3 feeders (**Appendix 3**).

Interestingly, more cell numbers at indicated days in $\Delta Np63^{-/-}$ epidermal cells ($\Delta Np63^{-/-}$ keratinocytes have a similar result, data not shown) showed hyperproliferation and longer culture showed stem-like cell morphology in vitro (**Figure 24A & B**).

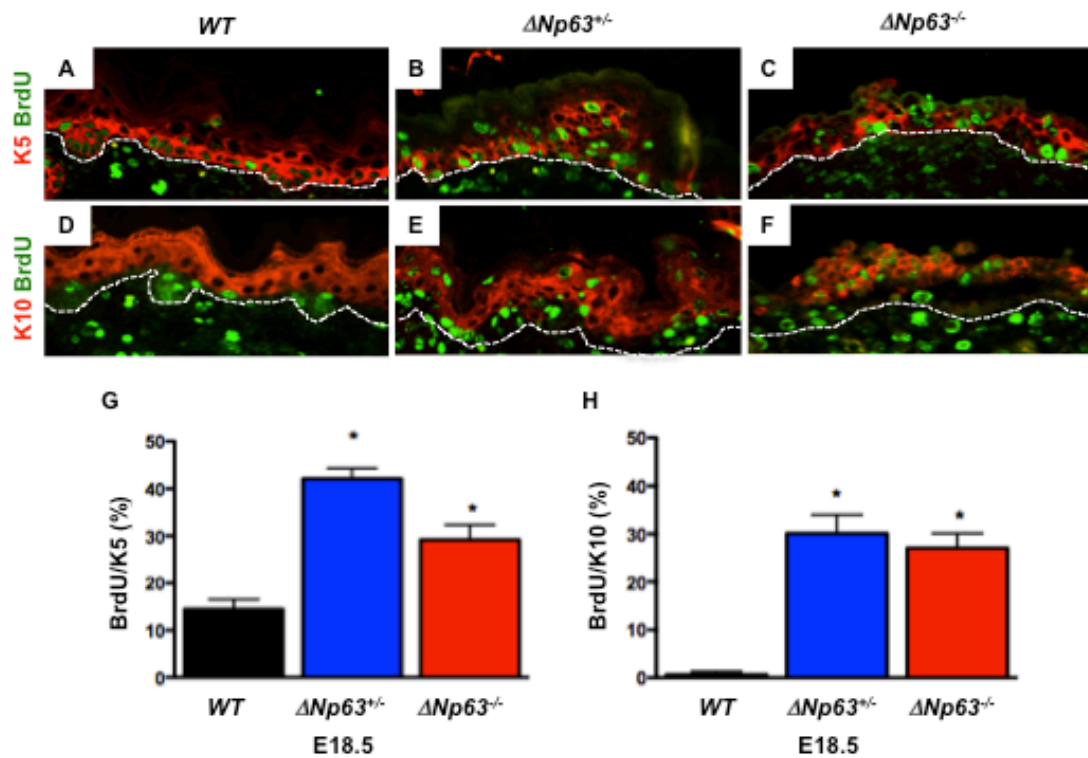


Figure 21. $\Delta Np63$ mutant mice have a hyperproliferative epidermis.

A-F) Double immunofluorescence using skin from E18.5 day embryos of the indicated genotypes. Antibodies used are as follows: **(A-C)** keratin 5 (K5, red) and BrdU (green) and **(D-F)** keratin 10 (K10, red) and BrdU (green). DAPI was used as a counterstain. Magnification 400X. **G)** Percentage of BrdU positive cells expressing K5. **H)** Percentage of BrdU positive cells expressing K10. Asterisks indicate statistical significance, ($p < 0.001$).

4.6. Molecular mechanism contributing to the regulation of epithelial differentiation of $\Delta Np63$

4.6.1. $\Delta Np63$ mutant mice phenocopy of $DGCR8^{fl/fl};K14Cre+$ and $Dicer^{fl/fl};K14Cre+$ mice hair follicle outgrowing.

Phenotypic defects in stratification and proliferation observed in skin from the $DGCR8^{fl/fl};K14Cre+$ and $Dicer^{fl/fl};K14Cre+$ mice (Yi et al., 2006; Yi et al., 2009) were similar to phenotypes observed in the absence of $\Delta Np63$, which include expansion of the basal layer, hyperproliferation, hair follicles evagination and a defect in differentiation. To determine whether there is outgrowing hair germ in $\Delta Np63^{+/-}$ and $\Delta Np63^{-/-}$ epidermis, like $DGCR8^{fl/fl};K14Cre+$ and $Dicer^{fl/fl};K14Cre+$ mice, double staining on $\Delta Np63^{fl/fl};K14Cre+$ and $\Delta Np63^{fl/+};K14Cre+$ were performed for Lef1 as a hair germ marker (**Figure 22**) (Merrill et al., 2001). The $\Delta Np63^{+/-}$ and $\Delta Np63^{-/-}$ embryo epidermis at E18.5 showed hair germ outgrowth by confirmation of Lef1 expression (**Figure 22B, C, F & G**). Hence, I hypothesize that $\Delta Np63$ regulates $DGCR8$ and/or $Dicer$ in mice skin.

4.6.2. $DGCR8$ is a unique target gene of $\Delta Np63$.

$DGCR8$ forms a complex with Drosha, which processes primary microRNAs to precursor microRNAs in the nucleus. Studies from the Flores laboratory (Su & Chakravarti et al., 2010) have reported that TAp63 transcriptionally regulates $Dicer$.

With phenotypic similarities between *DGCR8^{fl/fl};K14Cre+* and *Dicer^{fl/fl};K14Cre+* mice with respect to epidermal development, I wanted to determine whether Δ Np63 regulates expression of the 3 microRNA-processing component genes. To address this question, q-RT PCR was performed with primers for *Dicer*, *DGCR8* and *Drosha* using RNA from E18.5 wild type and *Δ Np63^{-/-}* mice skin. Interestingly, Δ Np63 only down modulates *DGCR8* mRNA expression. However, none of *Dicer* and *Drosha* mRNA levels seemed to differ between two genotypes (**Figure 22G**). It prompted me to ask whether TAp63 also regulates *DGCR8* mRNA as similar in *Dicer* regulation (Su & Chakravarti et al., 2010). To address this question, q-RT PCR was also performed for *DGCR8* using RNA extracted from *TAp63^{-/-}* keratinocytes. However, in the absence of *TAp63*, a *DGCR8* mRNA expression levels are not down modulated (**Figure 22H**), which indicates that Δ Np63 is a unique regulator of *DGCR8* mRNA expression.

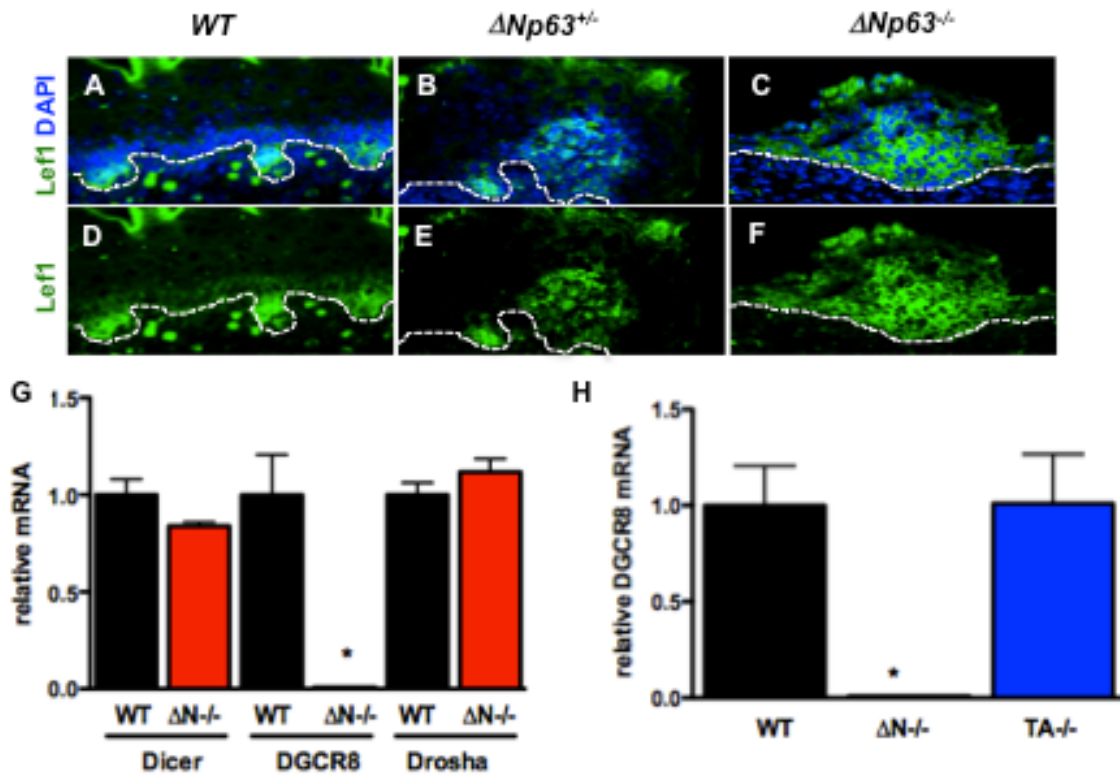


Figure 22. $\Delta Np63$ deficient mice epidermis is reminiscent to $DGCR8^{fl/fl};K14Cre+$ and $Dicer^{fl/fl};K14Cre+$ mice.

Immunofluorescence using skin from E18.5 day embryos of the indicated genotypes. **A-C**) Lef1 (green) and DAPI (blue) or **D-F**) Lef1 (green) only. **G**) qRT-PCR for *Dicer*, *DGCR8* and *Drosha* using total RNA from wild-type (WT) and $\Delta Np63^{-/-}$ ($\Delta N^{-/-}$) epidermal cells. **H**) qRT-PCR for *DGCR8* using total RNA from wild-type (WT), $\Delta Np63^{-/-}$ ($\Delta N^{-/-}$) and *Tap63*^{-/-} epidermal cells.

4.6.3. Δ Np63 transcriptionally regulates *DGCR8* via direct binding to its promoter

To further understand how Δ Np63 regulates *DGCR8* gene expression and to address whether the *DGCR8* gene down-regulation results from absence of p63 to transactivate the gene, chromatin immunoprecipitation (ChIP) analysis was performed using specific antibody for p63. 2 putative sites (site 1 and site 2) in the Intron1 of *DGCR8* were found to be a binding consensus region where p63 could bind, however p63 only bound to site1 of *DGCR8* promoter (**Figure 23A**). To verify whether that site is a specific binding site of p63, a set of non-specific primers were designed and located at 500bp upstream from the site 1, indicating site 1 is specific for binding (**Figure 23B**). To further verify its binding on the promoter of *DGCR8* can functionally regulate gene transcription, the *DGCR8-Luciferase* reporter gene construct (dgcr8 S) was constructed which included site1 sequence. Dgcr8 S was mutated (dgcr8 Sm) using a site-directed mutagenesis kit to change the consensus site from (ctgCATGtatctcctaagaagcCTTGcca) to (ctgTTTTtatctcctaagaagcTTTTcca), using a binding site that contains putative p63 binding site from ChIP as a negative control. Dgcr8 S or dgcr8 Sm were transfected with a p63 isoform expressing plasmid, TAp63 α , β or γ or Δ Np63 α , β or γ (**Figure 23D**) into *p53*^{-/-};*p63*^{-/-} MEFs. Only Δ Np63 isoforms could transactivate *luciferase* reporter gene activity but the mutated reporter construct was not transactivated by any of p63 isoforms (**Figure 23D**). This indicates that the binding site is specific for Δ Np63, but not for TAp63. This result is consistent with q-RT PCR for *DGCR8* mRNA expression (**Figure 22**).

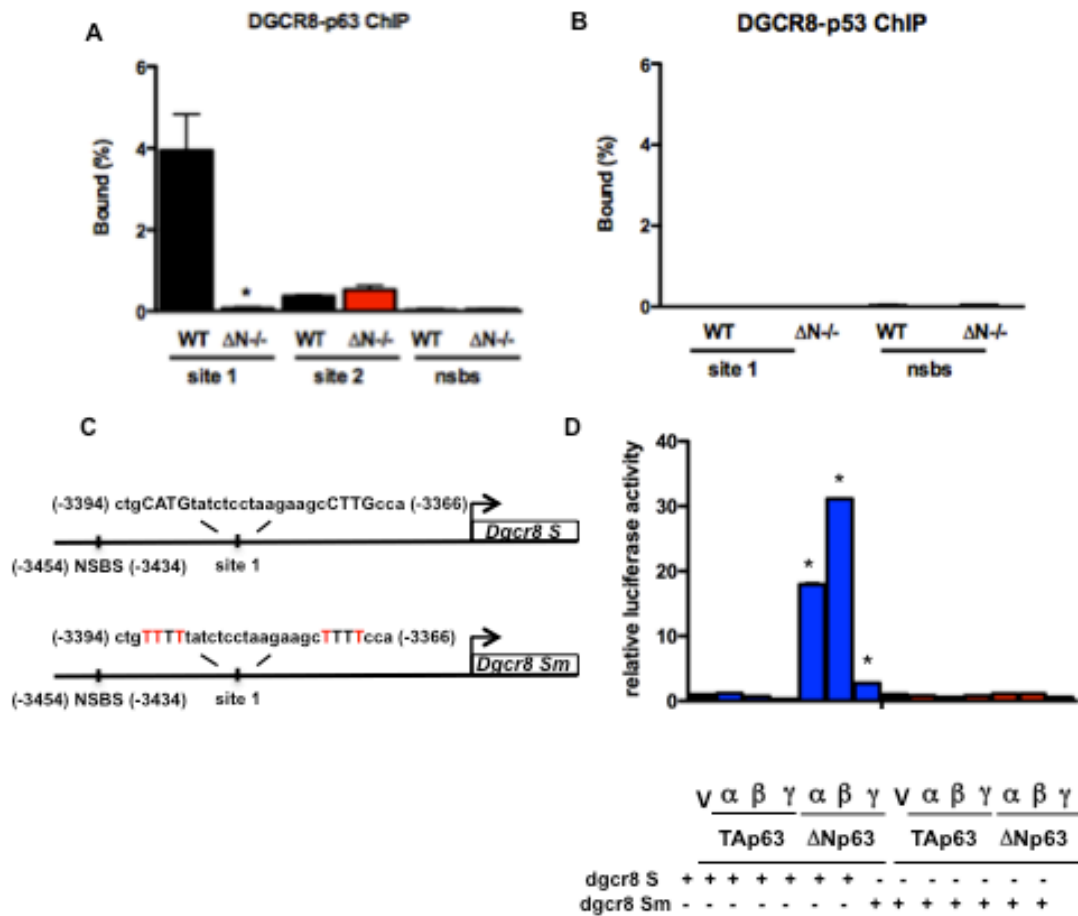


Figure 23. *DGCR8* is transactivated by $\Delta Np63\alpha$, $\Delta Np63\beta$ and $\Delta Np63\gamma$.

A & B) qRT-PCR of ChIP assay using wild-type (WT) and $\Delta Np63^{-/-}$ ($\Delta N^{-/-}$) epidermal cells and indicating p63-binding site (site 1) or no binding of p63 to site 2 or non-specific binding site (NSBS) (**A**) or no binding of p53 to the indicated sites (**B**). **C**) Schematic showing *DGCR8*-site 1 (*dgcr8 S*-) and *DGCR8*-mutant of site 1 (*dgcr8 Sm*-)

luciferase reporter genes. **D)** Luciferase assay for *DGCR8* in *p53*^{-/-};*p63*^{-/-} MEFs transfected with the indicated p63 isoforms and the indicated *luciferase* reporter gene. Each bar represents the average of the fold activation of three independent experiments. The asterisks indicate statistical significance (p-value <0.001).

4.6.4. Loss of $\Delta Np63$ results in higher expression of the pluripotency regulators, *Oct4*, *Sox2* and *Nanog*.

We have seen the failure of terminal differentiation in $\Delta Np63$ lacking skin. To characterize thoroughly the role of $\Delta Np63$, I isolated cells and deleted the allele acutely to understand down stream consequence. Loss of $\Delta Np63$ shows a hyperproliferation phenotype in embryos at E18.5 and also in vitro epidermal cell culture (**Appendix 3**). Interestingly, I observed that $\Delta Np63^{-/-}$ epidermal cells exhibit a unique undifferentiated morphology that does not resemble keratinocytes. Moreover, when I ablated $\Delta Np63$ by administering adenovirus-cre recombinase to $\Delta Np63^{fl/fl}$ keratinocytes, a similar undifferentiated phenotype was observed within hours of $\Delta Np63$ deletion (compare **Figure 24A & B**). Consistent with our model, $DGCR8^{-/-}$ embryonic stem (ES) cells have a hyperproliferation phenotype and a delayed differentiation defect (Melton et al., 2010; Suh et al., 2010). Also, in $DGCR8^{-/-}$ embryonic stem cells (ES), expression of *Oct4*, *Sox2* and *Nanog* genes were not diminished by differentiation stimulators, it resulted in delayed differentiation and hyperproliferation (Melton et al., 2010). To further elucidate the roles of $\Delta Np63$ in differentiation, an in vitro system using primary epidermal cells was employed and cells were subjected to high calcium (1.6mM, Ca^{2+}) to induce terminal differentiation (Su et al., 2009; Flores et al., 2000). To determine the efficiency of differentiation in vitro cell system, western analysis was performed to test protein expression levels with the use of differentiation markers (**Figure 24C**). Interestingly, filaggrin, a terminal differentiation marker, expression was too low to detect under high

calcium conditions. It indicates the possibility of delayed or improper differentiation both *in vivo* and *in vitro* due to loss of $\Delta Np63$.

I tried to address the question whether pluripotency regulating genes expression is modulated in $\Delta Np63^{-/-}$ epidermal cells. I observed that in $\Delta Np63$ KO and cKO epidermal cells display high expression of *Oct4*, *Sox2* and *Nanog* (**Figure 24D-F**). This corresponds to the pluripotent genes, *Oct4*, *Sox2* and *Nanog*, in which the expression is concomitantly elevated in $\Delta Np63$ deficient cells. Hence, I hypothesized that $\Delta Np63$ represses pluripotency regulators expression through the transcriptional regulation of *DGCR8*. To understand the molecular mechanism between DGCR8 and pluripotency regulators, its genes expression level was tested. The expression of pluripotent genes was down regulated to wild type level after DGCR8 restoration in the $\Delta Np63^{-/-}$ epidermal cells (**Figure 24B-D**). An alternative approach to test the hypothesis was to perform a loss of function experiment with infecting of short-hairpin DGCR8 (shDGCR8) virus into wild type epidermal cells and then expression levels of the pluripotency genes was determined. The expression pattern was found to be increased in shDGCR8 infected wild type epidermal cells (**Appendix 4**).

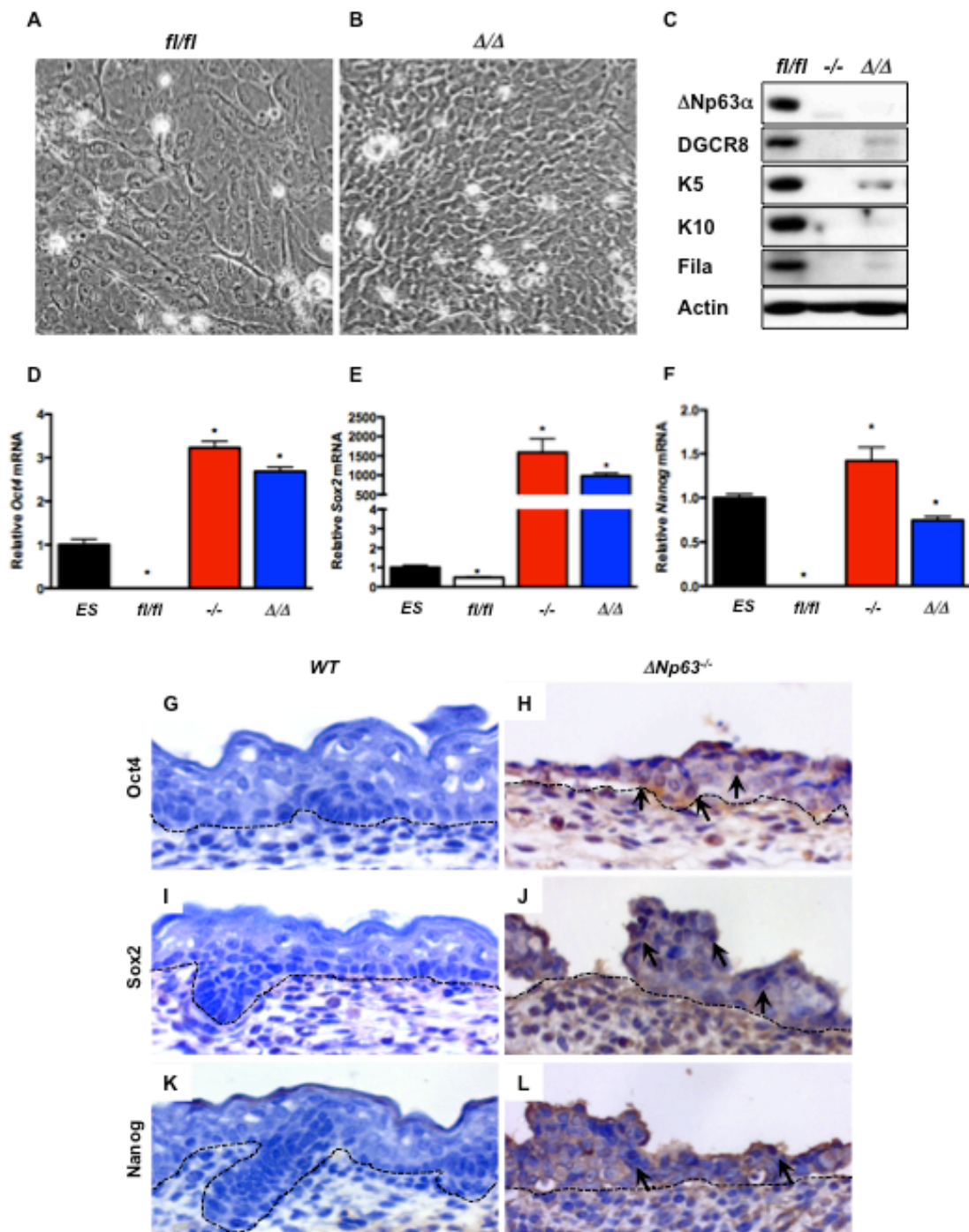


Figure 24. *Oct4*, *Sox2* and *Nanog* are upregulated in $\Delta Np63$ deficient epidermal

cells.

A & B) Epidermal cells derived from the skin of $\Delta Np63$ conditional knock out mice (fl/fl) (**A**) and $\Delta Np63fl/fl$ epidermal cells infected with adenovirus-cre for 6 hours to generate $\Delta Np63$ deficient (Δ/Δ) epidermal cells. **C)** Western blot analysis of epidermal cells derived from mice of the indicated genotypes grown under conditions that promote keratinocyte differentiation (High Ca^{2+}) and using the indicated antibodies. Actin was used as a loading control. **D-F)** qRTPCR using total RNA from mouse embryonic stem cells (ES) and epidermal cells of the indicated genotypes for *Oct4* (**D**), *Sox2* (**E**), and *Nanog* (**F**). Asterisks indicate statistical significance (p-value <0.001). **G-L)** Immunohistochemistry for Oct4 (G&H), Sox2 (I&J), and Nanog (K&L) in cross sections of E18.5 skin from embryos of the following genotypes: wild-type (**G, I&K**), and $\Delta Np63^{-/-}$ (**H, J&K**).

4.6.5. Repression of mir470 and mir145 in $\Delta Np63^{-/-}$ and Δ/Δ epidermal cells correspond to elevated mRNA levels of *Oct4*, *Sox2* and *Nanog*.

ΔNp63 deficient epidermal cells had diminished expression of *DGCR8*, well-known microRNA processor complex protein. This prompted us to search for microRNAs that might involve in this stem-like morphological phenotype in *ΔNp63Δ/Δ* epidermal cells. Earlier, Tay et al., and Xu et al. reported miR470 and miR145 are important regulators to commit embryonic stem cell undergoing differentiation (Tay et al., 2008; Xu et al., 2009). These microRNAs repress *Oct4*, *Sox2* and *Nanog*, when ES cells commit to differentiation (Tay et al., 2008). Hence, the new hypothesis was whether *ΔNp63* induces differentiation via *DGCR8* regulation through miR470 and miR145. To test this hypothesis, Taqman based real time PCR was performed for *miR470* and *miR145*. As expected, *miR470* and *miR145* were repressed by loss of *ΔNp63*. Indeed, this level was similar to ES cells in *ΔNp63^{-/-}* epidermal cells and slightly higher in *ΔNp63* acute deleted epidermal cells, *ΔNp63Δ/Δ* (**Figure 25B-D**). To further understand the molecular mechanism, *DGCR8* was restored using Flag-*DGCR8* retrovirus infection. *MiR470* and *miR145* expressions were found to be similar to the wild type epidermal cells (**Figure 25E & F**). These data indicate that *ΔNp63* deficient epidermal cells might obtain pluripotency as a result of misregulation of repression of microRNAs, *miR470* and *miR145*, on *Oct4*, *Sox2* and *Nanog* via diminution of *DGCR8*.

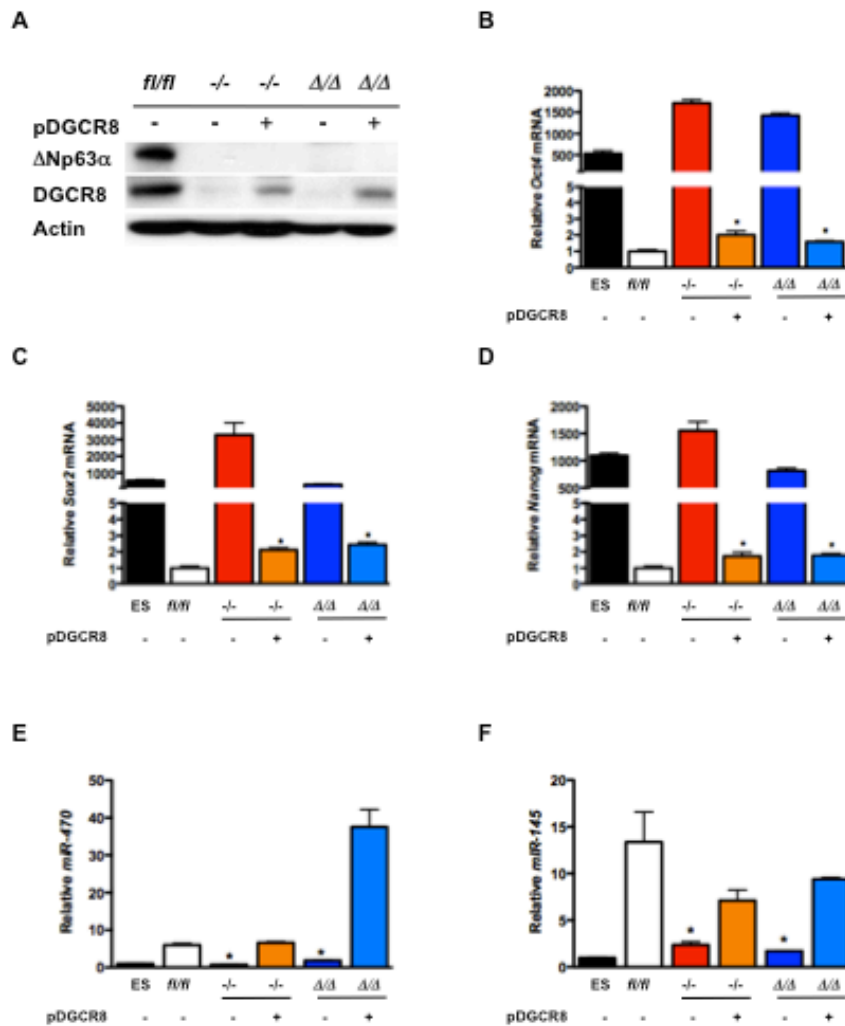


Figure 25 Restoration of DGCR8 rescues defect in differentiation in Δ Np63 deficient epidermal cells

A) Western blot analysis of epidermal cells of the indicated genotypes with the antibodies shown. **B-D)** qRT-PCR using total RNA from epidermal cells of the indicated genotypes. Cells expressing DGCR8 are indicated by (pDGCR8). Expression of *Oct4* (**B**), *Sox2* (**C**), and *Nanog* (**D**) were analyzed. **E & F)** TaqMan reverse transcriptase

mediated PCR for *miR-470* (E) and *miR-145* (F) using RNA from the indicated samples.

Asterisks indicate statistical significance (p-value <0.001)

4.6.6. $\Delta Np63$ regulates cell fate and cell differentiation via the regulation of *DGCR8*.

$\Delta Np63$ mutant cells resulted in transcriptional down regulation of *DGCR8* that gave rise to pluripotency characteristics. I hypothesized that $\Delta Np63$ governs proper terminal differentiation by transcriptional regulation of *DGCR8* in the mouse epidermis. Previous studies have demonstrated that overexpression of Oct4 in wild type mouse keratinocytes changed their cell fate from keratinocytes to neuronal cells, when it cultured in neuroectodermal media (Grinnell et al., 2007). To test whether loss of *$\Delta Np63$* led cells to differentiate to multiple cell fates, *$\Delta Np63\Delta/\Delta$* epidermal cells were cultured in neuroectodermal media. To determine whether *DGCR8* is necessary for differentiation, I cultured cells absent or present *DGCR8* in neuroectodermal media. As previously shown by Grinnell, epidermal cells changed cellular morphology to neuronal cells which were confirmed by the expression of neuronal cell markers, *Nestin* for neuronal membrane marker and *NeuN* for neurons by q-RT PCR primers designed against mRNA, with or without *DGCR8* restoration in *$\Delta Np63\Delta/\Delta$* epidermal cells (**Figure 26A-C**). It seems *$\Delta Np63\Delta/\Delta$* epidermal cells no longer have keratinocyte cell fate, so they will be called epidermal cells. I transfected *DGCR8* plasmid into acute deleted *Δ/Δ* epidermal cells and subjected cells the high calcium (Ca^{2+} , 1.6mM) to induce epidermal cells differentiation for a period of 3days. Differentiation marker western blot analyses were performed to determine whether terminal differentiation is rescued by restoration of *DGCR8* (**Figure 26D & E**). I inferred from the western blot

analysis that restoration of DGCR8 rescued the differentiation defect in epidermal cells. The restoration of DGCR8 in $\Delta Np63$ deficient cells rescued improper epidermal cell differentiation. Importantly, restoration of DGCR8 in $\Delta Np63$ deficient cells resulted in the different cell fate to neuronal cells. Hence, transcriptional regulation of *DGCR8* by $\Delta Np63$ enabled processing the mature miR470 and miR145 to repress pluripotency genes, *Oct4*, *Sox2* and *Nanog*, thereby differentiation defects were rescued in the $\Delta Np63$ ^{-/-} mice skin (**Figure 26D & E**).

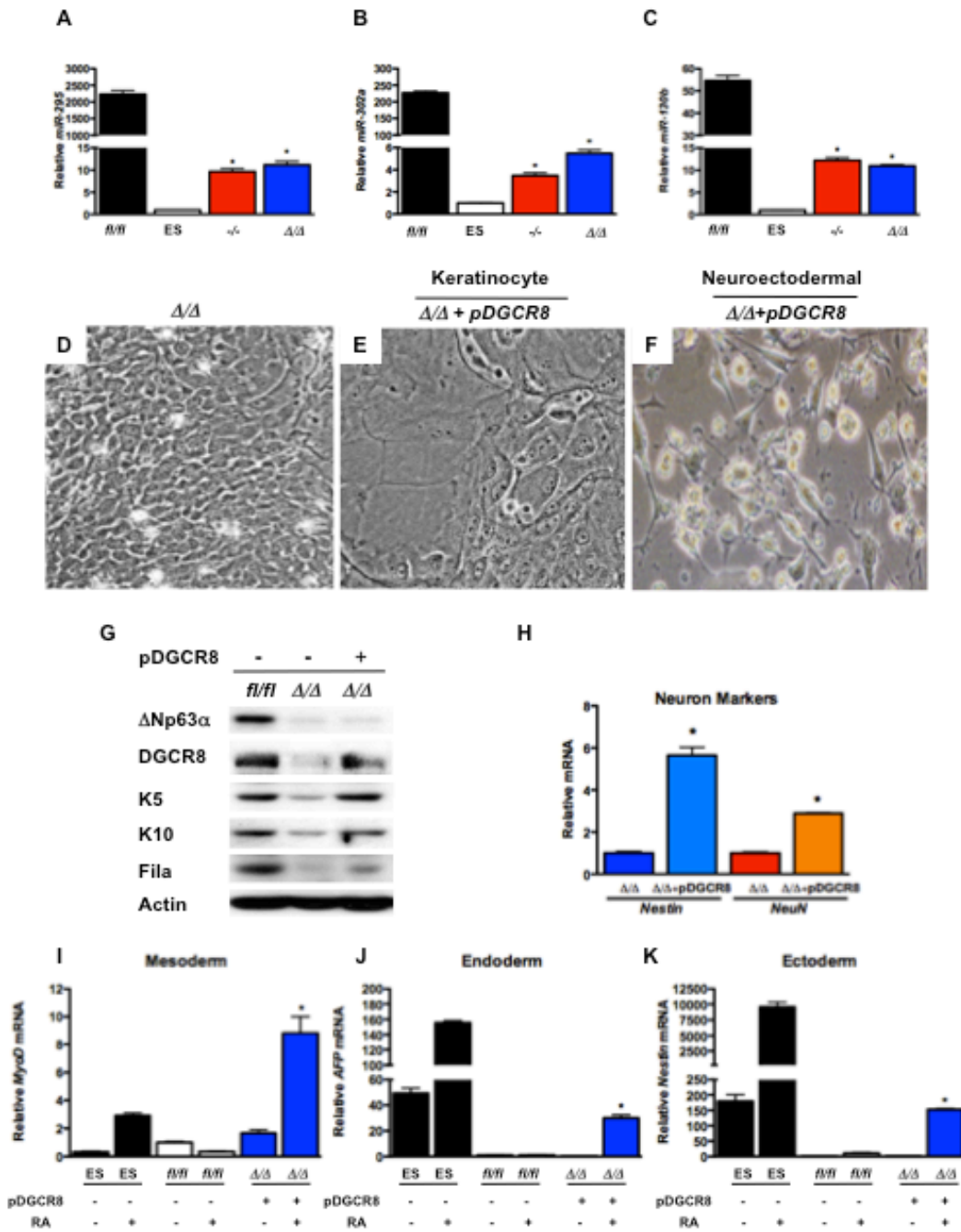


Figure 26. $\Delta Np63$ deficient epidermal cells are pluripotent and can self-renew.

A-C) TaqMan reverse transcriptase mediated PCR for *miR-295* (**A**), *miR-302a* (**B**) and *miR-130b* (**C**) using RNA from the indicated samples. Asterisks indicate statistical significance (p-value <0.001), **D-F)** $\Delta Np63$ deficient epidermal cells (Δ/Δ) cultured under the following conditions: **(D)** keratinocyte media Low Ca²⁺, **(E)** keratinocyte differentiation media (High Ca²⁺), and **(F)** neuroectodermal media. **G)** Western blot analysis of epidermal cells of the indicated genotypes with (+pDGCR8) or without (-pDGCR8) DGCR8 and using the antibodies shown. Actin was used as a loading control. **H)** qRT-PCR for *nestin* and *NeuN* using total RNA from the epidermal cells of the indicated genotypes. **I-K)** qRT-PCR using total RNA from epidermal cells of the indicated genotypes with (+retinoic acid: RA) or without (-retinoic acid: RA) RA. Cells expressing DGCR8 are indicated by (pDGCR8). Expression of *MyoD*; a mesoderm marker (**I**), *AFP*, an endoderm marker (**J**), and *Nestin*, an ectoderm marker (**K**) were analyzed.

4.7. Loss of $\Delta Np63$ results in obtaining self-renewal capacity in epidermal cells

To characterize whether $\Delta Np63$ ablated epidermal cells obtain stem cell properties, such as self-renewal capacity, a clone formation assay was performed as previously described (Barrandon and Green, 1987; Flores et al., 2000). 4×10^5 acutely ablated $\Delta Np63$ (Δ/Δ) epidermal cells were cultured on J2-3T3 feeders for 7 days interval until passage 5 (**Figure 26F**). To determine self-renewing capacity, cell numbers were counted and a BrdU incorporation assay was performed. Δ/Δ epidermal cells maintained their proliferative capacity that was confirmed by cell numbers and percentage of BrdU positivity (**Figure 26G & H**) indicating the ability to self-renew.

To determine whether the expression of pluripotency markers was sustained after serial passage in $\Delta Np63$ deficient epidermal cells, I examined mRNA levels of *Oct4*, *Sox2*, and *Nanog* in wild-type ($\Delta Np63^{fl/fl}$) and $\Delta Np63\Delta/\Delta$ epidermal cells from passage 1 to 5 (**Figure 26I-K**).

Taken together, current model is built according to my study in terms of differentiation from these results indeed suggests that $\Delta Np63$ induces terminal differentiation through regulation of *DGCR8* as a key factor during embryo development (**Figure 27**).

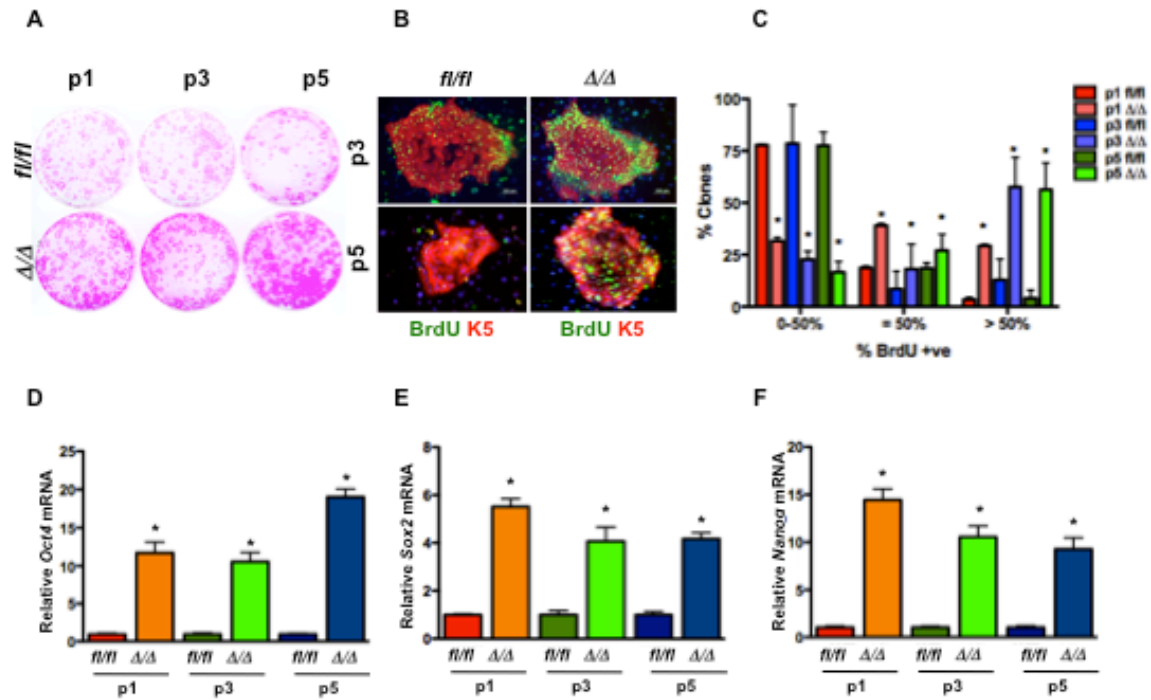


Figure 27. $\Delta Np63$ initiates epidermal differentiation through *DGCR8*.

A) Epidermal colonies from wild-type and $\Delta Np63$ deficient epidermal cells (Δ/Δ) cultured on J2 3T3 feeder layers and stained with rhodamine B. Passages 1 (P1), 3 (P3), and 5 (P5) are shown. **B)** Immunostaining for BrdU (green) and K5 (red) in passage 3 and 5 wild-type ($\Delta Np63^{fl/fl}$) and $\Delta Np63\Delta/\Delta$ (Δ/Δ) epidermal cells. DAPI (blue) was used as a counterstain. White bar indicates 100 μ m. **C)** Quantification of BrdU incorporation in colonies after 8 days in culture. Passages 1, 3, and 5 are shown. Experiments performed in triplicate. Asterisks indicate statistical significance (p-value <0.001). **D-F)** qRT-PCR from total RNA derived from wild-type ($\Delta Np63^{fl/fl}$) and

$\Delta Np63\Delta/\Delta$ (Δ/Δ) epidermal cells at passages 1, 3, and 5. Expression of *Oct4* (**D**), *Sox2* (**E**), and *Nanog* (**F**) were analyzed. Experiments performed in triplicate. Asterisks indicate statistical significance (p-value <0.001).

CHAPTER 5.

Roles of Δ Np63 in limb development, wound healing, and asymmetric cell division

5.1. Limb development and epidermal differentiation

Rationale: Recently, I have demonstrated that $\Delta Np63$ transcriptionally regulates *brachyury* gene expression and that low levels of *brachyury* result in truncated limbs of *p63* null mice (Cho et al., 2010). As expected, $\Delta Np63^{-/-}$ mice also develop truncated limbs indicating that $\Delta Np63$ is a regulator for limb formation (Cho et al. 2010; Cho et al., under review 2011). *Brachyury* was expressed at early embryonic day E5.5-E12.5 and was regulated by $\Delta Np63$ (Cho et al.). *p63* was already expressed at embryonic day E8.5 before stratification occurred (Cho et al.; Koster et al., 2004; Laurikkala et al., 2006).

Stratification occurs with formation of limb bud at embryonic day E9.5 and is coincident with expression of K5 and K14 (Sun et al.). I tested whether $\Delta Np63$ ablation between before- and after-differentiation differs from proper limb development. Hence, to delete $\Delta Np63$ after commitment to differentiation, $\Delta Np63^{fl/fl}$ mice mated with *K14Cre* transgenic mice (Jonkers et al., 2001) to obtain $\Delta Np63^{fl/fl};K14Cre$.

Hypothesis: I hypothesized that $\Delta Np63$ regulates proper limb development before the limb bud starts differentiation.

5.1.1. Cre recombines 90% of $\Delta Np63$ alleles in $\Delta Np63^{fl/fl};K14Cre+$ (Δ/Δ) mice.

To determine whether $\Delta Np63$ functions before differentiation begins, *K14Cre* transgenic mice were used to delete $\Delta Np63$ allele after differentiation began. *K14Cre* mice are transgenic mice. Cre is a recombinase that was controlled under the *K14* promoter (Jonkers et al., 2001). To segregate the difference between a germ line deletion and deletion after differentiation using *K14Cre* transgenic mice, $\Delta Np63^{fl/fl};K14Cre+$ (Δ/Δ) mice were generated by crossing $\Delta Np63^{fl/fl}$ mice and *K14Cre* transgenic mice (Jonkers et al., 2001). Since *K14Cre* transgenic mice were crossed to remove $\Delta Np63$ allele conditionally in K14 positive cells, to determine how much deletion of $\Delta Np63$ took place in the basal layer of epidermis, IHC staining was performed using $\Delta Np63$ specific antibody showed greater than 90% of $\Delta Np63$ was deleted (**Figure 28D**).

Epidermal differentiation remarkably occurred in $\Delta Np63^{fl/fl};K14Cre+$ (Δ/Δ) mice. The multi-layered epidermis existed (**Figure 29B & D**) in $\Delta Np63^{fl/fl};K14Cre+$ (Δ/Δ) mice.

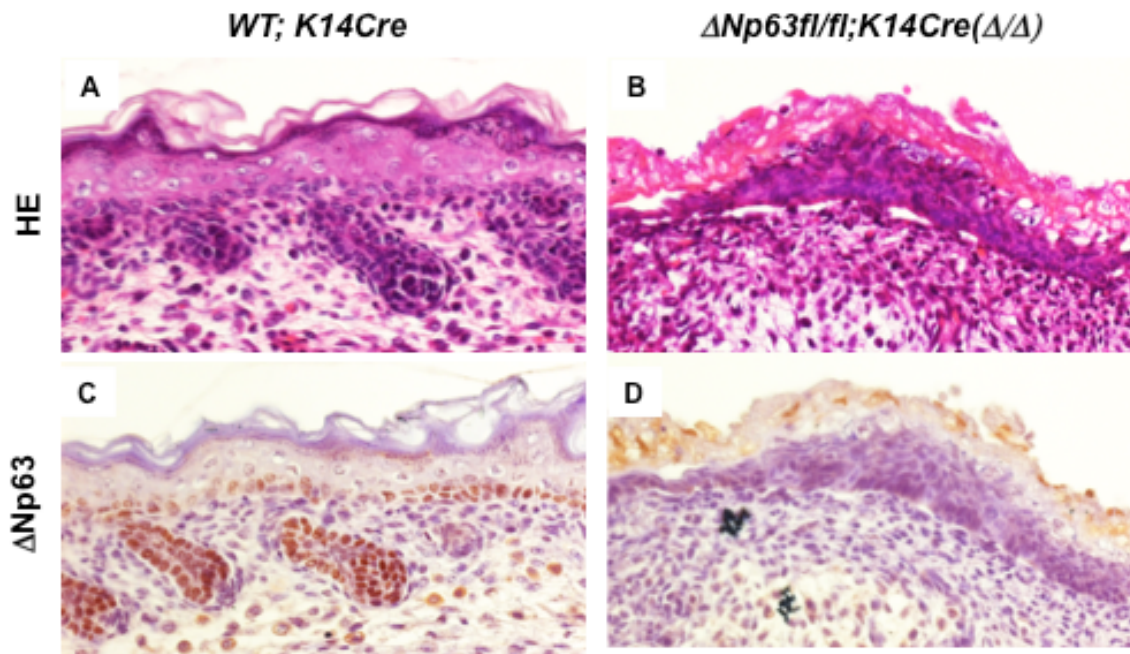


Figure 28. Stratification occurred in $\Delta Np63^{fl/fl};K14Cre^+$ (Δ/Δ) mice epidermis.

A & B) Hematoxylin and eosin stained cross sections of the skin of E18.5 embryos of the following genotypes: *WT; K14Cre* and *$\Delta Np63^{fl/fl};K14Cre$ (Δ/Δ)*. **C & D)** Immunohistochemistry antibody against $\Delta Np63$ stained cross sections of the skin of E18.5 embryos of the following genotypes: *WT; K14Cre* and *$\Delta Np63^{fl/fl};K14Cre$ (Δ/Δ)*.

(Cho & Flores, unpublished)

5.1.2. $\Delta Np63$ acts early in limb development and epidermal skin differentiation.

A very interesting observation from $\Delta Np63^{fl/fl}; K14Cre+$ (Δ/Δ) mice, fore- and hind limbs formed in $\Delta Np63^{fl/fl}; K14Cre+$ (Δ/Δ) mice. *Brachyury* was regulated by $\Delta Np63$ isoforms to form limbs, which I already demonstrated in *in vitro* cell system (Cho et al., 2010) and as previously shown in Chapter 4 in this thesis: $\Delta Np63$ isoforms regulated *brachyury* during limb development and $\Delta Np63^{-/-}$ mice developed truncated limbs and died within hours after birth with fragile and disorganized epidermis appearance (Cho et al., 2011 submitted). Koster (2007) and Cho (2010) have reported that $\Delta Np63$ is expressed from embryonic day at E8.5~ E9.5. To further understand how $\Delta Np63$ plays a role in limb developmental defects as seen in the $p63^{-/-}$ and $\Delta Np63^{-/-}$ mice (Mills et al., 1999; Yang et al., 1999; Cho et al., submitted 2011), $\Delta Np63^{fl/fl}$ mice were crossed with the *K14Cre* transgenic mice (Jonkers et al., 2001) to obtain double heterozygous mice ($\Delta Np63^{fl/+}; K14Cre+$). Subsequent mating by intercrossing a female $\Delta Np63^{fl/+}; K14Cre+$ and a male $\Delta Np63^{fl/+}; K14Cre+$ mice gave rise to $\Delta Np63^{fl/fl}; K14Cre+$ (Δ/Δ) mice. Progenies were born with a Mendelian ratio and $\Delta Np63^{fl/fl}; K14Cre+$ mice were viable at birth; however, they also died within hours after birth as observed in $p63^{-/-}$ and $\Delta Np63^{-/-}$ mice. Importantly, the phenotype of $\Delta Np63^{fl/fl}; K14Cre+$ mice was dramatically different than $p63^{-/-}$ and even $\Delta Np63^{-/-}$ (**Figure 29**). $\Delta Np63^{fl/fl}; K14Cre+$ (Δ/Δ) mice developed proper face, ear and nose structures; in particular, limbs were remarkably well formed with little shortening in size and limbs from Δ/Δ mice

even had separate digit formation (**Figure 29E, F, G& H**). The digits are not completely separated but folded. They look similar to human's foot and hand disfiguring appearances (AEC and EEC) (**Figure 4**).

Additionally, in the dorsal view of $\Delta Np63^{fl/fl}; K14Cre+$ (Δ/Δ) mice limbs display thinner blood vessels. This result also indicates that $\Delta Np63$ functions early in development, especially the differentiation of limb, epidermis and blood vessel formation. However, further investigations of blood vessel formation and complete limb formation have remained to be done.

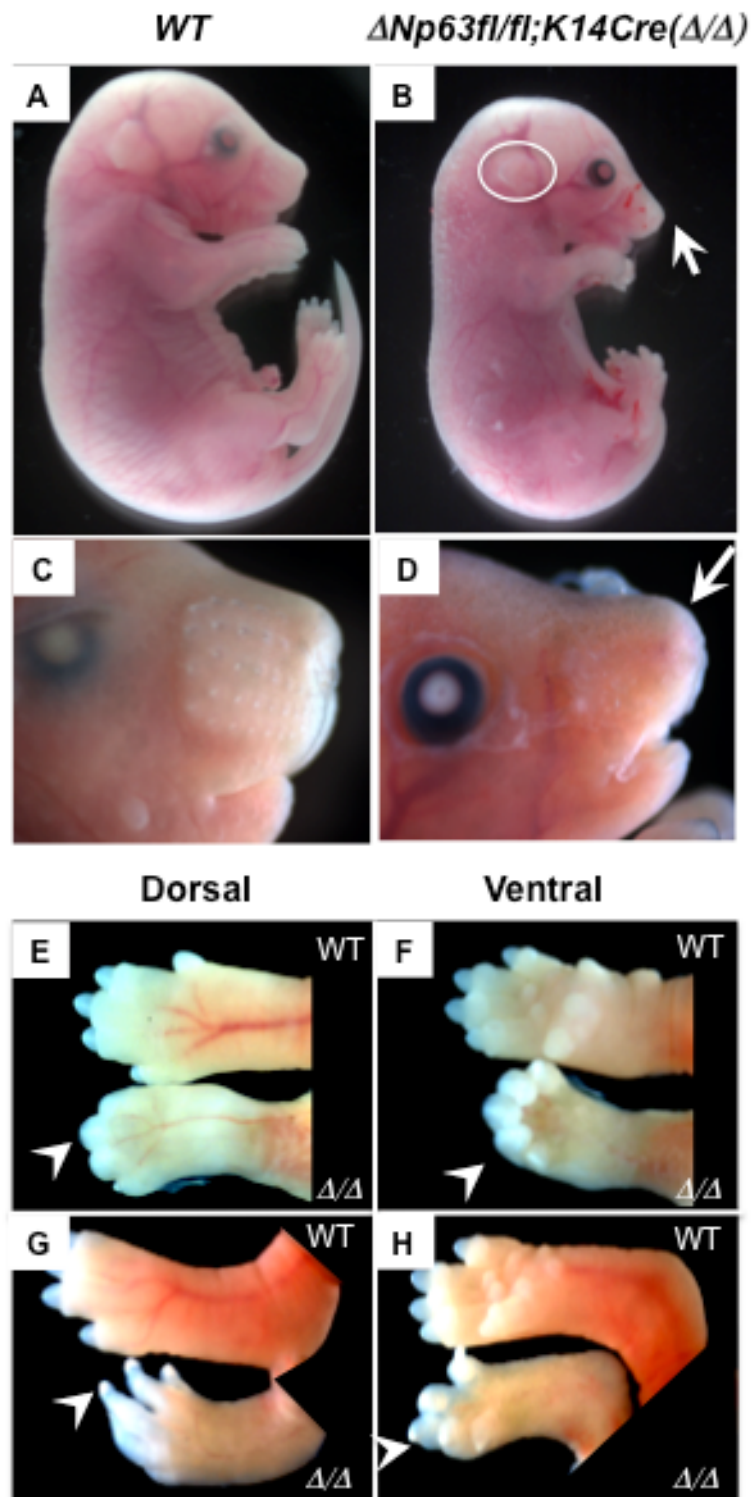


Figure 29. The view of $\Delta Np63^{fl/fl};K14Cre+$ (Δ/Δ) mice embryonic day at E18.5

A & B) Macroscopic view of wild type and $\Delta Np63^{fl/fl};K14Cre+$ (Δ/Δ) embryos at day E18.5. (White arrow indicates lip area in $\Delta Np63^{fl/fl};K14Cre+$ and white circle indicated proper developed ear in $\Delta Np63^{fl/fl};K14Cre+$. **C & D)** Mouth developed properly in $\Delta Np63^{fl/fl};K14Cre+$ that does not show cleft lip but still eye lids are covered incompletely and **E, F, G & H)** limb and digit dorsal and ventral views from wild type and $\Delta Np63^{fl/fl};K14Cre+$ (white arrow head indicates folded digits) (**Cho and Flores, unpublished**).

5.2. The role of $\Delta Np63$ in Wound healing

Rationale: Since $\Delta Np63^{-/-}$ and $\Delta Np63^{fl/fl};K14Cre^{+}(\Delta/\Delta)$ mice prematurely die, it becomes too difficult to study functions of $\Delta Np63$ at adulthood, I decided to use an inducible knock out strategy to generate $\Delta Np63^{-/-}$ mice at the adult stage using $\Delta Np63^{fl/fl};K14Cre^{ER}$ (Vasioukhin et al., 1999) conditional knock out mice ($\Delta Np63$ becomes null upon induction of Cre recombinase). Cre-recombinase is activated by an estrogen receptor induction in K14 positive cells. This transgenic mouse is very useful upon consideration of early death of $\Delta Np63^{-/-}$ and $\Delta Np63^{fl/fl};K14Cre^{+}(\Delta/\Delta)$ mice.

Hypothesis: $\Delta Np63$ plays a critical role in the maintenance of proper epithelialization through life.

5.2.1. Loss of $\Delta Np63$ accelerates healing process by hyperproliferation after wound.

Accelerated proliferation and improper differentiation seemed to be the main characteristics exhibited by loss of $\Delta Np63$. To further decipher this phenomenon, a wound-healing assay was performed to 5-week-old mice from wild type, $p63^{+/-}$, $\Delta Np63^{+/-}$, $\Delta Np63^{fl/+};K14Cre^{ER+}$ and $\Delta Np63^{fl/fl};K14Cre^{ER+}$. The wound healing assay tests the capacity of the epidermal cells to differentiate and proliferate in vivo during adulthood (Su et al., 2009b). To generate a wound, I used the punch biopsy approach in

wild type and $\Delta Np63^{+/-}$ at 5 week-old-age mice since $\Delta Np63^{-/-}$ mice do not survive until adulthood, and we have seen a hyperproliferation phenotype in epidermal layers, basal and spinous layer of epidermis, from $\Delta Np63^{+/-}$ mice (**Figure 20**). A wound healed more rapidly in $\Delta Np63^{+/-}$ mice than wild type mice (**Figure 30A**). This was consistent with previous proliferation assay using skin sections from embryos (**Figure 20**).

I also used $\Delta Np63^{fl/fl};K14Cre^{ER+}$ mice to recombine $\Delta Np63$ allele to delete only in K14 positive basal layer of cells by tamoxifen administration at 5week-old-age; $\Delta Np63$ was ablated to about 50%, as confirmed by PCR analyses (**Figure 30C**). Tamoxifen was administrated by painting method once a day for 3days (100ul of 100mg/ml). After tamoxifen treatment for 3days, the skin was irritated and showed thickening and fragility in $\Delta Np63^{fl/fl};K14Cre^{ER+}$ mice. Then I wounded on back skin by punch biopsy and measured the percent of open wounds. $\Delta Np63^{fl/fl};K14Cre^{ER+}$ healed faster than control, $WT;K14Cre^{ER+}$ and $\Delta Np63^{fl/+};K14Cre^{ER+}$ (**Figure 30B**). Since recombination rate is about 50% (Δ/Δ), it was thought to be $\Delta Np63^{+/-}$. Wound from $\Delta Np63\Delta/\Delta$ mice showed faster healing than wild type and $\Delta Np63\Delta/+$ (**Figure 30B**) suggesting that dosage of $\Delta Np63$ is important to maintain cell proliferation and differentiation. However a rigorous study is still warranted to understand this matter further.

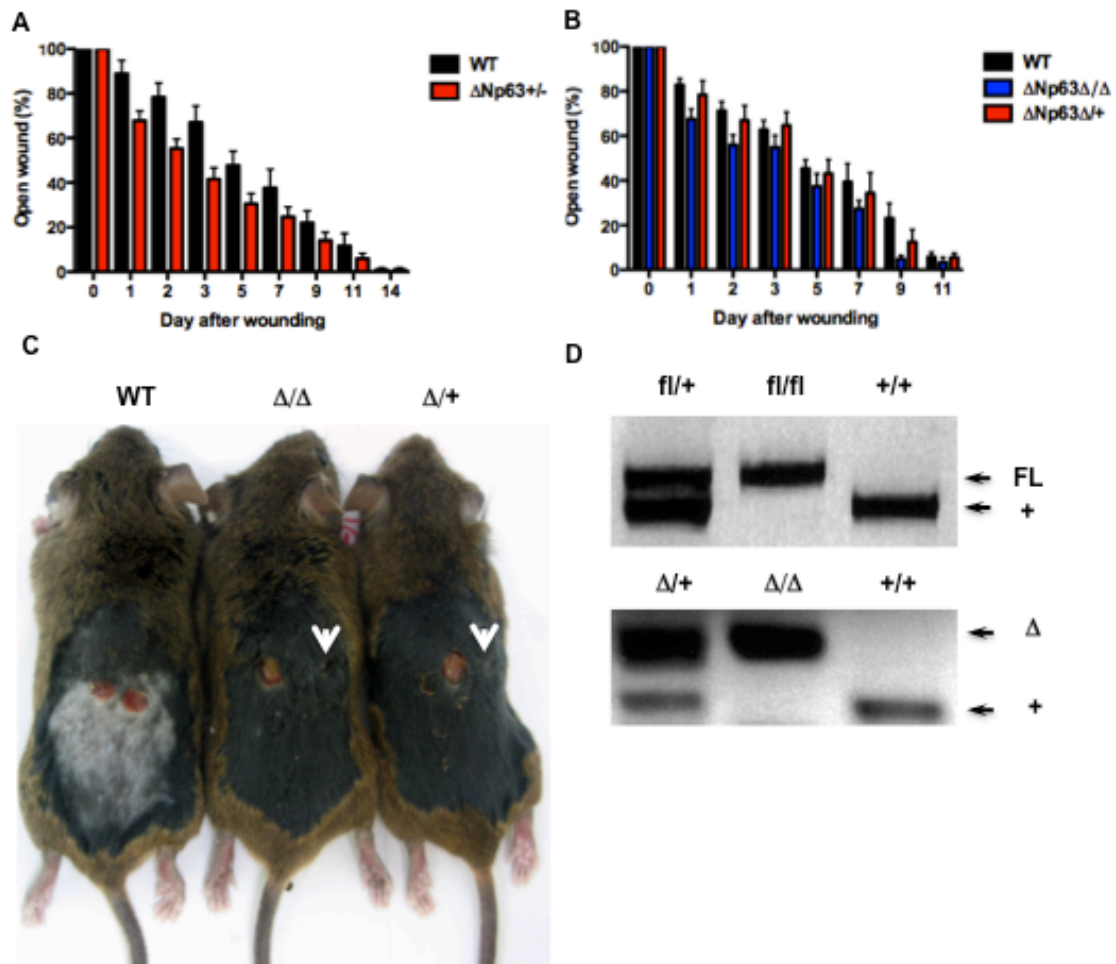


Figure 30. Wound healing is accelerated in $\Delta N63$ deficient mice skin

A) A graph of open wound (%) measured every day after wounding in 5week-old mice. The following genotypes are used for *WT* and $\Delta Np63^{+/-}$, **B)** A graph of open wound (%) measured everyday after wound in 5week-old mice. The following genotypes are used for *WT*, $\Delta Np63^{\Delta/\Delta}$ and $\Delta Np63^{\Delta/+}$, **C)** *WT*, $\Delta Np63^{\Delta/\Delta}$ and $\Delta Np63^{\Delta/+}$ mice wounding after 5 days, white arrows indicate closed one and **D)** PCR analysis to check recombination after tamoxifen treatment. (Cho & Flores, unpublished)

5.2.2. Hyperproliferation results in rapid healing after wound in $\Delta Np63^{+/-}$

To determine whether faster healing occurs in later adulthood, I used 9-month-old mice. Indeed, even 9-month-old $\Delta Np63^{+/-}$ mice still healed faster than wild type mice. To figure out what promotes faster healing, I performed BrdU incorporation before I collected wounded skins to test proliferation. I observed hyperproliferation in $\Delta Np63^{+/-}$ mice epidermis (**Figure 31**). Indeed, there were two epithelial tongues in $\Delta Np63^{+/-}$ but one in wild type and $p63^{+/-}$ (**Figure 31C, F & I**). A healing process was faster in $\Delta Np63^{+/-}$ mice than in both wild type and $p63^{+/-}$ mice. Proliferation was higher in $\Delta Np63^{+/-}$ mice epidermis (**Figure 31**) with aberrant proliferation not only in basal layer but also in none basal layer, the spinous layer of embryonic epidermis (**Figure 20**).

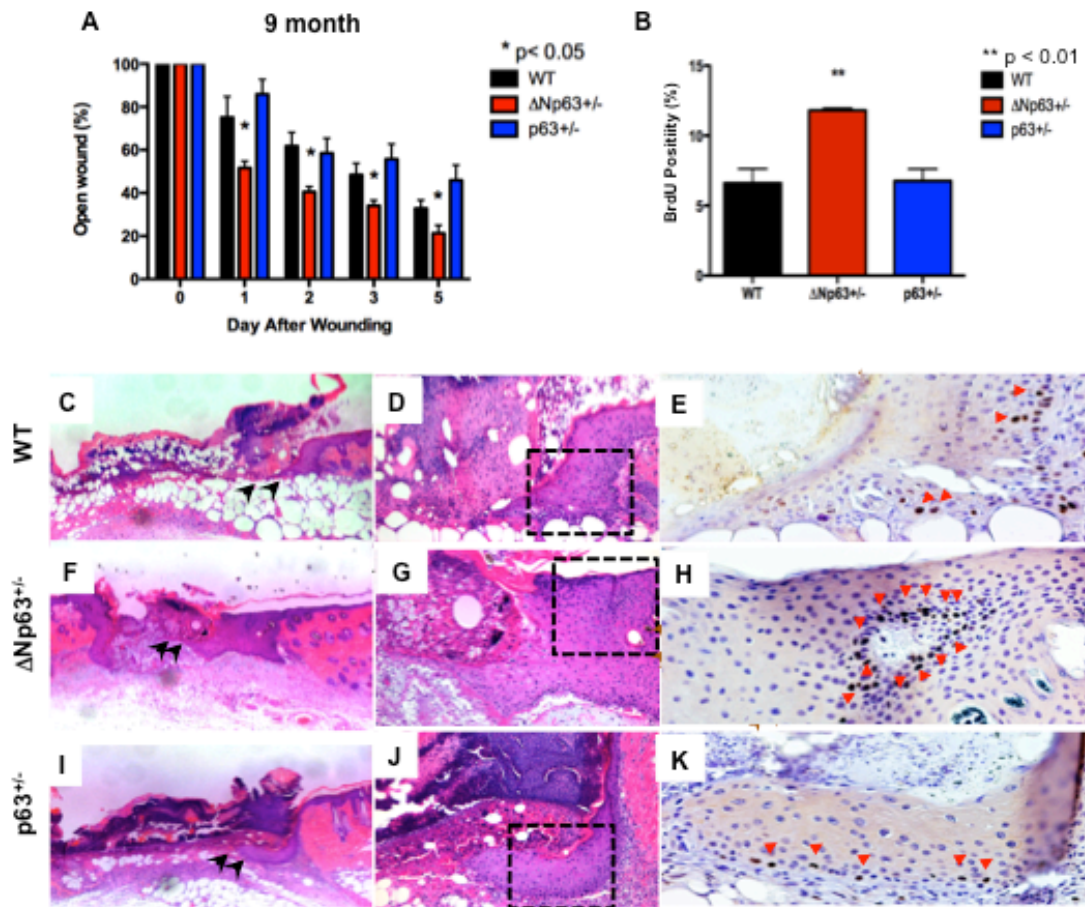


Figure 31. A graph of open wound (%) measured everyday after wound in 9 month old mice A) and incorporation of BrdU at wound healing region, B) Hematoxylin and eosin stained cross sections of the skin of 9 month old mice after wound healing in the following genotypes: C, D) *WT*, F, G) $\Delta Np63^{+/-}$ and I, J) $p63^{+/-}$ (6X magnification: C, F, I and 40X magnification: D, G, J) BrdU stained cross sections of the skin of 9 month old mice after wound healing in the following genotypes: E) *WT*, H) $\Delta Np63^{+/-}$ and K) $p63^{+/-}$ (200X magnification: E, H, K) Black arrow heads indicate epithelial tongue and red arrow heads indicate BrdU positive cells. (Cho & Flores, unpublished)

5.2.3. Loss of $\Delta Np63$ cells has a defect in orientation of cell division during development

During the healing process after wounding, I demonstrated that non-basal layer cells retained proliferative capacity in $\Delta Np63^{+/-}$ skin. Under wounded condition, epithelial cells divide fast to make up for the loss during wound repair. During early embryonic stages, cells divide symmetrically before differentiation and then asymmetric cell division occurs while undergoing differentiation (Lechler and Fuchs, 2005). Asymmetric cell division promotes stratification and differentiation in skin (Lechler and Fuchs, 2005). The Fuchs laboratory showed that LGN is a regulator of cell division orientation (Lechler and Fuchs, 2005).

Because of defects in the hyperproliferation and differentiation in our mouse model, I tested the orientation of cell division. I examined day E18.5 embryo skins from wild type, $\Delta Np63^{-/-}$ and $TAp63^{-/-}$ (**Figure 32 A- C**) when the cells have already undergone differentiation. To determine orientation of mitotic cell division, wild type, $\Delta Np63^{-/-}$ and $TAp63^{-/-}$ skin were used. Wild type and $TAp63^{-/-}$ skin cells followed a perpendicular division pattern about 70% of epidermal cells while $\Delta Np63^{-/-}$ epidermal cells have been divided in parallel division orientation (**Table 3**).

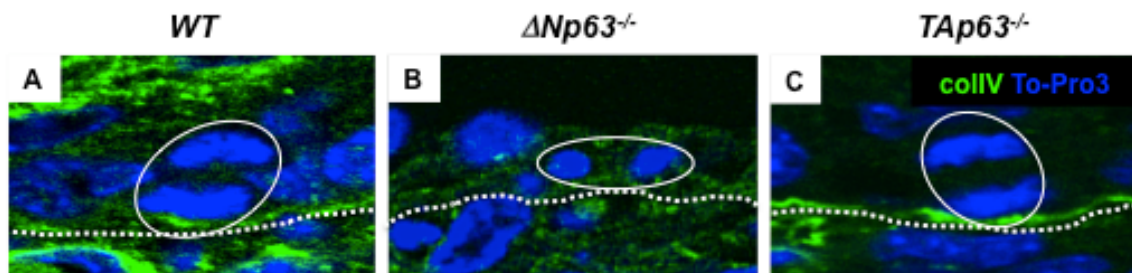


Figure 32. Asymmetric cell division is impaired by loss of $\Delta Np63$ embryo at day E18.5. Immunofluorescence using an antibody for Collagen type IV (ColIV), a marker of basement membrane and counterstained with TO-PRO3. Genotypes of analyzed embryos are: **A) *WT***, **B) $\Delta Np63^{-/-}$** and **C) *TAp63^{-/-}***. White broken circle indicates a mitotic cell and white broken line for basement membrane. (Cho & Flores, unpublished)

Table 3. Cell division ratio (Cho & Flores, unpublished)

	WT	$\Delta Np63^{-/-}$	<i>TAp63^{-/-}</i>
Parallel	26.3%	66.7%	22.2%
Perpendicular	73.7%	33.3%	77.8%

5.2.4. Δ Np63 regulates *LGN*, a marker of cell orientation, by indirectly binding to its promoter.

Hyperproliferation occurred in epidermal cells of *DGCR8^{fl/fl};K14Cre* mice (Yi et al. 2009) and loss of *DGCR8* in embryonic stem cells (ESC) showed a hyperproliferation phenotype (Melton et al., 2010). In Chapter 4, I showed that Δ Np63 regulates *DGCR8* and a diminution of *DGCR8* also has differentiation defect in Δ Np63 ablated epidermal cells. Asymmetric cell division controls stratification and differentiation that is regulated by *LGN* (Lechler and Fuchs, 2005).

To further understand how Δ Np63 regulates cell division and promotes wound repair, I tested mRNA levels of *LGN* found that it is expressed locally in the nucleus during asymmetric cell division (Lechler and Fuchs, 2005). I observed downregulation of *LGN* in Δ Np63^{-/-} skin but not in *TAp63*^{-/-} skin indicating that Δ Np63 specifically regulates for *LGN* gene expression and cell division orientation (**Figure 33A**). This result is consistent with asymmetric cell division that occurs in wild type and *TAp63*^{-/-} skin (**Figure 33**).

To further understand whether *LGN* downregulation results from transcriptional regulation of Δ Np63, I performed chromatin immunoprecipitation (ChIP) analysis using p63 and p53 antibodies. I searched 2000bp upstream of the 5'UTR of the *LGN* gene and found 3 putative sites where p63/p53 might bind to the promoter of *LGN*. However, p63 did not bind to *LGN* promoter whereas p53 did in Δ Np63^{-/-} epidermal cells (**Figure 33B & C**). This clearly implicates binding activity of p53 to the promoter of *LGN*. This data

could imply that there is a correlation between $\Delta Np63$ and p53 to regulate *LGN*. However, further analysis is still required.

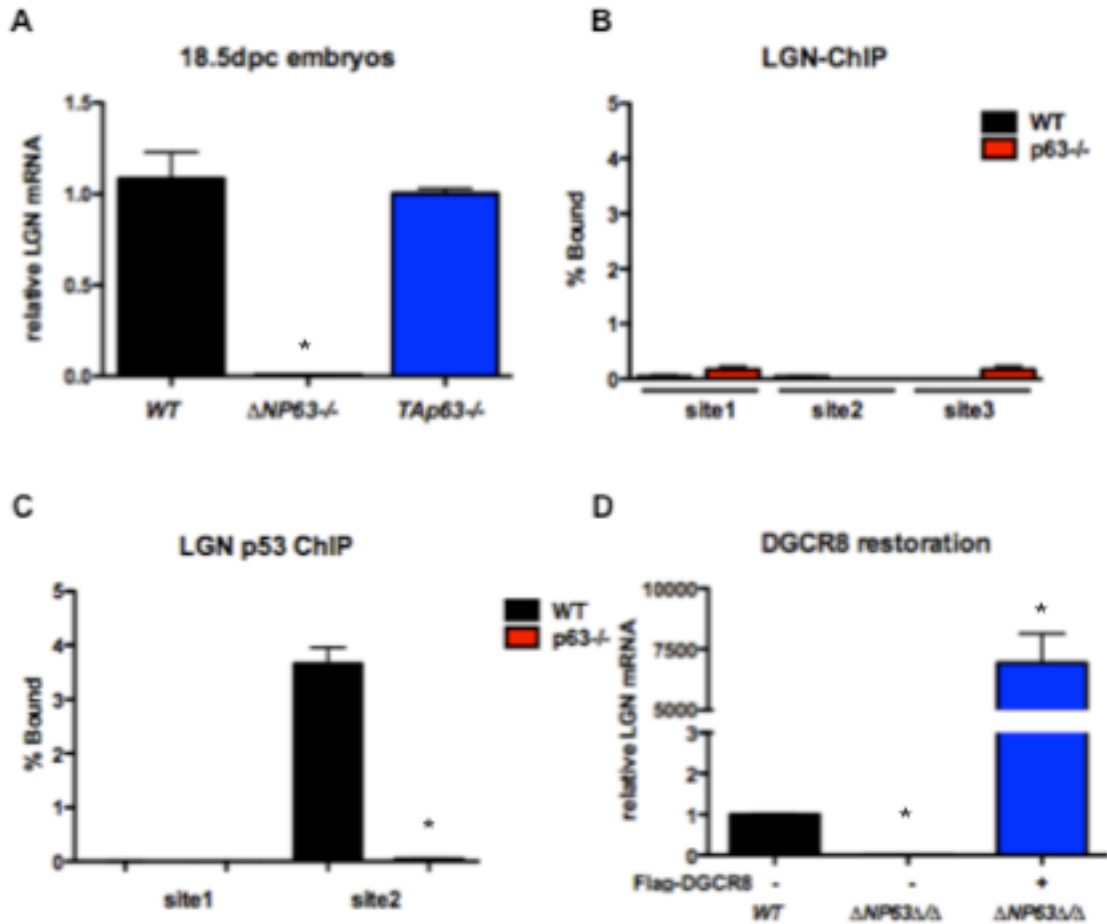


Figure 33. *LGN* is downregulated in $\Delta Np63^{-/-}$ epidermal cells through *DGCR8* regulation. A) The value is normalized to IgG from *wild type*, $\Delta Np63^{-/-}$ and $TAp63^{-/-}$ embryos skin, Real time PCR analysis using 2 primer sets for *LGN* using ChIP-DNA using antibodies p63 B) and p53 C) from *WT* and $p63^{-/-};p19^{-/-}$ keratinocytes. D) After

DGCR8 restoration, cells are harvested and q-RT PCR for for *LGN* in RNA from *wild type* and $\Delta Np63^{4a}$ with or without DGCR8. The asterisks indicate statistical significance (p-value <0.001). **(Cho & Flores, unpublished)**

5.2.5. Restoration of DGCR8 rescues expression of *LGN* in $\Delta Np63^{-/-}$ keratinocytes

There is another question of whether any regulation exists between DGCR8 and *LGN* in $\Delta Np63^{-/-}$. *LGN* is implicated in asymmetric cell division that results in defects in stratification and differentiation (Lechler and Fuchs, 2005). *DGCR8*^{-/-} embryonic stem cells (ESC) showed proliferation and differentiation defects (Melton et al., 2010). To address this question, DGCR8 was restored into $\Delta Np63^{-/-}$ epidermal cells. The result is that the expression level of *LGN* mRNA was dramatically increased in $\Delta Np63^{-/-}$ epidermal cells (**Figure 33D**). This data indicates that DGCR8 regulates controlling *LGN* to control asymmetric cell division in $\Delta Np63^{-/-}$ epidermal cells. However, further analysis is still desired.

5.2.6. Loss of $\Delta Np63$ shows a straight orientation of hair follicle growth.

Another interesting observation from $\Delta Np63^{+/-}$ skin is that hair follicle orientation is perpendicular to the basement membrane of epidermis (**Figure 34B**). This hair follicle orientation is controlled by cell division and morphogenesis regulating signals during development (Ciruna et al., 2006; Gong et al., 2004). About 30% of epidermal skin demonstrated hair follicle orientation defect in $\Delta Np63^{+/-}$ skin.

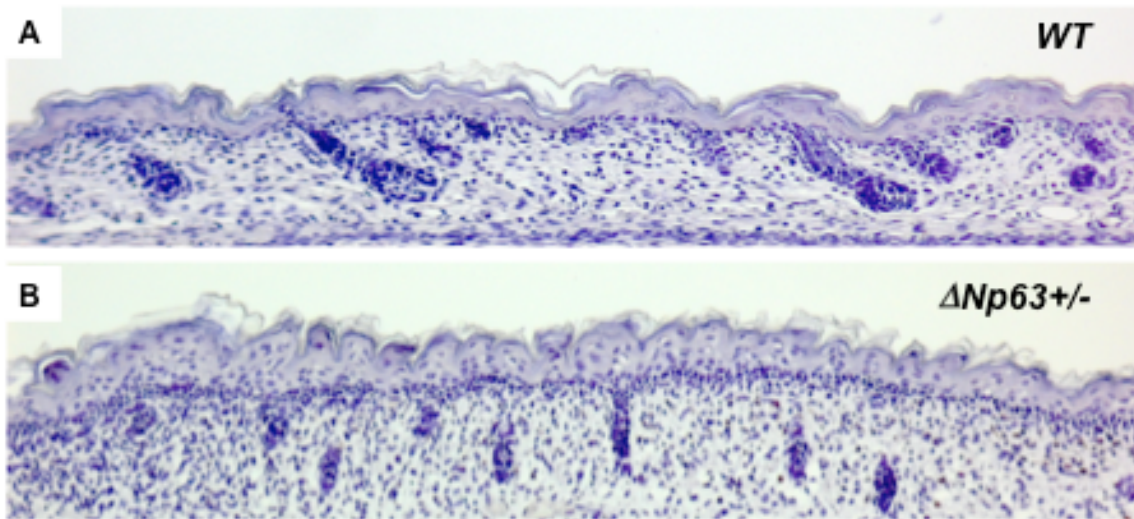


Figure 34. The orientation of hair follicle growth is straight in $\Delta Np63$ heterozygote embryos at E18.5. Hematoxylin stained cross sections of the skin of E18.5 embryos of the following genotypes: *WT* and $\Delta Np63^{+/-}$. (Cho & Flores, unpublished)

CHAPTER 6.
CONCLUSION & DISCUSSIONS

Some parts of this chapter were modified from the following journals.

- 1. Cho MS, Chan IL and Flores ER. *Cell Cycle* 9:12, 1-8; June 15, 2010 Δ Np63 transcriptionally regulates *brachyury*, a gene with diverse roles in limb development, tumorigenesis and metastasis. **Reproduced with permission from Cho et al. and copyright clearance center.****
- 2. Su X, Cho MS, Gi Y, Ayanga BA, Sherr CJ, and Flores ER. *EMBO J.* 2009 Jul 8;28(13):1904-15. Rescue of key features of the *p63*-null epithelial phenotype by inactivation of Ink4a and Arf. **Reproduced with permission from Su et al. and copyright clearance center.****
- 3. Min Soon Cho, Xiaohua Su, Deepavali Chakravarti, Arianexys Aquino, Nicole Müller, Avinashnarayan Venkatanarayan, Io Long Chan, Young Jin Gi, & Elsa R. Flores. Δ Np63 induces terminal differentiation through transcriptional regulation of DGCR8 and suppression of pluripotency factors.**

Chapter6. Conclusions and Discussions

During my thesis work, I demonstrated that one of the essential functions necessary for the maintenance of the epithelium is tied to the repression of the *Ink4a-Arf* locus by p63, especially $\Delta Np63$ isoforms and a complex network of genes regulated by p63 in multiple processes: stem cell proliferation, differentiation and adhesion for the maintenance of the integrity and development of the skin (Su et al., 2009).

Second, I showed that the transcriptional network regulated by $\Delta Np63$ during limb development and tumorigenesis acts through the transcriptional activation of *brachyury* (Cho et al., 2010). The biological significance of $\Delta Np63$ overexpression is not completely understood in cancer. Previous studies have shown that $\Delta Np63$ primarily serves to inactivate p53 and the full-length isoforms of p63 and p73, TAp63 and TAp73, leading to a diminution in the ability of these p53 family members to induce apoptosis, cell cycle arrest, and other critical anti-tumorigenic processes that ultimately lead to tumor formation (Lanza et al., 2006; Yang et al., 1998).

Third, I showed that $\Delta Np63$ is a critical factor for the induction of epidermal differentiation and appropriate stratification (Cho et al., submitted 2011). In the absence of $\Delta Np63$, a rudimentary and disorganized epidermis forms around the developing mouse embryo. $\Delta Np63^{+/-}$ mice show an even more striking phenotype in terms of the disorganization of the developing epidermis with evaginating hair germs. These epidermal phenotypes are reminiscent of mice lacking *DGCR8* and *Dicer* expression in

the skin (Yi et al., 2006; Yi et al., 2009). Accordingly, $\Delta Np63$ deficiency resulted in low levels of *DGCR8* and the *miR-470* and *miR-145*, which were critical repressors of the pluripotency factors, *Oct4*, *Sox2*, and *Nanog* (Tay et al., 2008; Xu et al., 2009) (**Figure 27**). I found that in the absence of $\Delta Np63$ all three of these pluripotency factors were expressed at levels comparable to that found in mouse embryonic stem cells and that $\Delta Np63$ deficient epidermal cells could self renew and differentiate into multiple cell fates after re-expression of *DGCR8*. Importantly, I found that $\Delta Np63$ is a transcriptional activator of *DGCR8*. These data indicate that $\Delta Np63$ is a critical regulator of terminal differentiation through the transcriptional activation of a critical factor in miRNA biogenesis.

6.1 Rescue of key features of the $p63^{-/-}$ epithelial phenotype by inactivation of *Ink4a* and *Arf*.

Two *p63*-null mouse models have been generated. Each shows similar phenotypes such as defects in stratified epithelium, truncated limbs, severe defects in craniofacial structures and ectodermal derived appendage malformation. However, there are at least two distinct interpretations of the data because of the complexity of the transcriptional network regulated by *p63* (Mills et al., 1999; Vigano and Mantovani, 2007; Yang et al., 1999). *p63* regulates numerous transcriptional network of target genes in the maintenance of the integrity of stratified epithelium with essential functions in differentiation and cell adhesion (Vigano and Mantovani, 2007). Recent evidence has

also indicated that *p63* is essential for the proliferative potential of the epidermal stem cells (Senoo et al., 2007). Prior to our study, the mechanisms governing epidermal differentiation and maintenance of stem cell proliferation were not known.

As a tumor suppressor gene *Ink4a-Arf* is well studied. Recent study showed that repression of the *Ink4a-Arf* locus by Bmi-1 (a polycomb complex protein) plays a pivotal role in the maintenance of stem cell properties both in hematopoietic stem cells and neural stem cells (Bracken et al., 2007; Bruggeman et al., 2005; Molofsky et al., 2005; Molofsky et al., 2003). Bmi-1 represses the *Ink4a-Arf* locus. The epidermis is also an essential organ to continue homeostasis in order to maintain skin structure and is needed to retain stem cell proliferation and differentiation through life. However Bmi-1 is not required for the development of the epithelium indicating that other repressors of the *Ink4a-Arf* locus exist in the epidermis to allow for stem cell renewal and proliferation (Senoo et al., 2007; van der Lugt et al., 1994). Indeed, inactivation of *Arf* or *Ink4a* rescues many of the defects seen in the *p63*-null mouse limb formation and epidermal cell proliferation. We demonstrated this by generating *p63*^{-/-};*Arf*^{-/-} or *p63*^{-/-};*Ink4a*^{-/-} mice. Both of these double mutant mice showed a remarkable rescue of the *p63*^{-/-} phenotype exhibiting K5 and K10-expressing epidermal sheets around most of the embryos. The rescue is more impressive in the *p63*^{-/-};*Ink4a*^{-/-} mice with 85% of the skin of the 20 embryos examined having K5 and K10 positive cells. Remarkably, these mice exhibited evidence of hair follicles that stain positively for the hair follicle marker Lhx2 and K15 (Liu et al., 2003b; Rhee et al., 2006) indicating some degree of restoration in the

epidermal stem cell compartment. In contrast, K5 positive cells were only apparent in 0.3% of the skin in the twenty *p63*^{-/-} embryos consistent with previously published data. While the epithelium in the double mutants surrounded the embryo, the skin on these mice was still fragile and detached easily from the embryo as be shown in Fig. 8C & D. *p63* has previously been shown to regulate genes involved in cell–cell adhesion. Loss of *Ink4a* or *Arf* rescues the proliferative and differentiation markers expression defects in keratinocytes deficient for *p63*. These data suggest the presence of a complex network of *p63* targets in the development of a stratified epithelium. Here, we show a clear rescue of the proliferation defect of *p63*^{-/-} keratinocytes; cells lacking *Ink4a* or *Arf* and *p63* proliferate to wild type levels by BrdU incorporation assay.

p63 has been shown to have *p53*-dependent and -independent activities to promote cell survival and stem cell maintenance (Truong et al., 2006). Our analysis of *p53*^{-/-};*p63*^{-/-} embryos are compatible with these findings. Apart from that, these genetic experiments strongly support the view that *Ink4a* and *Arf* have *p53*-independent activities in the rescue of keratinocytes stem cell proliferation in absence of *p63*.

Here, we demonstrated that one of the essential functions necessary for the maintenance of the epithelium is tied to the repression of the *Ink4a-Arf* locus by *p63*, and especially the Δ N*p63* isoform (Su et al., 2009a). This argues for a complex network of genes regulated by *p63* in multiple processes: stem cell proliferation, differentiation and adhesion for the maintenance of the integrity and development of the skin. These data reveal a novel *p53*-independent mechanism for the restoration of the proliferative

potential of epidermal stem cells in the absence of *p63*. The molecular mechanisms regarding cell adhesion still remain to be addressed.

6.2 $\Delta Np63$ transcriptionally regulates *brachyury*, a gene with diverse roles in limb development, tumorigenesis and metastasis.

I have identified *brachyury*, a gene that plays diverse roles in limb development and tumorigenesis, as a novel transcriptional target of p63, especially the $\Delta Np63$ isoform. Importantly, *brachyury* is critical for appropriate formation of the apical ectodermal ridge (AER) that is essential for limb formation during embryogenesis (Liu et al., 2003). Similarly, *p63* is expressed on the AER and is also essential for limb formation (Mills et al., 1999; Yang et al., 1999; Lo Iacono et al., 2008). Here, I provide evidence that *p63*, specifically the $\Delta Np63\alpha$ and $-\beta$ but not $-\gamma$ isoforms are critical for transcriptional regulation of *brachyury* during embryogenesis when the AER is formed.

Interestingly, *brachyury* is highly expressed in many cancers, reminiscent of the pattern of expression of the $\Delta Np63$ isoforms in many human tumors. I have shown that $\Delta Np63$ is also essential for expression of *brachyury* in tumors and that downregulation of $\Delta Np63$ in cells from these tumors results in a diminution of *brachyury* expression and a decrease in cell proliferation. Our data provides a basis for further investigation of treatment of tumors with high levels of *brachyury* through inhibition of $\Delta Np63$.

The transcriptional network regulated by $\Delta Np63$ during limb development and tumorigenesis is not well understood. Based on the knowledge that p63 transcriptionally

regulates a large network of genes in multiple processes, p53-dependent or –independent way, it is likely that p63 also transcriptionally regulates multiple targets during limb development. A recent study has shown that p63 transcriptionally regulates *Dlx5* and *Dlx6*, transcription factors that play important roles in limb morphogenesis (Lo Iacono et al., 2008). This study found that the $\Delta Np63\alpha$ isoform leads to the highest transactivation of *Dlx5* and *Dlx6*. Similarly, we found that the $\Delta Np63$ isoforms had the highest activity at the *brachyury* promoter; however, $\Delta Np63\alpha$ and $\Delta Np63\beta$, and not $\Delta Np63\gamma$, resulted in transactivation of a *brachyury-luciferase* reporter gene. Together, these results suggest that the $\Delta Np63$ isoforms likely transcriptionally regulate distinct sets of targets in limb development. Our data are further supported by the *in vivo* phenotypes of the *p63*^{-/-} mice (Mills et al., 1999; Yang et al., 1999), which have severely truncated limbs, and the *TAp63*^{-/-} mice, which develop normal limbs (Su et al., 2009) and have no transcriptional activity at the brachyury promoter, indicating that only the $\Delta Np63$ isoforms are critical for appropriate limb development. High levels of expression of $\Delta Np63$ have been detected in many tumors. $\Delta Np63$ is highly expressed in tumors of epithelial origin like some head and neck squamous cell carcinomas and prostate, lung, and mammary adenocarcinomas (Flores, 2007; Flores et al., 2005). The biological significance of $\Delta Np63$ over expression is not completely understood in cancer. Previous studies have shown that $\Delta Np63$ primarily serves to inactivate p53 and the full-length isoforms of p63 and p73, TAp63 and TAp73, leading to a diminution in the ability of these p53 family members to induce apoptosis, cell cycle arrest, and other critical anti-tumorigenic

processes that ultimately lead to tumor formation (Lanza et al., 2006; Yang et al., 1998). Our data demonstrate that $\Delta Np63$ also plays an active role in transactivating genes involved in the tumorigenic process through transcriptional activation of *brachyury*. Importantly, *brachyury* is highly expressed in chordoid cancer cells, chordoma, and chondrosarcoma, a malignant bone tumor originating in the cartilage (Yang et al., 2009; Vujovic et al., 2006). Chordoid cells are those that resemble notochordal tissue. Because *brachyury* is essential for notochord formation and differentiation, misexpression or overexpression of *brachyury* can lead to the formation of tumors with chordoid features. Interestingly, $\Delta Np63$ is highly expressed in invasive urothelial carcinomas with a chordoid morphology that resembles chondrosarcoma (Cox et al., 2009). Consequently, *brachyury* and $\Delta Np63$ are important biomarkers for these tumors and their expression is likely intimately linked.

Taken together, I have shown that $\Delta Np63$ can transcriptionally regulate *brachyury*. This regulation is critical during limb development and in the formation of tumors arising from the notochord. Given the transcriptional regulation of *brachyury* by $\Delta Np63$ and the diminution in cell proliferation in tumor cells after concomitant knockdown of $\Delta Np63$ and *brachyury*, $\Delta Np63$ is also a potential target for therapy of patients with tumors that have chordoid features. Further investigation into therapeutic outcomes of patients with high levels of $\Delta Np63$ and *brachyury* is essential to determine whether inhibitors of $\Delta Np63$ will benefit cancer patients with alterations in this pathway.

6.3. $\Delta Np63$ induces terminal differentiation through transcriptional regulation of *DGCR8* and suppression of pluripotency factors.

Here, we show that $\Delta Np63$ is a critical factor for the induction of epidermal differentiation and appropriate stratification. In the absence of $\Delta Np63$, a rudimentary, disorganized epidermis forms around the developing mouse embryo. $\Delta Np63$ heterozygous mice show an even more striking phenotype in terms of the disorganization of the developing epidermis with evaginating hair germs. These epidermal phenotypes are reminiscent of mice lacking *DGCR8* and *Dicer* expression in the skin (Yi et al., 2006; Yi et al., 2009). Accordingly, $\Delta Np63$ deficiency resulted in low levels of *DGCR8* and miRNAs, *miR-470* and *miR-145*, which are critical repressors of the pluripotency factors, *Oct4*, *Sox2*, and *Nanog* (Tay et al., 2008; Xu et al., 2009) (Appendix 5). We found that in the absence of $\Delta Np63$ all three of these pluripotency factors were expressed at levels comparable to that found in mouse embryonic stem cells and that $\Delta Np63$ deficient epidermal cells can self renew and differentiate into multiple cells fates after re-expression of *DGCR8*. Importantly, we found that $\Delta Np63$ is a transcriptional activator of *DGCR8*. These data indicate that $\Delta Np63$ is a critical regulator of terminal differentiation through the transcriptional activation of a critical factor in miRNA biogenesis (Appendix 5). The presence of a rudimentary epidermis in $\Delta Np63^{-/-}$ mouse embryos and the ability of $\Delta Np63$ deficient epidermal cells to self-renew was quite surprising. The roles of *p63* in epidermal morphogenesis have been the subject of heated controversy. Experimental evidence supports a role for *p63* in both stem cell

proliferation and in the initiation of differentiation (Koster et al., 2004; Mills et al., 1999; Senoo et al., 2007; Yang et al., 1999). Elegant experiments using *p63* deficient epithelial cells demonstrated that *p63* is required for stem cell proliferation (Senoo et al., 2007). Also, data from an equal number of studies using *p63*^{-/-} mice showed that *p63* is required for proper differentiation of epithelial tissues (Koster et al., 2004). Most of these studies were performed using mouse models that are deficient for all isoforms of *p63* making the interpretation of the data difficult to decipher due to the existence of multiple *p63* isoforms. More recently, experiments have been performed using *in vivo* siRNA knock down of $\Delta Np63\alpha$, the isoform predominantly expressed in the skin. While this mouse model has provided valuable insight into transcriptional targets of $\Delta Np63\alpha$, it differs from our $\Delta Np63$ knockout mice in two ways: 1.) the deletion of $\Delta Np63$ was incomplete due to siRNA technology and 2.) $\Delta Np63$ was deleted in K14-expressing cells, after the commitment to differentiation.

Therefore, our unique mouse model has unveiled unknown functions of the $\Delta Np63$ isoforms in epidermal stem cell proliferation and in the induction of epidermal differentiation. Importantly, $\Delta Np63$ indirectly regulates the expression of the pluripotency factors *Oct4*, *Sox2*, and *Nanog* by direct transactivation of *DGCR8*.

Our data indicate that expression of *DGCR8* is critical for terminal differentiation of $\Delta Np63$ deficient cells into multiple cell fates. The phenotype of $\Delta Np63^{+/-}$ and $\Delta Np63^{-/-}$ embryos is similar to that of mice with *DGCR8* ablated in K14 expressing cells within the epidermis. All three of these mouse models have a hyperproliferative epidermis and

hair germs that evaginate instead of invaginate (Yi et al., 2006; Yi et al., 2009). Moreover, *DGCR8*^{-/-} embryonic stem cells continue to self-renew and fail to undergo terminal differentiation.

Similarly, $\Delta Np63$ ^{-/-} epidermal cells continued to self-renew in clonogenic assays while wild-type epidermal cells senesced. $\Delta Np63$ ^{-/-} epidermal cells also continue to express markers of pluripotency, *Oct4*, *Sox2*, and *Nanog*, after multiple passages and only terminally differentiate after re-expression of *DGCR8*. Contrary to one of the current models that proposes that expression of $\Delta Np63$ induces pluripotency, our data favor a model whereby complete deletion of $\Delta Np63$ induces pluripotency in epidermal stem cells and likely in other progenitor cells where $\Delta Np63$ is normally expressed.

In summary, $\Delta Np63$ is required for transcriptional activation of *DGCR8* in the developing epidermis. *DGCR8* is essential for epidermal morphogenesis; therefore, in the absence of $\Delta Np63$, the epidermal stem cells in the developing skin fail to suppress expression of *Oct4*, *Sox2*, and *Nanog* and therefore fail to terminally differentiate. These findings have important implications for the function of $\Delta Np63$ in cancer where its expression is often dysregulated (Flores, 2007). In the future, understanding the mechanisms employed by the individual *p63* isoforms in maintaining progenitor and stem cells in various tissues is key to understanding its complex roles in cancer development and metastasis.

6.4. $\Delta Np63$ indirectly controls asymmetric cell divisions through *LGN* via

regulation of *DGCR8*.

Based on other studies on asymmetric cell divisions, we knew that this event is required for deciding cell fate during embryogenesis (Artavanis-Tsakonas et al., 1999; Rohrschneider and Nance, 2009; Schuurmans and Guillemot, 2002; Segalen and Bellaiche, 2009). However, in adult mouse epidermis, perpendicular spindle orientation is observed in only ~3% of cells. This is too small a fraction to account for the asymmetric divisions in this tissue. Thus, alternative mechanisms might exist to achieve the asymmetric stem cell division in this system. Asymmetric cell divisions are also implicated in skin epidermal differentiation. That is critical for stratification and differentiation (Lechler and Fuchs, 2005). In this study, p63 was implicated as an important gene, as *p63*^{-/-} epidermal cells showed a defect in asymmetric cell division. However, underlying molecular mechanisms are largely unknown. Here I reported my preliminary data showing *LGN*, which is one of spindle asymmetric orientation regulator genes, to be regulated by Δ Np63, not TAp63. It is consistent with *TAp63*^{-/-} exhibiting no asymmetric cell division defect. By restoring *DGCR8*, its mRNA expression level was elevated to wild type level. However, chromatin immunoprecipitation (ChIP) assay showed that *LGN* was indirectly regulated by Δ Np63. Using p53 antibody for immunoprecipitation in *p63*^{-/-} epidermal cells, I observed binding at the *LGN* promoter which indicates that Δ Np63 is required but not p53. p53 has not yet been implicated in asymmetric cell divisions. In summary, *LGN* might be regulated by indirectly Δ Np63 in

asymmetric cell division. There may be some other mediators involved in the regulation between $\Delta Np63$ and LGN that could be p53 dependent.

In summary, $\Delta Np63$ is required for transcriptional activation of *DGCR8* for proliferation and differentiation in developing epidermis. *DGCR8* is essential for epidermal morphogenesis; therefore, in the absence of $\Delta Np63$, the epidermal stem cells in the developing skin fail to suppress expression of *Oct4*, *Sox2*, and *Nanog* and therefore fail to terminally differentiate. Even in repression of the *Ink4a-Arf* locus in p63 null background, epidermal terminal differentiation is still not complete since there is no *DGCR8* involvement to differentiate by losing $\Delta Np63$. These findings have important implications for the function of $\Delta Np63$ in cancer where its expression is often dysregulated (Flores, 2007). In the future, understanding the mechanisms employed by the individual *p63* isoforms in maintaining progenitor and stem cells in various tissues will be key to understanding its complex roles in cancer development and metastasis. The unique isoform specific conditional knock out mice model from Flores laboratory will provide a robust model with which to explore these questions.

BIBLIOGRAPHIES

Alvarez-Garcia, I., and Miska, E.A. (2005). MicroRNA functions in animal development and human disease. *Development* 132, 4653-4662.

Ambrosio, D.L., Barbosa, C.F., Vianna, V.F., and Cicarelli, R.M. (2004). Trypanosoma cruzi: establishment of permeable cells for RNA processing analysis with drugs. *Mem Inst Oswaldo Cruz* 99, 617-620.

Artavanis-Tsakonas, S., Rand, M.D., and Lake, R.J. (1999). Notch signaling: cell fate control and signal integration in development. *Science* 284, 770-776.

Barrandon, Y., and Green, H. (1987). Three clonal types of keratinocyte with different capacities for multiplication. *Proc Natl Acad Sci U S A* 84, 2302-2306.

Barrow, L.L., van Bokhoven, H., Daack-Hirsch, S., Andersen, T., van Beersum, S.E., Gorlin, R., and Murray, J.C. (2002). Analysis of the p63 gene in classical EEC syndrome, related syndromes, and non-syndromic orofacial clefts. *J Med Genet* 39, 559-566.

Bertwistle, D., Zindy, F., Sherr, C.J., and Roussel, M.F. (2004). Monoclonal antibodies to the mouse p19(Arf) tumor suppressor protein. *Hybrid Hybridomics* 23, 293-300.

Bracken, A.P., Kleine-Kohlbrecher, D., Dietrich, N., Pasini, D., Gargiulo, G., Beekman, C., Theilgaard-Monch, K., Minucci, S., Porse, B.T., Marine, J.C., *et al.* (2007). The Polycomb group proteins bind throughout the INK4A-ARF locus and are disassociated in senescent cells. *Genes Dev* 21, 525-530.

Brivanlou, A.H., Gage, F.H., Jaenisch, R., Jessell, T., Melton, D., and Rossant, J. (2003). Stem cells. Setting standards for human embryonic stem cells. *Science* *300*, 913-916.

Bruggeman, S.W., Valk-Lingbeek, M.E., van der Stoop, P.P., Jacobs, J.J., Kieboom, K., Tanger, E., Hulsman, D., Leung, C., Arsenijevic, Y., Marino, S., *et al.* (2005). Ink4a and Arf differentially affect cell proliferation and neural stem cell self-renewal in Bmi1-deficient mice. *Genes Dev* *19*, 1438-1443.

Candi, E., Dinsdale, D., Rufini, A., Salomoni, P., Knight, R.A., Mueller, M., Krammer, P.H., and Melino, G. (2007a). TAp63 and DeltaNp63 in cancer and epidermal development. *Cell Cycle* *6*, 274-285.

Candi, E., Rufini, A., Terrinoni, A., Dinsdale, D., Ranalli, M., Paradisi, A., De Laurenzi, V., Spagnoli, L.G., Catani, M.V., Ramadan, S., *et al.* (2006). Differential roles of p63 isoforms in epidermal development: selective genetic complementation in p63 null mice. *Cell Death Differ* *13*, 1037-1047.

Candi, E., Rufini, A., Terrinoni, A., Giamboi-Miraglia, A., Lena, A.M., Mantovani, R., Knight, R., and Melino, G. (2007b). DeltaNp63 regulates thymic development through enhanced expression of FgfR2 and Jag2. *Proc Natl Acad Sci U S A* *104*, 11999-12004.

Candi, E., Schmidt, R., and Melino, G. (2005). The cornified envelope: a model of cell death in the skin. *Nat Rev Mol Cell Biol* *6*, 328-340.

Carroll, D.K., Brugge, J.S., and Attardi, L.D. (2007). p63, cell adhesion and survival. *Cell Cycle* *6*, 255-261.

Carroll, D.K., Carroll, J.S., Leong, C.O., Cheng, F., Brown, M., Mills, A.A., Brugge, J.S., and Ellisen, L.W. (2006). p63 regulates an adhesion programme and cell survival in epithelial cells. *Nat Cell Biol* 8, 551-561.

Celli, J., Duijf, P., Hamel, B.C., Bamshad, M., Kramer, B., Smits, A.P., Newbury-Ecob, R., Hennekam, R.C., Van Buggenhout, G., van Haeringen, A., *et al.* (1999). Heterozygous germline mutations in the p53 homolog p63 are the cause of EEC syndrome. *Cell* 99, 143-153.

Chia, W., Cai, Y., Morin, X., Tio, M., Udolph, G., Yu, F., and Yang, X. (2001). The cell cycle machinery and asymmetric cell division of neural progenitors in the *Drosophila* embryonic central nervous system. *Novartis Found Symp* 237, 139-151; discussion 151-163.

Cho, M.S., Chan, I.L., and Flores, E.R. DeltaNp63 transcriptionally regulates brachyury, a gene with diverse roles in limb development, tumorigenesis and metastasis. *Cell Cycle* 9.

Ciruna, B., Jenny, A., Lee, D., Mlodzik, M., and Schier, A.F. (2006). Planar cell polarity signalling couples cell division and morphogenesis during neurulation. *Nature* 439, 220-224.

Cox, R.M., Schneider, A.G., Sangoi, A.R., Clingan, W.J., Gokden, N., and McKenney, J.K. (2009). Invasive urothelial carcinoma with chordoid features: a report of 12 distinct cases characterized by prominent myxoid stroma and cordlike epithelial architecture. *Am J Surg Pathol* 33, 1213-1219.

Craig, A.L., Holcakova, J., Finlan, L.E., Nekulova, M., Hrstka, R., Gueven, N., DiRenzo, J., Smith, G., Hupp, T.R., and Vojtesek, B. DeltaNp63 transcriptionally regulates ATM to control p53 Serine-15 phosphorylation. *Mol Cancer* 9, 195.

Crook, T., Nicholls, J.M., Brooks, L., O'Nions, J., and Allday, M.J. (2000). High level expression of deltaN-p63: a mechanism for the inactivation of p53 in undifferentiated nasopharyngeal carcinoma (NPC)? *Oncogene* 19, 3439-3444.

Farley, F.W., Soriano, P., Steffen, L.S., and Dymecki, S.M. (2000). Widespread recombinase expression using FLPeR (flipper) mice. *Genesis* 28, 106-110.

Flores, E.R. (2007). The roles of p63 in cancer. *Cell Cycle* 6, 300-304.

Flores, E.R., Allen-Hoffmann, B.L., Lee, D., and Lambert, P.F. (2000). The human papillomavirus type 16 E7 oncogene is required for the productive stage of the viral life cycle. *J Virol* 74, 6622-6631.

Flores, E.R., Sengupta, S., Miller, J.B., Newman, J.J., Bronson, R., Crowley, D., Yang, A., McKeon, F., and Jacks, T. (2005). Tumor predisposition in mice mutant for p63 and p73: evidence for broader tumor suppressor functions for the p53 family. *Cancer Cell* 7, 363-373.

Flores, E.R., Tsai, K.Y., Crowley, D., Sengupta, S., Yang, A., McKeon, F., and Jacks, T. (2002). p63 and p73 are required for p53-dependent apoptosis in response to DNA damage. *Nature* 416, 560-564.

Friedl, P., and Wolf, K. (2003). Tumour-cell invasion and migration: diversity and escape mechanisms. *Nat Rev Cancer* 3, 362-374.

Fuchs, E. (2008). Skin stem cells: rising to the surface. *The Journal of cell biology* *180*, 273-284.

Gong, Y., Mo, C., and Fraser, S.E. (2004). Planar cell polarity signalling controls cell division orientation during zebrafish gastrulation. *Nature* *430*, 689-693.

Grinnell, K.L., and Bickenbach, J.R. (2007). Skin keratinocytes pre-treated with embryonic stem cell-conditioned medium or BMP4 can be directed to an alternative cell lineage. *Cell Prolif* *40*, 685-705.

Grinnell, K.L., Yang, B., Eckert, R.L., and Bickenbach, J.R. (2007). De-differentiation of mouse interfollicular keratinocytes by the embryonic transcription factor Oct-4. *J Invest Dermatol* *127*, 372-380.

Hall, B.K. (2000a). A role for epithelial-mesenchymal interactions in tail growth/morphogenesis and chondrogenesis in embryonic mice. *Cells Tissues Organs* *166*, 6-14.

Hall, B.K. (2000b). Epithelial-mesenchymal interactions. *Methods Mol Biol* *137*, 235-243.

Hall, P.A. (1989). What are stem cells and how are they controlled? *J Pathol* *158*, 275-277.

Hall, P.A., and Watt, F.M. (1989). Stem cells: the generation and maintenance of cellular diversity. *Development* *106*, 619-633.

Han, J., Pedersen, J.S., Kwon, S.C., Belair, C.D., Kim, Y.K., Yeom, K.H., Yang, W.Y., Haussler, D., Belloch, R., and Kim, V.N. (2009). Posttranscriptional crossregulation between Drosha and DGCR8. *Cell* *136*, 75-84.

Hu, L.Y., Sun, Z.G., Wen, Y.M., Cheng, G.Z., Wang, S.L., Zhao, H.B., and Zhang, X.R. ATP-mediated protein kinase B Akt/mammalian target of rapamycin mTOR/p70 ribosomal S6 protein p70S6 kinase signaling pathway activation promotes improvement of locomotor function after spinal cord injury in rats. *Neuroscience* *169*, 1046-1062.

Ihrie, R.A., Marques, M.R., Nguyen, B.T., Horner, J.S., Papazoglu, C., Bronson, R.T., Mills, A.A., and Attardi, L.D. (2005). Perp is a p63-regulated gene essential for epithelial integrity. *Cell* *120*, 843-856.

Inman, K.E., and Downs, K.M. (2006). Localization of Brachyury (T) in embryonic and extraembryonic tissues during mouse gastrulation. *Gene Expr Patterns* *6*, 783-793.

Iwakuma, T., Lozano, G., and Flores, E.R. (2005). Li-Fraumeni syndrome: a p53 family affair. *Cell Cycle* *4*, 865-867.

Izumi, Y., Hirose, T., Tamai, Y., Hirai, S., Nagashima, Y., Fujimoto, T., Tabuse, Y., Kemphues, K.J., and Ohno, S. (1998). An atypical PKC directly associates and colocalizes at the epithelial tight junction with ASIP, a mammalian homologue of *Caenorhabditis elegans* polarity protein PAR-3. *J Cell Biol* *143*, 95-106.

Jacks, T., Remington, L., Williams, B.O., Schmitt, E.M., Halachmi, S., Bronson, R.T., and Weinberg, R.A. (1994). Tumor spectrum analysis in p53-mutant mice. *Curr Biol* *4*, 1-7.

Joberty, G., Petersen, C., Gao, L., and Macara, I.G. (2000). The cell-polarity protein Par6 links Par3 and atypical protein kinase C to Cdc42. *Nat Cell Biol* 2, 531-539.

Johansson, A., Driessens, M., and Aspenstrom, P. (2000). The mammalian homologue of the *Caenorhabditis elegans* polarity protein PAR-6 is a binding partner for the Rho GTPases Cdc42 and Rac1. *J Cell Sci* 113 (Pt 18), 3267-3275.

Johnson, R.L., and Tabin, C.J. (1997). Molecular models for vertebrate limb development. *Cell* 90, 979-990.

Jonkers, J., Meuwissen, R., van der Gulden, H., Peterse, H., van der Valk, M., and Berns, A. (2001). Synergistic tumor suppressor activity of BRCA2 and p53 in a conditional mouse model for breast cancer. *Nat Genet* 29, 418-425.

Kemphues, K. (2000). PARsing embryonic polarity. *Cell* 101, 345-348.

Kemphues, K.J., Kusch, M., and Wolf, N. (1988a). Maternal-effect lethal mutations on linkage group II of *Caenorhabditis elegans*. *Genetics* 120, 977-986.

Kemphues, K.J., Priess, J.R., Morton, D.G., and Cheng, N.S. (1988b). Identification of genes required for cytoplasmic localization in early *C. elegans* embryos. *Cell* 52, 311-320.

Kengaku, M., Capdevila, J., Rodriguez-Esteban, C., De La Pena, J., Johnson, R.L., Izpisua Belmonte, J.C., and Tabin, C.J. (1998). Distinct WNT pathways regulating AER formation and dorsoventral polarity in the chick limb bud. *Science* 280, 1274-1277.

Keyes, W.M., Vogel, H., Koster, M.I., Guo, X., Qi, Y., Petherbridge, K.M., Roop, D.R., Bradley, A., and Mills, A.A. (2006). p63 heterozygous mutant mice are not prone to spontaneous or chemically induced tumors. *Proc Natl Acad Sci U S A* *103*, 8435-8440.

Kim, V.N. (2005). MicroRNA biogenesis: coordinated cropping and dicing. *Nat Rev Mol Cell Biol* *6*, 376-385.

Koster, M.I., Dai, D., Marinari, B., Sano, Y., Costanzo, A., Karin, M., and Roop, D.R. (2007). p63 induces key target genes required for epidermal morphogenesis. *Proc Natl Acad Sci U S A* *104*, 3255-3260.

Koster, M.I., Kim, S., Mills, A.A., DeMayo, F.J., and Roop, D.R. (2004). p63 is the molecular switch for initiation of an epithelial stratification program. *Genes Dev* *18*, 126-131.

Koster, M.I., Lu, S.L., White, L.D., Wang, X.J., and Roop, D.R. (2006). Reactivation of developmentally expressed p63 isoforms predisposes to tumor development and progression. *Cancer Res* *66*, 3981-3986.

Lambert, J.D., and Nagy, L.M. (2002). Asymmetric inheritance of centrosomally localized mRNAs during embryonic cleavages. *Nature* *420*, 682-686.

Lanza, M., Marinari, B., Papoutsaki, M., Giustizieri, M.L., D'Alessandra, Y., Chimenti, S., Guerrini, L., and Costanzo, A. (2006). Cross-talks in the p53 family: deltaNp63 is an anti-apoptotic target for deltaNp73alpha and p53 gain-of-function mutants. *Cell Cycle* *5*, 1996-2004.

Laurikkala, J., Mikkola, M.L., James, M., Tummers, M., Mills, A.A., and Thesleff, I. (2006). p63 regulates multiple signalling pathways required for ectodermal organogenesis and differentiation. *Development* 133, 1553-1563.

Lechler, T., and Fuchs, E. (2005). Asymmetric cell divisions promote stratification and differentiation of mammalian skin. *Nature* 437, 275-280.

Lee, R., Feinbaum, R., and Ambros, V. (2004). A short history of a short RNA. *Cell* 116, S89-92, 81 p following S96.

Lena, A.M., Shalom-Feuerstein, R., Rivetti di Val Cervo, P., Aberdam, D., Knight, R.A., Melino, G., and Candi, E. (2008). miR-203 represses 'stemness' by repressing DeltaNp63. *Cell Death Differ* 15, 1187-1195.

Lewandoski, M., Wassarman, K.M., and Martin, G.R. (1997). Zp3-cre, a transgenic mouse line for the activation or inactivation of loxP-flanked target genes specifically in the female germ line. *Curr Biol* 7, 148-151.

Liefer, K.M., Koster, M.I., Wang, X.J., Yang, A., McKeon, F., and Roop, D.R. (2000). Down-regulation of p63 is required for epidermal UV-B-induced apoptosis. *Cancer Res* 60, 4016-4020.

Lim, L.P., Glasner, M.E., Yekta, S., Burge, C.B., and Bartel, D.P. (2003). Vertebrate microRNA genes. *Science* 299, 1540.

Lin, Y.L., Sengupta, S., Gurdziel, K., Bell, G.W., Jacks, T., and Flores, E.R. (2009). p63 and p73 transcriptionally regulate genes involved in DNA repair. *PLoS Genet* 5, e1000680.

Liu, C., Nakamura, E., Knezevic, V., Hunter, S., Thompson, K., and Mackem, S. (2003a). A role for the mesenchymal T-box gene Brachyury in AER formation during limb development. *Development* *130*, 1327-1337.

Liu, Y., Lyle, S., Yang, Z., and Cotsarelis, G. (2003b). Keratin 15 promoter targets putative epithelial stem cells in the hair follicle bulge. *J Invest Dermatol* *121*, 963-968.

Lo Iacono, L., and Gross, C. (2008). Alpha-Ca²⁺/calmodulin-dependent protein kinase II contributes to the developmental programming of anxiety in serotonin receptor 1A knock-out mice. *J Neurosci* *28*, 6250-6257.

Looijenga, L.H., Stoop, H., de Leeuw, H.P., de Gouveia Brazao, C.A., Gillis, A.J., van Roozendaal, K.E., van Zoelen, E.J., Weber, R.F., Wolffenbuttel, K.P., van Dekken, H., *et al.* (2003). POU5F1 (OCT3/4) identifies cells with pluripotent potential in human germ cell tumors. *Cancer Res* *63*, 2244-2250.

Marks, R. (2006). Skin disease in the elderly. *Eur J Dermatol* *16*, 460-461.

Massion, P.P., Taflan, P.M., Jamshedur Rahman, S.M., Yildiz, P., Shyr, Y., Edgerton, M.E., Westfall, M.D., Roberts, J.R., Pietenpol, J.A., Carbone, D.P., *et al.* (2003). Significance of p63 amplification and overexpression in lung cancer development and prognosis. *Cancer Res* *63*, 7113-7121.

McGrath, J.A., Duijf, P.H., Doetsch, V., Irvine, A.D., de Waal, R., Vanmolkot, K.R., Wessagowit, V., Kelly, A., Atherton, D.J., Griffiths, W.A., *et al.* (2001). Hay-Wells syndrome is caused by heterozygous missense mutations in the SAM domain of p63. *Hum Mol Genet* *10*, 221-229.

Melton, C., Judson, R.L., and Blelloch, R. Opposing microRNA families regulate self-renewal in mouse embryonic stem cells. *Nature* 463, 621-626.

Merrill, B.J., Gat, U., DasGupta, R., and Fuchs, E. (2001). Tcf3 and Lef1 regulate lineage differentiation of multipotent stem cells in skin. *Genes Dev* 15, 1688-1705.

Miller, M.W., Mooney, S.M., and Middleton, F.A. (2006). Transforming growth factor beta1 and ethanol affect transcription and translation of genes and proteins for cell adhesion molecules in B104 neuroblastoma cells. *J Neurochem* 97, 1182-1190.

Mills, A.A., Zheng, B., Wang, X.J., Vogel, H., Roop, D.R., and Bradley, A. (1999). p63 is a p53 homologue required for limb and epidermal morphogenesis. *Nature* 398, 708-713.

Molofsky, A.V., He, S., Bydon, M., Morrison, S.J., and Pardal, R. (2005). Bmi-1 promotes neural stem cell self-renewal and neural development but not mouse growth and survival by repressing the p16Ink4a and p19Arf senescence pathways. *Genes Dev* 19, 1432-1437.

Molofsky, A.V., Pardal, R., Iwashita, T., Park, I.K., Clarke, M.F., and Morrison, S.J. (2003). Bmi-1 dependence distinguishes neural stem cell self-renewal from progenitor proliferation. *Nature* 425, 962-967.

Niwa, H. (2009). [Transcription factor network governing cellular pluripotency]. *Rinsho Ketsueki* 50, 1524-1530.

Nose, A., Nagafuchi, A., and Takeichi, M. (1987). Isolation of placental cadherin cDNA: identification of a novel gene family of cell-cell adhesion molecules. *EMBO J* 6, 3655-3661.

Ohuchi, H., Takeuchi, J., Yoshioka, H., Ishimaru, Y., Ogura, K., Takahashi, N., Ogura, T., and Noji, S. (1998). Correlation of wing-leg identity in ectopic FGF-induced chimeric limbs with the differential expression of chick Tbx5 and Tbx4. *Development* 125, 51-60.

Palena, C., Polev, D.E., Tsang, K.Y., Fernando, R.I., Litzinger, M., Krukovskaya, L.L., Baranova, A.V., Kozlov, A.P., and Schlom, J. (2007). The human T-box mesodermal transcription factor Brachyury is a candidate target for T-cell-mediated cancer immunotherapy. *Clin Cancer Res* 13, 2471-2478.

Park, B.J., Lee, S.J., Kim, J.I., Lee, C.H., Chang, S.G., Park, J.H., and Chi, S.G. (2000). Frequent alteration of p63 expression in human primary bladder carcinomas. *Cancer Res* 60, 3370-3374.

Pattyn, F., Speleman, F., De Paepe, A., and Vandesompele, J. (2003). RTPrimerDB: the real-time PCR primer and probe database. *Nucleic Acids Res* 31, 122-123.

Racila, D., Winter, M., Said, M., Tomanek-Chalkley, A., Wiechert, S., Eckert, R.L., and Bickenbach, J.R. Transient expression of OCT4 is sufficient to allow human keratinocytes to change their differentiation pathway. *Gene Ther.*

Rhee, H., Polak, L., and Fuchs, E. (2006). Lhx2 maintains stem cell character in hair follicles. *Science (New York, NY)* 312, 1946-1949.

Rodda, D.J., Chew, J.L., Lim, L.H., Loh, Y.H., Wang, B., Ng, H.H., and Robson, P. (2005). Transcriptional regulation of nanog by OCT4 and SOX2. *J Biol Chem* 280, 24731-24737.

Rodriguez-Esteban, C., Tsukui, T., Yonei, S., Magallon, J., Tamura, K., and Izpisua Belmonte, J.C. (1999). The T-box genes *Tbx4* and *Tbx5* regulate limb outgrowth and identity. *Nature* 398, 814-818.

Rohrschneider, M.R., and Nance, J. (2009). Polarity and cell fate specification in the control of *Caenorhabditis elegans* gastrulation. *Dev Dyn* 238, 789-796.

Rothnagel, J.A., Seki, T., Ogo, M., Longley, M.A., Wojcik, S.M., Bundman, D.S., Bickenbach, J.R., and Roop, D.R. (1999). The mouse keratin 6 isoforms are differentially expressed in the hair follicle, footpad, tongue and activated epidermis. *Differentiation* 65, 119-130.

Schuermans, C., and Guillemot, F. (2002). Molecular mechanisms underlying cell fate specification in the developing telencephalon. *Curr Opin Neurobiol* 12, 26-34.

Segalen, M., and Bellaiche, Y. (2009). Cell division orientation and planar cell polarity pathways. *Semin Cell Dev Biol* 20, 972-977.

Senoo, M., Pinto, F., Crum, C.P., and McKeon, F. (2007). p63 Is essential for the proliferative potential of stem cells in stratified epithelia. *Cell* 129, 523-536.

Senoo, M., Tsuchiya, I., Matsumura, Y., Mori, T., Saito, Y., Kato, H., Okamoto, T., and Habu, S. (2001). Transcriptional dysregulation of the p73L / p63 / p51 / p40 / KET gene in human squamous cell carcinomas: expression of Delta Np73L, a novel dominant-

negative isoform, and loss of expression of the potential tumour suppressor p51. *Br J Cancer* 84, 1235-1241.

Sharpless, N.E., Bardeesy, N., Lee, K.H., Carrasco, D., Castrillon, D.H., Aguirre, A.J., Wu, E.A., Horner, J.W., and DePinho, R.A. (2001). Loss of p16Ink4a with retention of p19Arf predisposes mice to tumorigenesis. *Nature* 413, 86-91.

Sherr, C.J., and McCormick, F. (2002). The RB and p53 pathways in cancer. *Cancer Cell* 2, 103-112.

Shimomura, Y., Wajid, M., Shapiro, L., and Christiano, A.M. (2008). P-cadherin is a p63 target gene with a crucial role in the developing human limb bud and hair follicle. *Development* 135, 743-753.

Sontheimer, E.J., and Carthew, R.W. (2005). Silence from within: endogenous siRNAs and miRNAs. *Cell* 122, 9-12.

Su, X., Chakravarti, D., Cho, M.S., Liu, L., Gi, Y.J., Lin, Y.L., Leung, M.L., El-Naggar, A., Creighton, C.J., Suraokar, M.B., *et al.* TAp63 suppresses metastasis through coordinate regulation of Dicer and miRNAs. *Nature* 467, 986-990.

Su, X., Cho, M.S., Gi, Y.J., Ayanga, B.A., Sherr, C.J., and Flores, E.R. (2009a). Rescue of key features of the p63-null epithelial phenotype by inactivation of Ink4a and Arf. *EMBO J* 28, 1904-1915.

Su, X., and Flores, E.R. (2009). TAp63: The fountain of youth. *Aging (Albany NY)* 1, 866-869.

Su, X., Paris, M., Gi, Y.J., Tsai, K.Y., Cho, M.S., Lin, Y.L., Biernaskie, J.A., Sinha, S., Prives, C., Pevny, L.H., *et al.* (2009b). TAp63 prevents premature aging by promoting adult stem cell maintenance. *Cell Stem Cell* 5, 64-75.

Suh, N., Baehner, L., Moltzahn, F., Melton, C., Shenoy, A., Chen, J., and Belloch, R. MicroRNA function is globally suppressed in mouse oocytes and early embryos. *Curr Biol* 20, 271-277.

Sun, P., Yuan, Y., Li, A., Li, B., and Dai, X. Cytokeratin expression during mouse embryonic and early postnatal mammary gland development. *Histochem Cell Biol* 133, 213-221.

Taube, J.H., Allton, K., Duncan, S.A., Shen, L., and Barton, M.C. Foxa1 functions as a pioneer transcription factor at transposable elements to activate *Afp* during differentiation of embryonic stem cells. *J Biol Chem* 285, 16135-16144.

Tay, Y., Zhang, J., Thomson, A.M., Lim, B., and Rigoutsos, I. (2008). MicroRNAs to *Nanog*, *Oct4* and *Sox2* coding regions modulate embryonic stem cell differentiation. *Nature* 455, 1124-1128.

Thomson, J.A., Itskovitz-Eldor, J., Shapiro, S.S., Waknitz, M.A., Swiergiel, J.J., Marshall, V.S., and Jones, J.M. (1998). Embryonic stem cell lines derived from human blastocysts. *Science* 282, 1145-1147.

Thomson, J.A., and Marshall, V.S. (1998). Primate embryonic stem cells. *Curr Top Dev Biol* 38, 133-165.

Truong, A.B., and Khavari, P.A. (2007). Control of keratinocyte proliferation and differentiation by p63. *Cell Cycle* 6, 295-299.

Truong, A.B., Kretz, M., Ridky, T.W., Kimmel, R., and Khavari, P.A. (2006). p63 regulates proliferation and differentiation of developmentally mature keratinocytes. *Genes Dev* 20, 3185-3197.

Ulloa-Montoya, F., Verfaillie, C.M., and Hu, W.S. (2005). Culture systems for pluripotent stem cells. *J Biosci Bioeng* 100, 12-27.

Urist, M.J., Di Como, C.J., Lu, M.L., Charytonowicz, E., Verbel, D., Crum, C.P., Ince, T.A., McKeon, F.D., and Cordon-Cardo, C. (2002). Loss of p63 expression is associated with tumor progression in bladder cancer. *Am J Pathol* 161, 1199-1206.

van der Lugt, N.M., Domen, J., Linders, K., van Roon, M., Robanus-Maandag, E., te Riele, H., van der Valk, M., Deschamps, J., Sofroniew, M., van Lohuizen, M., *et al.* (1994). Posterior transformation, neurological abnormalities, and severe hematopoietic defects in mice with a targeted deletion of the bmi-1 proto-oncogene. *Genes Dev* 8, 757-769.

Vasioukhin, V., Degenstein, L., Wise, B., and Fuchs, E. (1999). The magical touch: genome targeting in epidermal stem cells induced by tamoxifen application to mouse skin. *Proc Natl Acad Sci U S A* 96, 8551-8556.

Vigano, M.A., Lamartine, J., Testoni, B., Merico, D., Alotto, D., Castagnoli, C., Robert, A., Candi, E., Melino, G., Gidrol, X., *et al.* (2006). New p63 targets in keratinocytes identified by a genome-wide approach. *The EMBO journal* 25, 5105-5116.

Vigano, M.A., and Mantovani, R. (2007). Hitting the numbers: the emerging network of p63 targets. *Cell cycle (Georgetown, Tex)* 6, 233-239.

Vujovic, S., Henderson, S., Presneau, N., Odell, E., Jacques, T.S., Tirabosco, R., Boshoff, C., and Flanagan, A.M. (2006). Brachyury, a crucial regulator of notochordal development, is a novel biomarker for chordomas. *J Pathol* 209, 157-165.

Wang, Y., Medvid, R., Melton, C., Jaenisch, R., and Blelloch, R. (2007). DGCR8 is essential for microRNA biogenesis and silencing of embryonic stem cell self-renewal. *Nat Genet* 39, 380-385.

Wilkinson, D.G., Bhatt, S., and Herrmann, B.G. (1990). Expression pattern of the mouse T gene and its role in mesoderm formation. *Nature* 343, 657-659.

Winter, J., Jung, S., Keller, S., Gregory, R.I., and Diederichs, S. (2009). Many roads to maturity: microRNA biogenesis pathways and their regulation. *Nat Cell Biol* 11, 228-234.

Xu, N., Papagiannakopoulos, T., Pan, G., Thomson, J.A., and Kosik, K.S. (2009). MicroRNA-145 regulates OCT4, SOX2, and KLF4 and represses pluripotency in human embryonic stem cells. *Cell* 137, 647-658.

Yamaguchi, K., Wu, L., Caballero, O.L., Hibi, K., Trink, B., Resto, V., Cairns, P., Okami, K., Koch, W.M., Sidransky, D., *et al.* (2000). Frequent gain of the p40/p51/p63 gene locus in primary head and neck squamous cell carcinoma. *Int J Cancer* 86, 684-689.

Yang, A., Kaghad, M., Wang, Y., Gillett, E., Fleming, M.D., Dotsch, V., Andrews, N.C., Caput, D., and McKeon, F. (1998). p63, a p53 homolog at 3q27-29, encodes multiple

products with transactivating, death-inducing, and dominant-negative activities. *Mol Cell* 2, 305-316.

Yang, A., Schweitzer, R., Sun, D., Kaghad, M., Walker, N., Bronson, R.T., Tabin, C., Sharpe, A., Caput, D., Crum, C., *et al.* (1999). p63 is essential for regenerative proliferation in limb, craniofacial and epithelial development. *Nature* 398, 714-718.

Yang, A., Zhu, Z., Kapranov, P., McKeon, F., Church, G.M., Gingeras, T.R., and Struhl, K. (2006). Relationships between p63 binding, DNA sequence, transcription activity, and biological function in human cells. *Molecular cell* 24, 593-602.

Yang, X.R., Ng, D., Alcorta, D.A., Liebsch, N.J., Sheridan, E., Li, S., Goldstein, A.M., Parry, D.M., and Kelley, M.J. (2009). T (brachyury) gene duplication confers major susceptibility to familial chordoma. *Nat Genet* 41, 1176-1178.

Yi, R., O'Carroll, D., Pasolli, H.A., Zhang, Z., Dietrich, F.S., Tarakhovsky, A., and Fuchs, E. (2006). Morphogenesis in skin is governed by discrete sets of differentially expressed microRNAs. *Nat Genet* 38, 356-362.

Yi, R., Pasolli, H.A., Landthaler, M., Hafner, M., Ojo, T., Sheridan, R., Sander, C., O'Carroll, D., Stoffel, M., Tuschl, T., *et al.* (2009). DGCR8-dependent microRNA biogenesis is essential for skin development. *Proc Natl Acad Sci U S A* 106, 498-502.

Yi, R., Poy, M.N., Stoffel, M., and Fuchs, E. (2008). A skin microRNA promotes differentiation by repressing 'stemness'. *Nature* 452, 225-229.

Yi, R., Qin, Y., Macara, I.G., and Cullen, B.R. (2003). Exportin-5 mediates the nuclear export of pre-microRNAs and short hairpin RNAs. *Genes Dev* 17, 3011-3016.

Yonei-Tamura, S., Endo, T., Yajima, H., Ohuchi, H., Ide, H., and Tamura, K. (1999). FGF7 and FGF10 directly induce the apical ectodermal ridge in chick embryos. *Dev Biol* 211, 133-143.

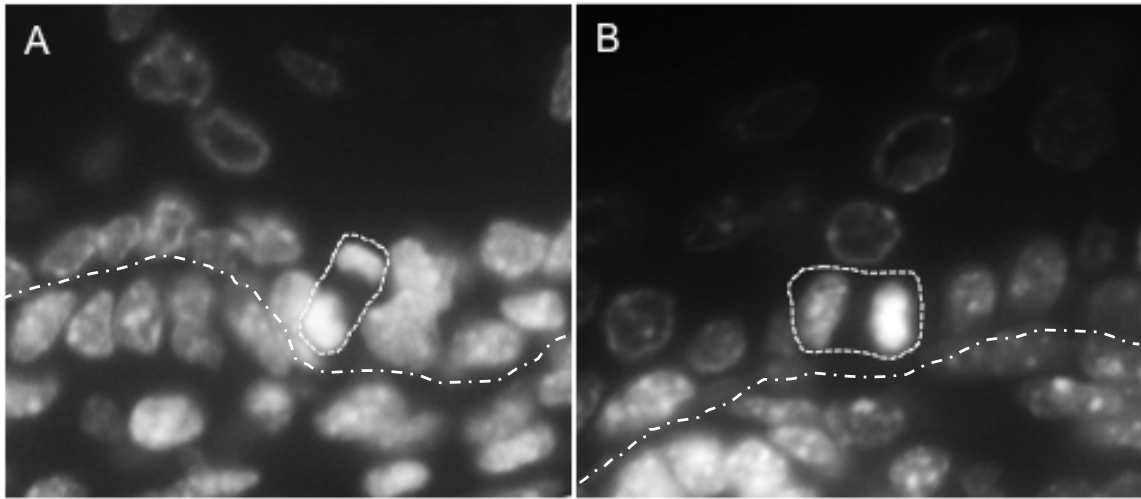
Yu, F., Ong, C.T., Chia, W., and Yang, X. (2002). Membrane targeting and asymmetric localization of *Drosophila* partner of *inscuteable* are discrete steps controlled by distinct regions of the protein. *Mol Cell Biol* 22, 4230-4240.

Zaehres, H., Lensch, M.W., Daheron, L., Stewart, S.A., Itskovitz-Eldor, J., and Daley, G.Q. (2005). High-efficiency RNA interference in human embryonic stem cells. *Stem Cells* 23, 299-305.

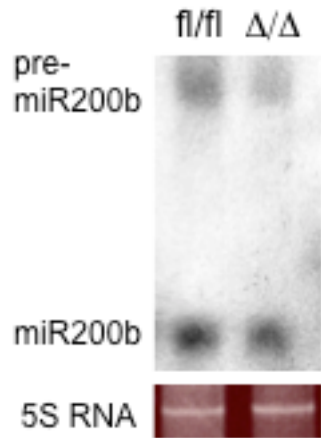
Zindy, F., Nilsson, L.M., Nguyen, L., Meunier, C., Smeyne, R.J., Rehg, J.E., Eberhart, C., Sherr, C.J., and Roussel, M.F. (2003a). Hemangiosarcomas, medulloblastomas, and other tumors in *Ink4c/p53*-null mice. *Cancer Res* 63, 5420-5427.

Zindy, F., Williams, R.T., Baudino, T.A., Rehg, J.E., Skapek, S.X., Cleveland, J.L., Roussel, M.F., and Sherr, C.J. (2003b). *Arf* tumor suppressor promoter monitors latent oncogenic signals in vivo. *Proc Natl Acad Sci U S A* 100, 15930-15935.

APPENDIX

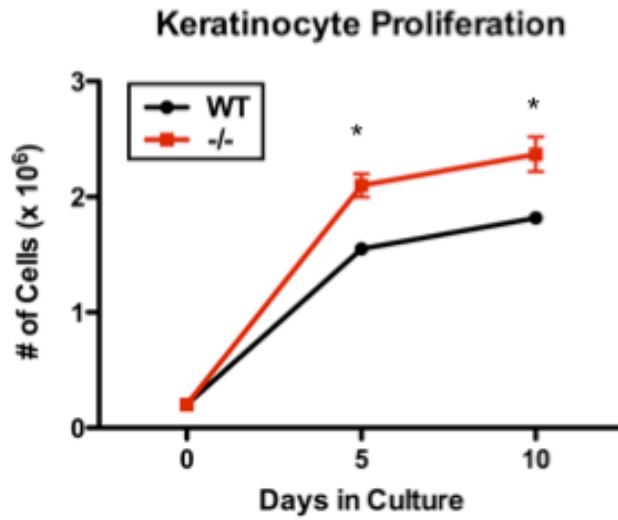


Appendix 1. Mitotic Figures in Developing Epidermis from a wild type embryo at 18.5 Days of epidermal keratinocytes in the basal layer of developing epidermis undergo apical-basal cell divisions (A), giving rise to cells in the intermediate layer, which divide laterally (B). (Cho & Flores Unpublished data) A broken white circle indicates a mitotic cell in the basal layer and broken line indicates a basement membrane between dermis and epidermis.



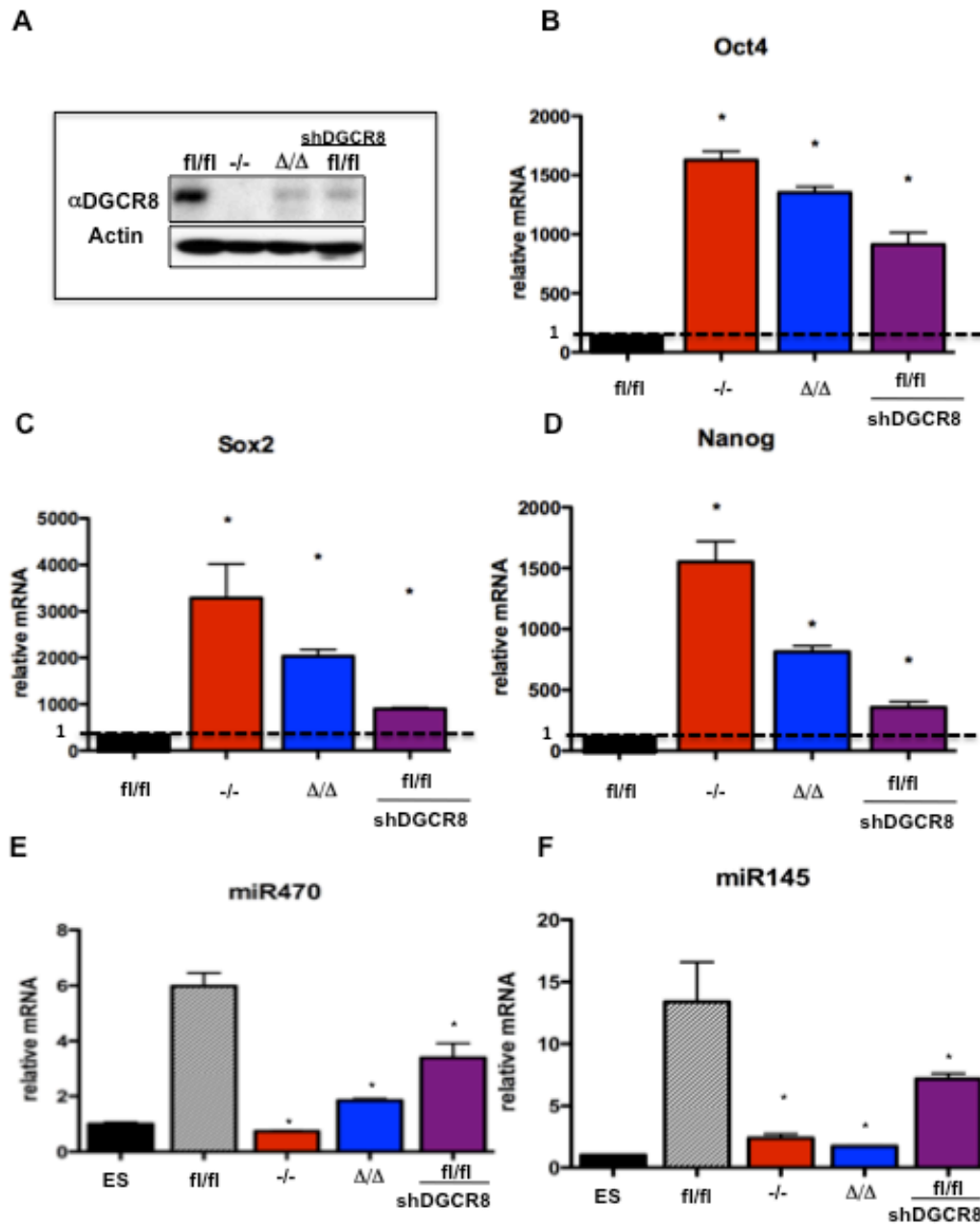
Appendix 2. Δ Np63 ablation shows lower microRNA expression.

Total RNA is extracted from Δ Np63^{fl/fl} and Δ Np63 Δ/Δ keratinocytes. Northern analysis was used to detect precursor and mature forms of microRNA 200b expression (**Cho & Flores Unpublished data**).



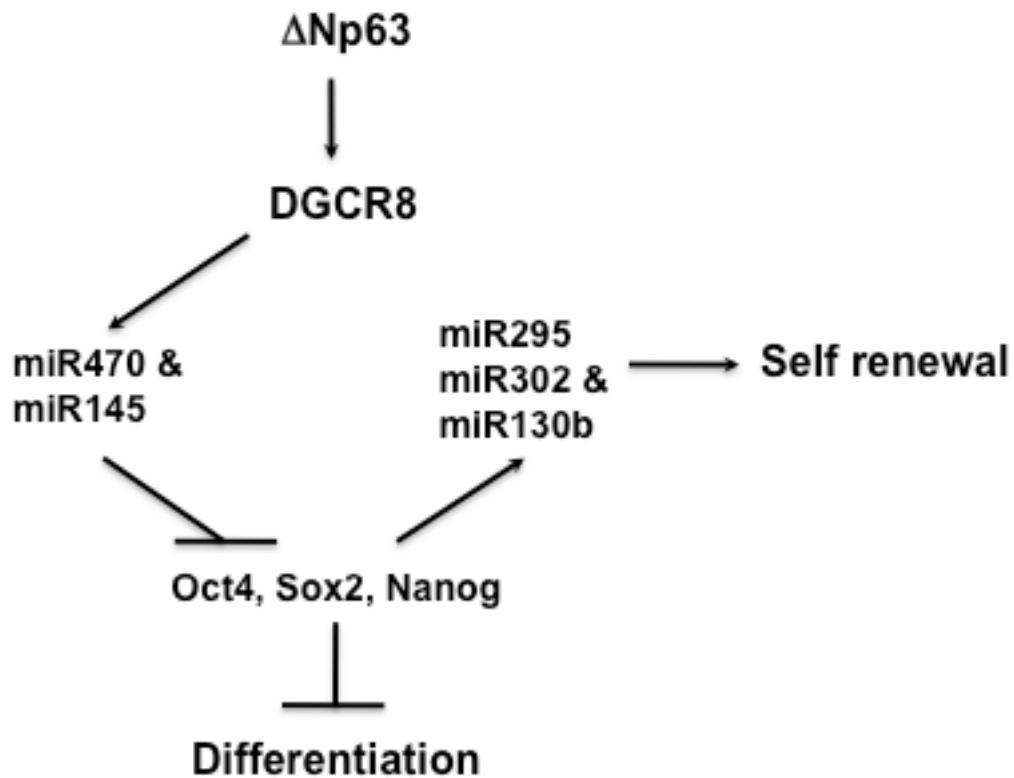
Appendix 3. Δ Np63 ablation shows hyperproliferation in epidermal cells.

* $p < 0.03$ A graph of cell numbers at indicated days (Day 0, 5 and 10). An asterisk showed statistically significant.



Appendix 4. DGCR8 knock down reminiscent gene expression. *Oct4*, *Nanog* and *Sox2* are downregulated in wild type epidermal cells by just knocking down DGCR8

using shDGCR8. **A)** Western blot analysis for DGCR8. **B, C & D)** qRT-PCR for Oct4, Nanog and Sox2 in RNA from *wild type* and $\Delta Np63^{-/-}$ epidermal cells and *miR470* and *miR145* are downregulated in *wild type* epidermal cells by just knocking down DGCR8 using shDGCR8. **E & F)** qRT-PCR for miR470 and miR145 in RNA from *wild type* and $\Delta Np63^{-/-}$ epidermal cells



Appendix 5. $\Delta Np63$ initiates epidermal differentiation through *DGCR8*.

In normal tissue differentiation, $\Delta Np63$ transcriptionally regulates *DGCR8*, a component of microRNA processors (DGCR8/Drosha) to process from primary microRNA to precursor microRNA. When $\Delta Np63$ transactivates *DGCR8*, its protein properly processes *microRNA470* (*miR470*) and *microRNA 145* (*miR145*). These two miRNAs repress *Oct4*, *Sox2* and *Nanog* transcripts and cells can undergo proper differentiation.

VITA

MinSoon Cho was born in Seoul, Republic of Korea on August 23rd (lunar calendar), 1972, the fourth daughter of my late father, Yoon Hak Cho and my mother, Boon Soon Jeong. After completing her work at Songgok Girl's high school, Seoul, Korea in 1991, she entered Seoul Women's University in Seoul, Korea. She received the degree of Bachelor of Science with a major in Biology from Seoul Women's University in Seoul, Korea in February, 1996. She received the degree of Master of Science with a major in Human Genetics from Seoul National University in Seoul, Korea in February, 1999. For a couple of years, she experienced and worked as a research assistant in several different institutes, including the school of medicine at the Aju university in Suwon, Korea, Baylor College of Medicine and MD Anderson Cancer Center in Houston, USA. In September of 2005, she entered The University of Texas Health Science Center at Houston Graduate School of Biomedical Sciences.

Permanent Address:

1885 El Paseo St. #1033, Houston, TX. 77054